VŠB – TECHNICAL UNIVERSITY OF OSTRAVA
FACULTY OF MECHANICAL ENGINEERING
DEPARTMENT OF CONTROL SYSTEMS AND INSTRUMENTATION

DIAGNOSTICS METHODS AND THEIR APPLICATION IN AUTOMOTIVE ENGINE

Study program: **P2301 Mechanical Engineering**

Field: **3902V010 Automation of Technological Processes**

PhD student: **Ing. Le Khac Binh**

Supervisor: **Prof. Ing. Jiří Tůma, CSc.**

Ostrava, 2012

CONTENT

List of figure…… 3

Nomenclature…… 7

Abstract…… 10

Outline of the doctoral thesis…… 11

1 INTRODUCTION…… 12

1.1 Equipments in modern engine…… 12

1.2 Overview of automotive engine control…… 15

1.3 Main control loops in SI engines…… 17

1.3.1 Air/Fuel Ratio Control…… 17

1.3.2 Ignition Control Loop…… 19

1.3.3 Knock control…… 20

1.3.4 Idle speed control system…… 22

1.4 Diagnostics technology theory…… 23

1.5 State of art in the automotive engine simulation…… 24

2 EXTENDING SI ENGINE MODEL BY MATLAB/SIMULINK…… 26

2.1 Engine…… 27

2.1.1 Throttle body model…… 29

2.1.2 Intake manifold model…… 32

2.1.3 Intake system model…… 37

2.1.4 Torque generation model…… 38

2.1.5 Mass moment of inertia…… 44

2.2 Sensors…… 49

2.2.1 Lambda sensor…… 49

2.2.2 Throttle position sensor…… 50

2.2.3 Engine speed sensor (crankshaft sensor)…… 53

2.2.4 Mass air flow sensor…… 54

2.2.5	Manifold absolute pressure sensor (MAP sensor)……	55
2.3	Electronic Control Unit (ECU) ……..	57
2.4	Actuators……..	58
2.4.1	Fuel injector…….	58
2.4.2	Exhaust gas recirculation valve (EGR)……	60
3	CONNECTING ENGINE MODEL TO dSPACE……...	62
3.1	Fundamental of dSPACE and Hardware-in-the-loop (HIL) simulation ……....	62
3.2	HIL Systems: Basics and Components ……..……	65
3.2.1	Basics of HIL System ……	65
3.2.2	Components of the HIL System……...	65
3.3	Testing Diagnostic Functions with HIL……...	67
4	SIMULATION RESULTS……..	69
4.1	Mass flow rate……...	69
4.2	Engine torque ……	71
4.3	Engine speed……..…….	76
4.4	Moment of inertia……	78
4.5	Crankshaft angular variation, velocity and acceleration…….	79
5	DIAGNOSTICS INTERNAL COMBUSTION ENGINE ……..……	82
5.1	Description of the diagnostic method……..	83
5.2	The relation between volume and pressure in the cylinder of SI engine……	84
5.3	Effect of the missing pulses in the signal from crankshaft on the frequency spectrum ……. ……..	85
5.4	Phase Demodulation using Hilbert Transform…….	87
5.5	Crankshaft variation measurement and evaluate the acceleration……...	93
6	CONCLUSIONS……..	98
7	REPERENCES……	101
8	LIST OF MY PAPERS……..	108

LIST OF FIGURE

Fig. 1.1	Wiring harness of a modern vehicle (Maybach)……..	13
Fig. 1.2	Layout of a modern engine management system…….	14
Fig. 1.3	Overview over a typical SI engine system structure……	15
Fig. 1.4	Basic SI engine control substructure……	17
Fig. 1.5	TWC and its conversion efficiency (after light-off, stationary behavior)…	18
Fig. 1.6	Electronic ignition system. ..……	19
Fig. 1.7	An example of ignition map ……..……	20
Fig. 1.8	Cylinder pressure output signal for non-knocking and knocking combustion…….. ……..	21
Fig. 1.9	Knock control with feed-forward adaptive ignition angle map……	22
Fig. 1.10	Complete ISCS structure……...	23
Fig. 1.11	General structure of a diagnosis application…….	24
Fig. 1.12	Integrated diagnostics process……...	24
Fig. 2.1	Schematic diagram of a spark-ignition engine……..	26
Fig. 2.2	Overall simulink model of the engine and control system ……...	27
Fig. 2.3	Engine torque control structure in a torque – based engine control unit……	28
Fig. 2.4	Engine block……..	28
Fig. 2.5	Throttle body……	29
Fig. 2.6	Throttle model…….	32
Fig. 2.7	Idealized Air Flows ……..……	34
Fig. 2.8	Throttle flow with valve angle and pressure ……	36
Fig. 2.9	Intake manifold vacuum……	36
Fig. 2.10	Four-stroke internal combustion engine……	37
Fig. 2.11	Intake manifold model……..	38
Fig. 2.12	Forces and acceleration of the piston-crankshaft mechanism …..……	39
Fig. 2.13	Spark advance table…….	41

Fig. 2.14 Spark advance from MBT 41

Fig. 2.15 Torque Generation block 43

Fig. 2.16 The engine brake torque as a function of engine speed and average amplitude..... 43

Fig. 2.17 Mass effect on the piston rod coordination 44

Fig. 2.18 Simulink engine model..... 48

Fig. 2.19 Engine exhaust gases and normalized A/F ratio λ 49

Fig. 2.20 Oxygen sensor location 48

Fig. 2.21 Zirconium dioxide sensor and its output voltage 50

Fig. 2.22 Air/fuel ratio for engine, fuel injection modulation 51

Fig. 2.23 Throttle position sensor 52

Fig. 2.24 Output voltage of throttle position sensor..... 52

Fig. 2.25 Engine speed sensor..... 53

Fig. 2.26 The waveform of engine speed sensor..... 53

Fig. 2.27 Hot wire MAF sensor..... 55

Fig. 2.28 MAF sensor signal voltage 55

Fig. 2.29 MAP sensor 56

Fig. 2.30 MAP sensor circuit and output voltage 56

Fig. 2.31 ECU and its inputs, outputs..... 57

Fig. 2.32 Electronic control unit block 58

Fig. 2.33 Fuel injector..... 58

Fig. 2.34 Piezoelectric injector map..... 60

Fig. 2.35 EGR system..... 60

Fig. 2.36 Actuators block..... 61

Fig. 3.1 The dSPACE simulation and its connector panel 62

Fig. 3.2 dSPACE Prototyping system..... 63

Fig. 3.3 Signal flows in a real system and HIL simulation 64

Fig. 3.4	Structure of an HIL simulator with integrated diagnostics ……	64
Fig. 3.5	Components of an HIL system ……	65
Fig. 3.6	Angular processing unit (APU) for the crank-angle-synchronous generation of crankshaft/camshaft signals and knock signals and for capturing injection and ignition signal …….	68
Fig. 4.1	Mass flow rate into the manifold…….	68
Fig. 4.2	Simulation result of manifold pressure in intake system……	70
Fig. 4.3	Simulation result of mass flow rate in cylinder for combustion…….	71
Fig. 4.4	Timing diagram for the ignition……..	72
Fig. 4.5	Difference of firing and misfire pressure in cylinder …….	73
Fig. 4.6	Engine torque via spark advance…….	75
Fig. 4.7	Engine brake torque as function of ignition angle……..	76
Fig. 4.8	Simulation result of engine idle speed as a function of time……...	77
Fig. 4.9	Simulation result of engine speed with load mode as a function of time …	78
Fig. 4.10	Moment of inertia of one cylinder engine vs. angle of rotation…….	79
Fig. 4.11	Cylinder pressure in the combustion chamber……..……..……	80
Fig. 4.12	Crankshaft angular variation, velocity and acceleration……	81
Fig. 5.1	Indicator diagram for a 4-stroke engine……	84
Fig. 5.2	Cylinder pressure vs. crankshaft angle……..	84
Fig. 5.3	Crankshaft signal when the flywheel has enough 60 teeth……	85
Fig. 5.4	The autospectrum of crankshaft signal……..	85
Fig. 5.5	Crankshaft signal when two teeth are removed……..……...	86
Fig. 5.6	The autospectrum of crankshaft signal ……...	86
Fig. 5.7	Phase modulated signal……	86
Fig. 5.8	Zoom of phase modulated signal …….	87
Fig. 5.9	Order spectrum when β=5..……	88
Fig. 5.10	Order spectrum when β=0.1……	88
Fig. 5.11	Evaluation of the analytical complex signal in real time……..	89

Fig. 5.12 The Hilbert Transform signal……. 89

Fig. 5.13 Zoom of the Hilbert Transform signal…….. 89

Fig. 5.14 Unwrapped phase of analytical signal……... 90

Fig. 5.15 Phase of analytical signal……. 90

Fig. 5.16 Zoom of phase of analytical signal…….. 91

Fig. 5.17 Detrended unwrapped phase of analytical signal…….. 91

Fig. 5.18 Normalized detrended unwrapped phase of analytical signal……. 91

Fig. 5.19 Crankshaft variation measurement……. 92

Fig. 5.20 Rotational pulse signal……. 93

NOMENCLATURE

Symbol	*Description*
ECU	Electronic control unit
IC	Internal combustion
SI	Spark ignition
TWC	Three-way converter
EGR	Exhaust gas recirculation
ISCS	Idle-speed control-system
OBD	Onboard diagnostics
APU	Angular processing unit
TDC	Top dead center
BDC	Bottom dead center
BTDC	Before top dead center
RPM	Revolution per minute
AC	Alternating current
MAF	Mass air flow
MAP	Intake manifold pressure
MBT	Minimum spark advance for the best torque
TPS	Throttle position sensor
ECM	Electronic control module
HIL	Hardware in the loop
I/O	Input/output
PC	Personal computer
RTW	Real-Time Workshop
CAN	Control area network
FFT	Fast Fourier Transform
ms	Millisecond

Symbol	*Description*	*Units*
P	Combustion pressure……..	[bar]
P_m	Manifold pressure……..….	[bar]
P_{amb}	Ambient (atmospheric) pressure……	[bar]
R	Specific gas constant……..	[-]
T	Temperature……..……..	[^{0}K]
V_m	Manifold volume…….……	[m^3]
V_{cyl}	Volume of the engine cylinders…….....	[m^3]
V_{1cyl}	Volume of one cylinder……..	[m^3]
T_e	Torque produced by the engine (running output torque)……	[Nm]
T_l	Load torque…….	[Nm]
T_l	Engine rotational moment of inertia……..	[kg-m^2]
A_{th}	Cross-sectional flow area of throttle body……..	[m^2]
M_a	Molecular weight of air……...	[-]
M_{egr}	Molecular weight of exhaust……...	[-]
k	Ratio of specific heats…….	[-]
A/F(λ)	Air to fuel ratio……	[-]
$u(t)$	Inputs to the diagnosis system……	[-]
$y(t)$	Outputs to the diagnosis system……	[-]
$\dot{m}_{ao}$	Mass flow rate of air out of the manifold……..	[g/s]
m_a	Mass of air in cylinder for combustion……	[g]
$\dot{m}_{al}$	Mass flow rate into manifold……	[g/s]
J_{crank}	Crankshaft inertia……..	[kg.m^2]
T_0	Corresponding ambient temperature……	[^{0}K]
F_i	Indicated force……..	[N]
F_f	Friction force……..	[N]

F_{cr}	Connecting rod force……..	[N]
F_{st}	Side thrust force……..	[N]
P_i	Indicated pressure…….	[Pa]
L	Connecting rod length……	[m]
N	Engine speed……...	[RPM]
r	Crankshaft radius……	[m]
s	Cylinder stroke……	[m]
z	Number of cylinder…….	[-]
δ	Piston pin offset……..	[m]
d	Bore…….	[m]
α_e	Effective ignition angle……..	[degree]
α_i	Open loop ignition angle from fixed map……	[degree]
α_k	Knock control ignition angle……	[degree]
α_l	Learned ignition angle from adaptive map……	[degree]
α	Throttle angle……..……	[degree]
τ_{id}	The self-inflammation delay……...	[s]
θ	Crank angle…….	[degree]
$\dot{\theta}$	Engine speed……..….	[rad/s]
$\ddot{\theta}$	Engine acceleration…….….	[rad/s^2]
σ	Spark advance…….……	[degree]
ϑ	Temperature within combustion chamber…….	[^{0}K]
η_v	Volumetric efficiency…….	[-]
ρ_0	Atmospheric density……..	[kg/m^3]

Abstract

Diagnostic of automotive engines is a very important field and has a long history. Since the automotive industry was born in the 19th century, the problem of finding faults in engines become necessary, but the diagnosis was conducted manually and off-board. By the time, when the field of automotive industry develops, most of engine are equipped electric and electronic devices, the role of diagnostic becomes very indispensable because it yields benefits on several front such as fuel efficiency, exhaust emission reduction, better delivery, and so that, on-board diagnosis also develops very quickly.

In modern automotive engine, most of systems are equipped with a control system architecture that comprises of a microcontroller, several sensors and actuators. The microcontroller, also called as the electronic control unit (ECU), continually identifies what the driver is demanding out of the engine. Accordingly, it continually selects the engine control inputs such as air flow rate, fuel flow rate, spark timing, etc…. The microcontroller also processes the information carried by several sensors for feedback control as well as for diagnostics. The methodology for designing the controller involves modeling the engine and developing the controller in simulated environment as a first step.

In this dissertation, many different subsystems of the engine are modeled and the engine phenomena of relevance in "control-oriented sense". Then integrating them, develop dynamic, control engine parameters, after that, these models will be connected with dSpace equipment with Lapsoft software to control an IC engine. Simulation results for the model in are presented. From the results, we can diagnose the faults of the engine. The developed models also could be useful for controller development for other models of engine operation as well such as transient operation, steady state running, etc. The controller development exercise and results can be useful in further study for other similar mode of engine operation, such as cruising.

In the current condition of Vietnam, when the science and technology are still low, control dynamic systems in general, automotive control in particular, diagnostics engine are still a new field. The completion of this thesis will be very important meaning for me as well as the science of Vietnam.

Goals of the doctoral thesis

1. My firstly target is to describe generally equipments in the modern car and engine. Then, the overview of automotive engine control and some main control loops in spark ignition engines such as: Air/Fuel ratio control; Ignition control; and Knock control are shown. Some methods of diagnostic automotive engine are presented as well.

2. Second target is to extend the engine model of Weeks, R.W. & Moskwa, J.J. by modeling of the non-uniform driving torque in contrast to the original model assuming uniform driving torque. The thesis contains a description of the individual subsystems in the simulation program Matlab/Simulink from linear to none linear form. It includes an overview of the engine and the control system model briefly describing the various subsystems. Addition detail is provided the engine model with subsystems: intake system, sensors, actuators and engine controller unit (ECU).

3. Next target of my thesis is to combine the created engine model with the HIL equipment to control and simulate the engine. The purposes of simulation are: reading the measurement signals; calculating and perform numeric integration and outputting the results. These data will be the basic for diagnostics engine.

4. The last target of my thesis focuses on diagnostics of the engine. The factor for diagnostic the engine is the signal from the crankshaft angular acceleration. By means of analyzing the signal, the engine running state and a lot of related faults can be gained. Under the normal working conditions, the motive force performance of each cylinder is unanimous basically; the spark ignition engine operates steadily. While when a certain cylinder is abnormal, the consistency of motive force is destroyed, the engine becomes bad to the stationary of operation and angular acceleration signal will be out of shape. By observing its fluctuation, the working process in each cylinder can be evaluated. The main interest is dealing with combustion and compression stroke of IC engines.

1. INTRODUCTION

1.1. Equipments in modern engine

In modern life, automotive is one of the greatest conveniences and internal combustion engines have become the most frequently used sources of propulsion energy in passenger cars. One of the main reasons that it is widely used is the very high energy density of liquid hydrocarbon fuels. As long as fossil fuel resources are used to fuel cars, there are no foreseeable alternatives that offer the same benefits in terms of cost, safety, pollutant emission and fuel economy. The improvement of internal combustion engines is still big potential for scientists. For example, how to make the diesel (compression ignition) engines to be cleaner and how to make the gasoline (spark ignition) engines to be much more fuel efficient. To achieve these goals, the role of control systems is indispensable in automotive engine. For that reasons, in modern automotive engine, there is about one third of their parts value in electric and electronic components. These devices are not only helping the engine reduces the fuel consumption and the emission of pollutant species, to increase safety, but also improving its reliability. When the electronic control systems become more complex and powerful, an ever increasing number of mechanical functions are being replaced by electric and electronic devices. Figure 1.1 is an example of such an advanced vehicle.

In this system, the engine is only one part within a larger structure. Input and output signals are the main objects and commands issued by the electronic control unit (ECU) or directly by the driver, and the load torque transmitted through the clutch into the engine's flywheel.

Figure 1.2 shows many kinds of actuators and sensors in a modern SI engine management system. Depending on the demands of the driver about the working mode of the engine, ECU receives the signals from many type of sensors as input signals. After processing and optimizing these data, output signals are sent to all actuators as control signals, taking into account constraints imposed by engine safety considerations and pollutant emission limitations.

Fig. 1.1. Wiring harness of a modern vehicle (Maybach) [48]

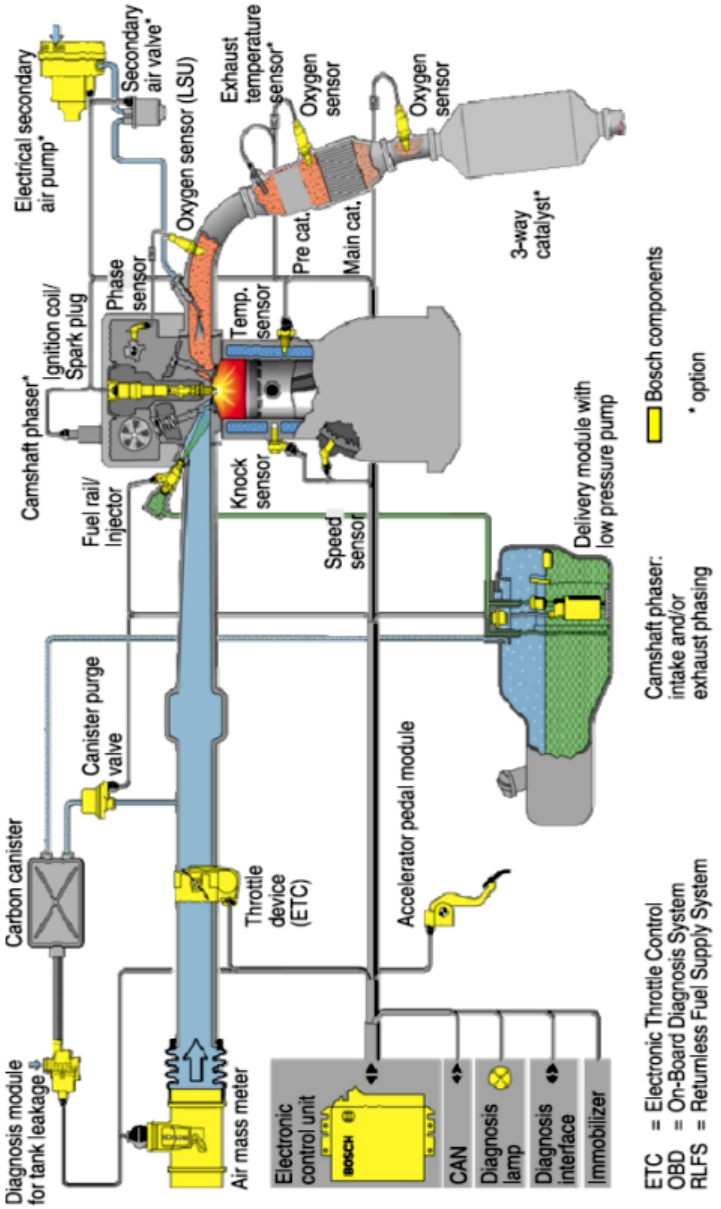

Fig. 1.2. Layout of a modern engine management system [36]

For reducing pollution purpose, in the modern engines management are equipped the three catalytic converters (TWC) and it will be described more detail in the next part. Three functions of the TWC are: the close-coupled TWC optimized for rapid light-off at cold start, the main TWC which is located downstream of the close-coupled TWC; and an optional underfloor catalytic converter. In order to control the complex exhaust after the treatment system, three exhaust gas oxygen sensors are equipped along the exhaust system: one located as close as possible to the exhaust valves; one installed between the close coupled and the main TWC; and the last one attached downstream of the main TWC. To prevent the damage of the catalytic converters due to overheating and to improve the overall control

system performance, the engine is also equipped an optional exhaust gas temperature sensor. The component of exhaust must be adapted to the specific pollutant emission limitations that are imposed by the environment laws. Normally, the smallest number of TWC and sensors are chosen with which these limitations can be met in order to realize the configuration.

1.2. Overview of automotive engine control

In almost of modern gasoline automotive engines, the port (indirect) injection spark-ignited are still equipped. The advantage of these engines is the time for mixing fuel and air longer, so the mixture is quite good and stoichiometric combustion of the engine process permits an extremely efficient exhaust gas purification with three-way catalytic converters and produces a very little particulate matter (PM). A standard configuration of such an engine is shown in figure 1.3.

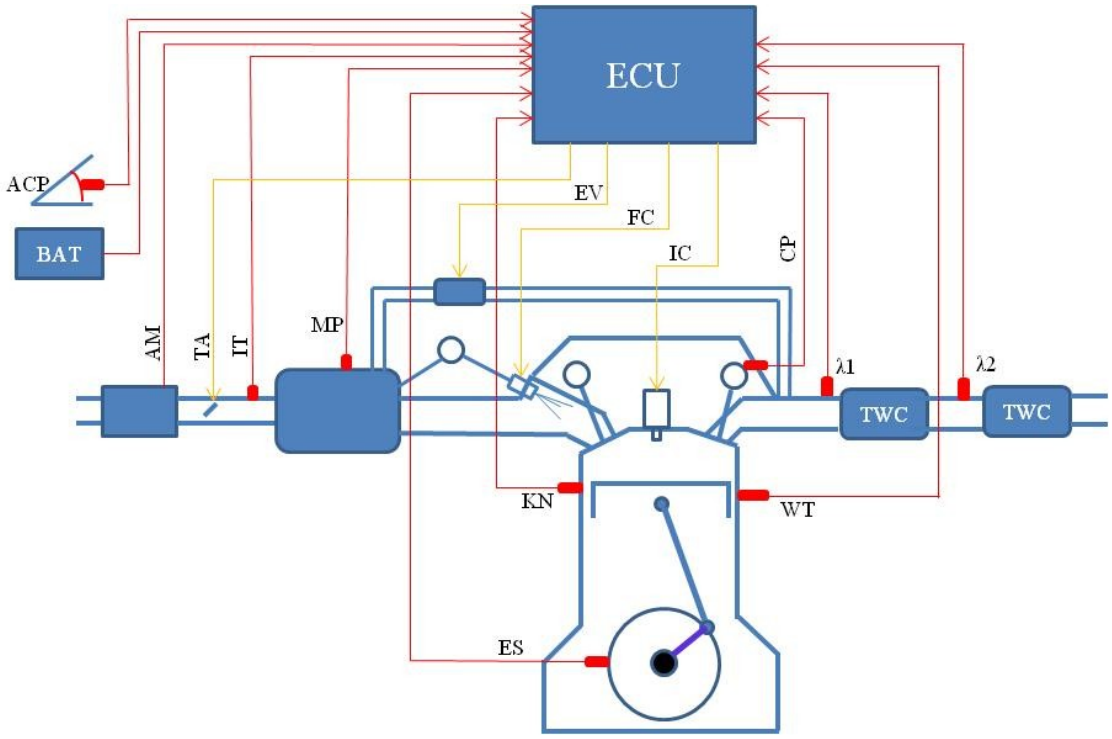

CP - camshaft sensor	ACP - acceleration pedal	ECU - controller
$\lambda_{1,2}$ - Oxygen sensors	BAT- battery	FC - fuel command
AM - air mass-flow sensor	IT - intake air temperature sensor	EV - EGR valve
ES - engine speed sensor	WT - water temperature sensor	IC - ignition command
KN - knock sensor	TWC - 3-way catalyst	TA – throttle angle

Fig.1.3. Overview over a typical SI engine system structure

The quality of the mixture affects directly to the torque of a stoichiometric engine in the cylinder during each stroke (the quality, i.e., the air/fuel ratio, remains constant). Typically, the quality of the mixture depends on many factors such as the intake pressure, the fuel injection quality, shape of the intake system, fuel quality, etc…. Not only that, when these factors change, the density of the air/fuel mixture is also change as well. Until now, a throttle plate is still the first choice for upstream of the combustion process in the intake system. Though this solution is relatively simple and reliable, but pumping losses is still a big problem that negatively affects the part-load efficiency of the engine. Novel approaches, such as an electronic throttle control, variable valve timing, etc., which offer improved fuel economy and pollutant emission, will be discussed below.

A simplified control-oriented substructure of an SI engine is shown in figure 1.4 [36]. The output of the block is the engine rotation ω, which takes into account the rotational inertia of the engine, whose inputs are the engine torque T_e and the load torque T_l is the most important output signal of the engine in this thesis. The knock signal y_ζ, which measured by the knock sensor and air/fuel ratio (A/F) (sometime called oxygen sensor) is measured by a λ sensor, which is located as close as possible to the exhaust valve are the important feedback output signals also.

From the figure 1.4, the four most important control loops are:

- The fuel-injection feedforward loop
- The air/fuel ratio feedback loop
- The ignition angle feedforward loop
- The knock feedback loop

In addition, the following feedforward or feedback loops are present in many engine systems:

- The idle and cruise speed control
- The exhaust gas recirculation EGR (for reducing emission during cold-start or for lean-burn engines)
- The secondary air injection (for faster catalyst light-off)
- The canister purge management (to avoid hydrocarbon evaporation)

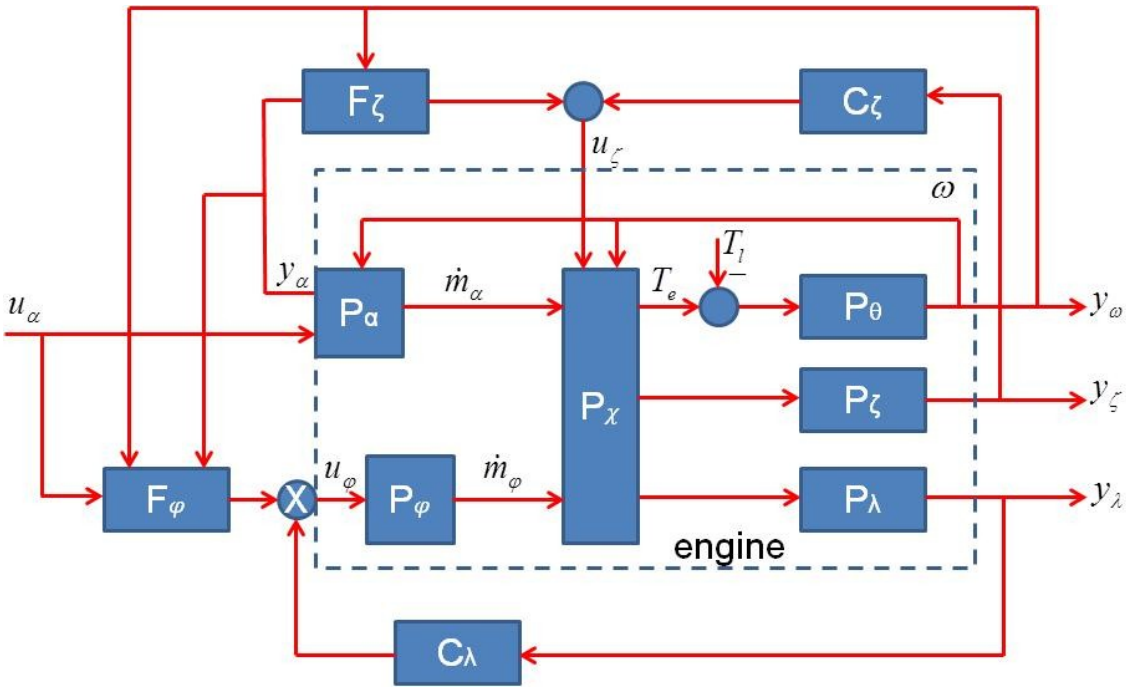

C - feedback controller	φ – fuel	ω - engine speed
F - feed – forward controller	χ – thermodynamics	u - input signal
θ - inertia	λ – air/fuel ratio	y - output signal
α – air	ζ – ignition	T_l - load torque

Fig.1.4. Basic SI engine control substructure

1.3. Main control loops in spark ignition engines (SI engines)

1.3.1. Air/fuel ratio control

The function of the air/fuel ratio control loop is to control the injection timing to get the optimal ratio of air and fuel (mixture) in each working mode of the engine. The purpose of this work is not only to save the fuel, but also to reduce the pollutant emission in exhaust. In modern automotive engines, by using the electronic control systems and appropriate sensors and actuators, the mean value of the air/fuel ratio can be kept within this narrow range. In this control loop, the air/fuel ratio sensor (λ sensor) is a very important component and an accurate fuel injection system also is necessary. This is currently realized using "sequential multiport injectors". Each intake port has its own injector, which injects fuel sequentially, i.e., only when the corresponding intake valves are closed.

Furthermore, the ECU must use appropriate control algorithms. Base on the measured air-path input information from either intake air mass flow rate and intake manifold pressure, or throttle plate angle and engine speed, the fuel-injection feedforward controller F_φ (figure 1.4) will send suitable injection timing to the injectors. Disturbance

occurs while controlling the system is unavoidable. In this case, the air/fuel ratio feedback control system C_λ will compensate the errors in the feedforward loop. While it guarantees the mean value of the air/fuel ratio to be at the stoichiometric level, it cannot prevent transient excursions in the air/fuel ratio.

The pollutant emission of SI engines is a big problem. It must be under the limits imposed by most regulatory boards, and in the future, the emission legislation will require substantial additional reductions of pollutant emission levels. To be satisfied these requirements, the modern engines must be equipped the exhaust gas after-treatment systems to reduce the factors in the exhaust which pollute the environment such as hydrocarbon (HC), carbon monoxide (CO), nitrogen oxide (NO_x), etc.

Until now, in order to reduce the pollutant emission in SI engines, three-way catalytic converter (TWC) is the best choice for this purpose because of its stationary conversion efficiency. A TWC and its conversion efficiency are shown in figure 1.5 [36].

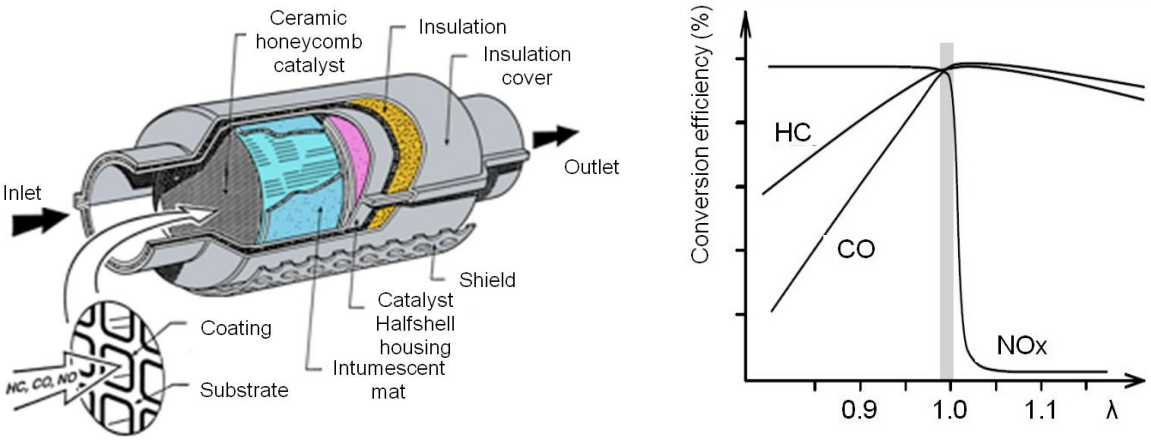

Fig.1.5. TWC and its conversion efficiency (after light-off, stationary behavior)

Three cases can be occurred:

- $\lambda \approx 1$: all three pollutant species present in the exhaust gas be almost completely converted to the innocuous components water and carbon dioxide.
- $\lambda > 1$ (lean mixture): the reduction of nitrogen oxide stops almost completely, because the now abundant free oxygen in the exhaust gas is used to oxidize the unburned hydrocarbon and the carbon monoxide.
- $\lambda < 1$ (rich mixture): the unburned hydrocarbon (HC) and the carbon monoxide (CO) act as agents reducing the nitrogen oxide on the catalyst, thereby causing the desired TWC behavior.

1.3.2. Ignition control loop

To initiate the chemical reaction between fuel and air in the cylinder charge of SI engines, the ignition system is used. The functions of this system for a multicylinder internal combustion engine are:

- To provide a sufficiently energetic spark to initiate the burning of the fuel-air mixture within each cylinder
- To control spark timing for optimum efficiency so that cylinder pressure reaches its maximum value shortly after the piston reaches the top of its compression stroke
- To select the correct cylinder fired.

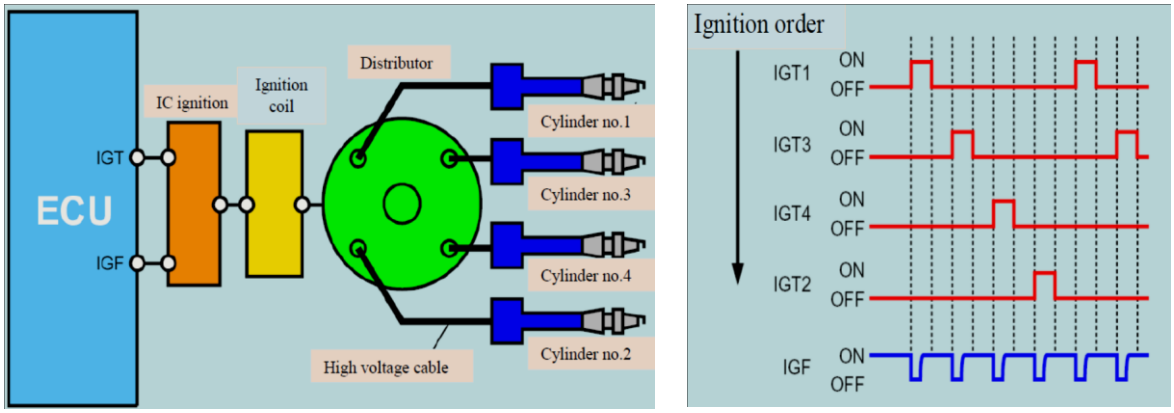

Fig.1.6. Electronic ignition system

Correct ignition timing over the entire engine operating range is very important. It is not only to reduce fuel consumption, emission rates but also can avoid the knock. Combustion within the cylinder can be divided into two phases:

- Inflammation delay (Time Proportional): the pressure and temperature in cylinders do not rise considerably within this time period. The inflammation delay time τ_{id} depends on the temperature, pressure and air-fuel ratio. The delay can be convoluted into an equivalent crankshaft angle which increases with engine speed.
- Combustion (Angle Proportional): The equivalent crankshaft angle for the second phase is almost constant over the entire engine operating range. Induced by the piston movement, turbulences accelerate with engine speed, as well as the combustion process.

If the combustion starts too late because of retarded ignition angles, the emission of hydrocarbons HC will increase. High pressure amplitudes at advanced ignition angles

increase the emission of NO_x. NO_x can be reduced by delaying the ignition at the expense of a higher fuel consumption.

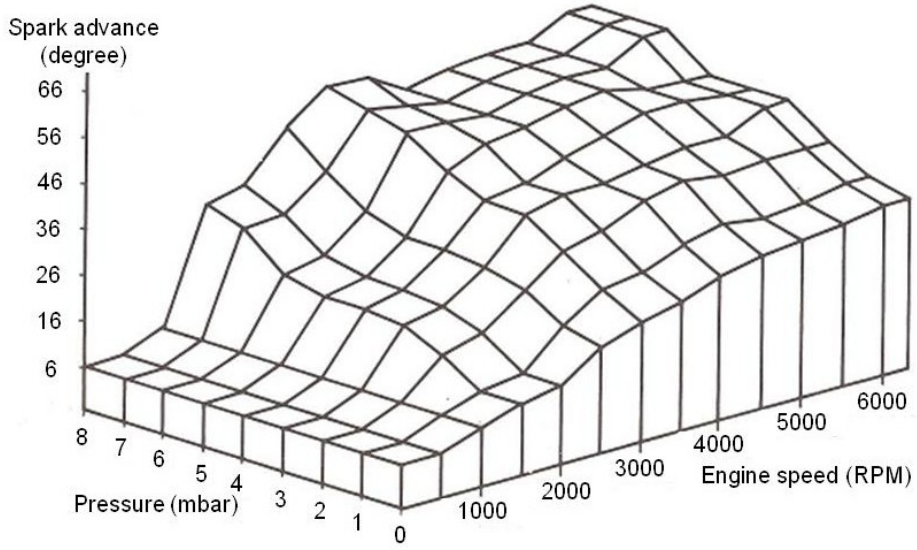

Fig.1.7. An example of ignition map [15]

In figure 1.4, based on the engine speed and load, which measured by manifold pressure sensor and other related signals, the nominal ignition angles will be controlled by the feedforward controller F_ζ. It is not only for realizing maximum brake torque while avoiding knock, but also for inordinate pollution levels of the engine. In order to get the stable and optimal correlation, the engine must be equipped the standard ECU and the ignition data was obtained during the calibration of the ECU. The function of the feedback control system C_ζ is to utilize the output of the knock detection system to adapt the ignition angle to a safe and fuel efficient value despite variations in environmental conditions, fuel quality, etc.

1.3.3. Knock control

Knock occurs when the combustion of the air/fuel mixture in the cylinder starts off correctly in response to ignition by the spark plug, but one or more pockets of A/F mixture explode outside the envelope of the normal combustion front. During a combustion stroke, one part of the air/fuel mixture may self-inflame, before it is reached by the flame front of the spark plug. Knock happens when the peak of the combustion process no longer occurs at the optimum moment for the four-stroke cycle shock wave creates the characteristic metallic "pinging" sound, and cylinder pressure increases dramatically.

The self-inflammation delay τ_{id} is approximated by Woschini [69]:

$$\tau_{id} = 0.44\text{ms}.\exp\left(\frac{4650K}{\vartheta}\right).\left(\frac{P}{P_{amb}}\right)^{-1.19} \quad (1.1)$$

Self-inflammation happens in the compression stroke when piston moves around at the locations within the combustion chamber, which are not so long distant from the spark plug. At that moment, the temperature and pressure in the cylinder are very high and stroke occurs. During the self-inflammation, the piston continues move to the TDC (Top Dead Center). When the piston reaches the position about 15 to 25 degrees before TDC, the spark plug ignites to burn the mixture in the cylinder. In this case, two flame fronts with opposite directions are generated. The result of this problem is the pressure peak in cylinder lower, the temperature of the engine increase, the engine work reduces and so on. The self-inflammation depends on many factors such as compress ratio; fuel quality (octane index of the fuel); geometry of the combustion chamber; engine condition; etc. Because of the knock, the resonances in the cylinder are superimposed to the normal pressure curve. Due to very high pressure gradients knock oscillations can lead to significant engine damages by cavitations. In some dangerous cases, the entire engine may be destroyed in a fraction of a minute.

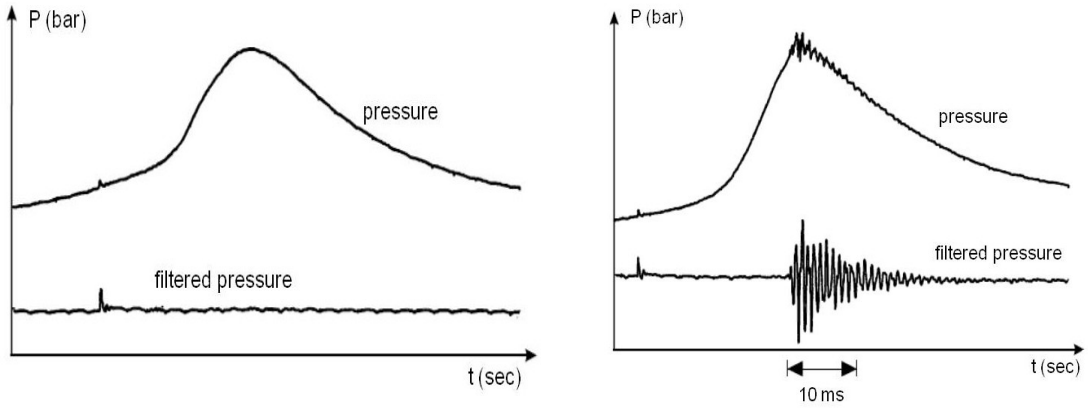

(a) (b)

Fig.1.8. Cylinder pressure output signal for non-knocking (a) and knocking (b) combustion [69]

The knock sometimes occurs at the dynamic engine transients because of mismatches of an ignition angle. In the modern automotive engine, knock control system is equipped to

reduce knock occurrence rate. By using a feed – forward control angle $\alpha_l(n)$, which was being optimized and stored in an adaptive ignition angle map to reduce the response time of the knock control.

Figure 1.7 is the ignition map, which shows the relation between engine rotational with spark advance, respectively. The values of the ignition angle map must therefore be adapted in every individual engine operating point for all cylinders.

As mentioned above, the ignition angle is a function of many factors and can be calculated by the formula [69]:

$$\alpha_e(n) = \alpha_i(n) + \alpha_k(n) + \alpha_l(n) \quad (1.2)$$

where

α_e- effective ignition angle

α_i - open loop ignition angle from fixed map

α_k- knock control ignition angle

α_l- learned ignition angle from adaptive map

n- discrete combustion cycle

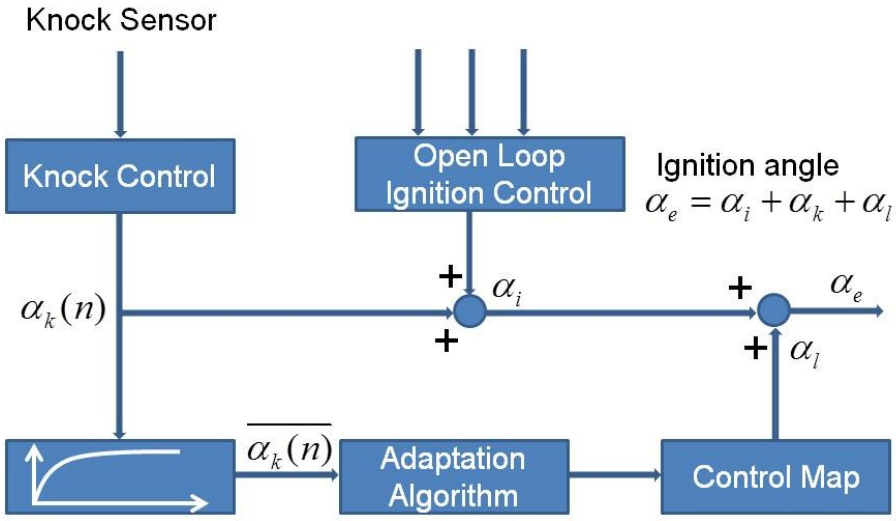

Fig.1.9. Knock control with feed-forward adaptive ignition angle map

1.3.4. Idle speed control system

Modern SI engines have rather low idle speeds of around 700 rpm in order to minimize fuel consumption and pollutant emission. The drawback is that sudden changes in engine torque (electric loads on the alternator, AC compressor, etc.) may stall the engine. A fast and robust idle-speed control-system (ISCS) is therefore mandatory.

The basic structure of a modern ISCS for SI engines is shown in figure 1.10. The engine speed is the main input signal, other engine variables (oil temperature, intake-air pressure and temperature, etc.) are used to compute the reference speed at which the engine should run.

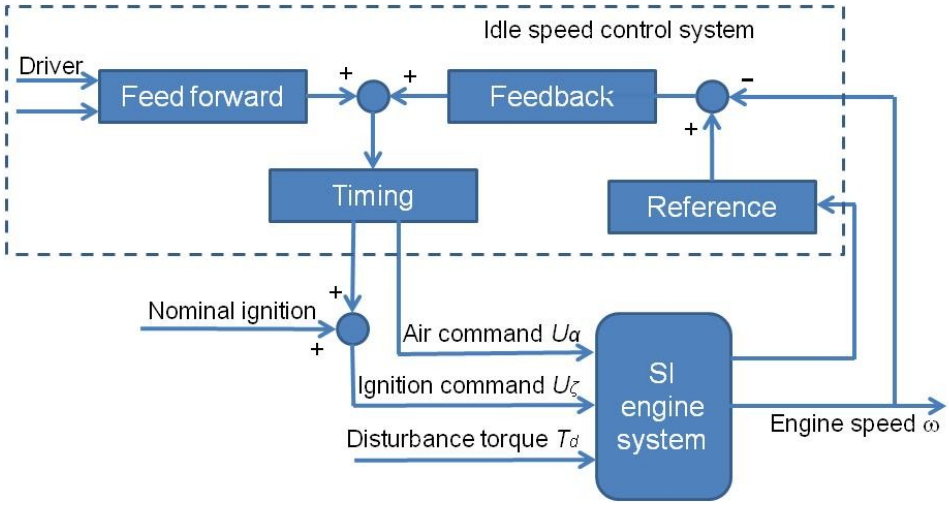

Fig.1.10. Complete ISCS structure

1.4. Diagnostics technology

Diagnostics of engines is a very important field in manufacturing, using and developing the vehicles' engine. From the results of diagnostics, not only the faults of the cars will be found out, but also to fix the problems and develop the engine, as well. In the modern automotive engines, electric and electronic devices are equipped in almost systems. This is the advantage for on-board diagnostics. The actuators and sensors are the components need to be diagnosed. All of these components must be in the allow limit. Further, the values must be consistent with each other.

The general structure of an application including a diagnosis system is shown in Fig.1.11. Inputs to the diagnosis system are the signal $u(t)$ and $y(t)$, which are equal to or a superset of control system signals. The plant is affected by faults and disturbances and the task of diagnosis system is to generate fault decision containing information about at least if a fault has occurred. When it occurred, and the location of the fault, i.e in what component the fault occurred.

With modern automotive engines, we need an integrated diagnostic process that naturally employs data-driven techniques, graph-based dependency models and a mathematical/physical model is necessary for faults diagnosis. An integrated diagnostics (figure 1.12) represents structured, systems engineering approach and the concomitant information-based architecture for maximizing the economic and functional performance of a system by integrating the individual diagnostic elements of design for testability, on-board diagnostics, automatic testing, manual troubleshooting, training, maintaining, technical information, and adaptation.

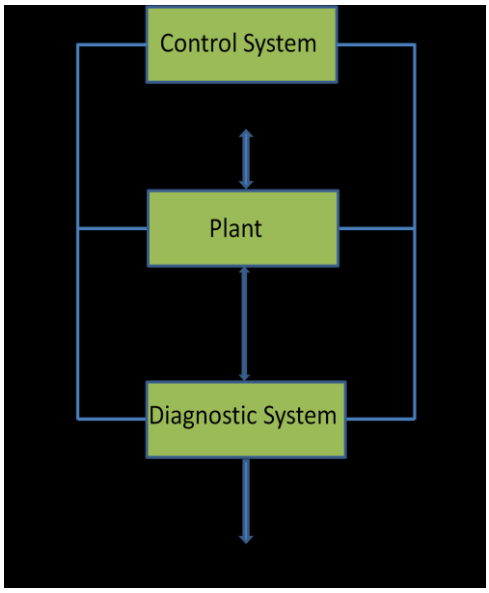

Fig.1.11. General structure of a diagnosis application [69]

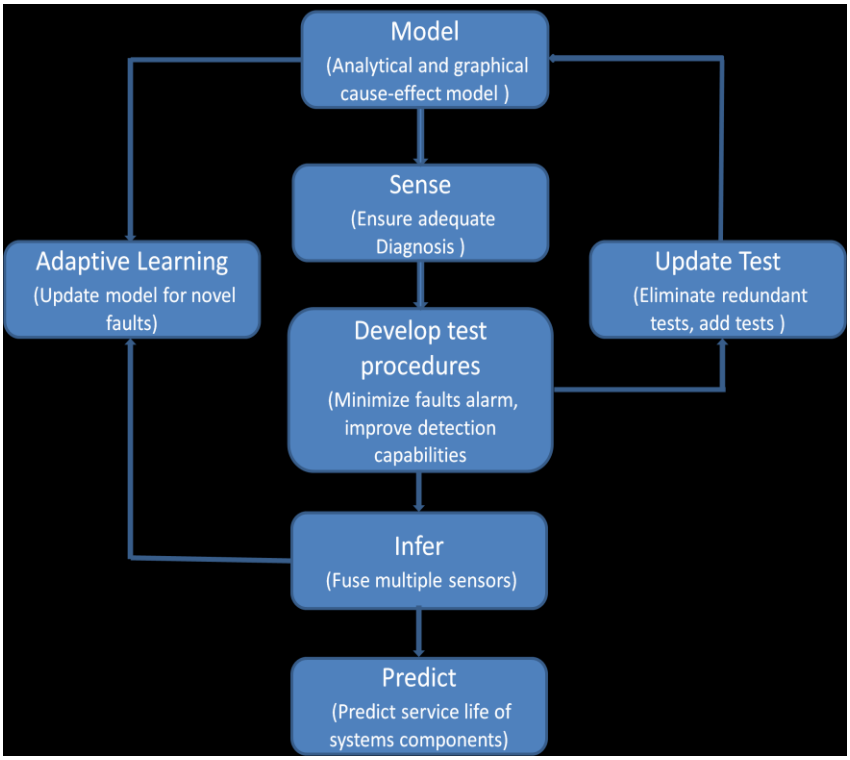

Fig1.12. Integrated diagnostics process [19]

1.5. State of art in the automotive engine simulation

As the development of the automotive engine industry, the roles of fault diagnostic in manufacturing, using and developing become more and more important in order to improve

the quality and reliability of the engine. Many fault diagnostic methods have been found by the scientists such as vibration spectrum analyzing, vibration wavelet theory, instantaneous rotary speed analyzing, lubrication oil iron-microboulde spectrum analyzing, lubrication oil copper-microboulde spectrum analyzing, etc. These methods have some disadvantages and must be conducted when the engine has operated for long time to obtain the accuracy result. The disadvantages of the above methods can be solved by using the model – wise methods. By using the controlling theory, the algorithm models, many systems of the engine are simulated. The simulation results are not only used for developing the engine, but also used for diagnosing the engine.

The angular acceleration signal from crankshaft, which can reflect directly the engine running state, the motive force performance of each cylinder, the spark ignition is one of the most important parameter to diagnose the engine. There are some scientists have been researched and found out the methods to evaluate the crankshaft angular acceleration. In [59], the variation of angular velocity/angular acceleration is calculated by using a crank signal sensor, but they are used for estimating the torque and combustion state. In [43], crank-angle domain investigation of the harmonic oscillations of the crankshaft of a six-cylinder diesel engine to diagnose the engine. The crankshaft angular acceleration of diesel engine is measured by using the high speed micro-controller AVR8535 which has unique function of automatically capturing the rising or falling edge of square wave [49]. The crankshaft acceleration estimation methods are also discussed in [31, 42, 52 & 78]. In [40], the indicate torque of the engine determination based on the engine speed is stated.

Concerning simulation of the engine the first model for Matlab/Simulink was created by Moskwa, J. J.; Hedrick, J. K and Weeks, R. W. [30, 54]. The simulation result of crankshaft acceleration is used for diagnostic engine, but in this case, the engine torque is supposed as the constant. In [1, 16, 17, 18, 21, 27, 36, 46 & 70], the authors concerned about the estimation, calculation as well as simulation many systems of the engine.

Presented in this thesis, the variation of angular acceleration is obtained by modeling the internal combustion engine in Matlab/Simulink, which is extended from the engine model of Weeks, R.W & Moskwa, J.J.. The original model with uniform driving torque will be replaced by the non-uniform driving torque. The simulation results of angular acceleration will be evaluated by using Hilbert transform to diagnose the engine. The driving torque simulations are the useful parameters to determine the spark advance in order to get the maximum brake torque.

2. EXTENDING SI ENGINE MODEL BY MATLAB/SIMULINK

Simulation in generally and simulation automotive engines in particular have a very important role in researching, designing and manufacturing. It saves the time and expense of building hardware or implementing and testing software in real engines. The current trend is toward simulations of larger systems whereas it was earlier considered sufficient with separate simulations of components and subsystems representing a more narrow area of the physical process.

This chapter describes a model engine with a description of the individual subsystems created in the simulation program Matlab/Simulink. The original engine model which was described in [30] will be extended for modern engines. It begins with an overview of the engine and control system model briefly describing the various subsystems. Addition detail is provided for the engine model's intake manifold subsystem before a series of other simulations are examined. These model simulations illustrate how mean torque predictive models can be useful for predicting a number of variables important to the control system engineering and the engine diagnostic.

The engine configuration can be shown schematically in figure 2.1. It is equipped with the mass air flow (MAF) sensor and with the intake manifold pressure (MAP) sensor. The temperature of air in the intake manifold is either measured or estimated.

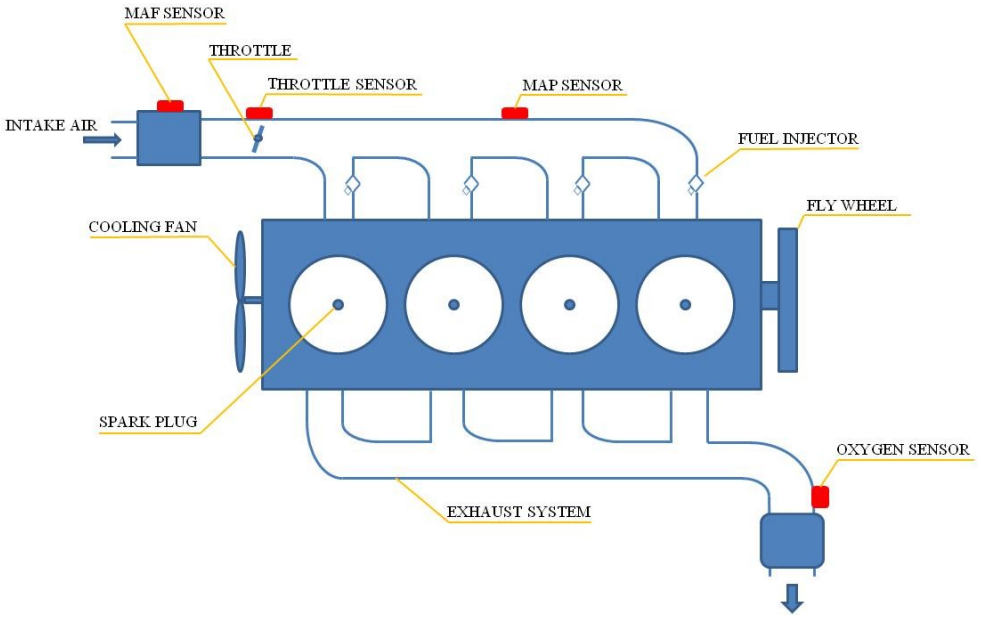

Fig.2.1. Schematic diagram of a spark-ignition engine

In the modern car, an engine, engine sensors, actuators and an ECU (electronic control unit) are the four main parts for building the engine model and its control system. The overall model of an automotive engine can be shown in figure 2.2. Throttle angle; an external load torque such as air conditioning compressor, water pump, coolant fan or transmission; ambient conditions (i.e., temperature and pressure of atmospheric) and actuator signal from various actuators such as fuel injectors, EGR valve, knock sensor, water temperature sensor, spark plug, etc are the inputs to the engine. All the important engine variables are vectored and made available to other subsystems such as sensors, actuators and data analysis.

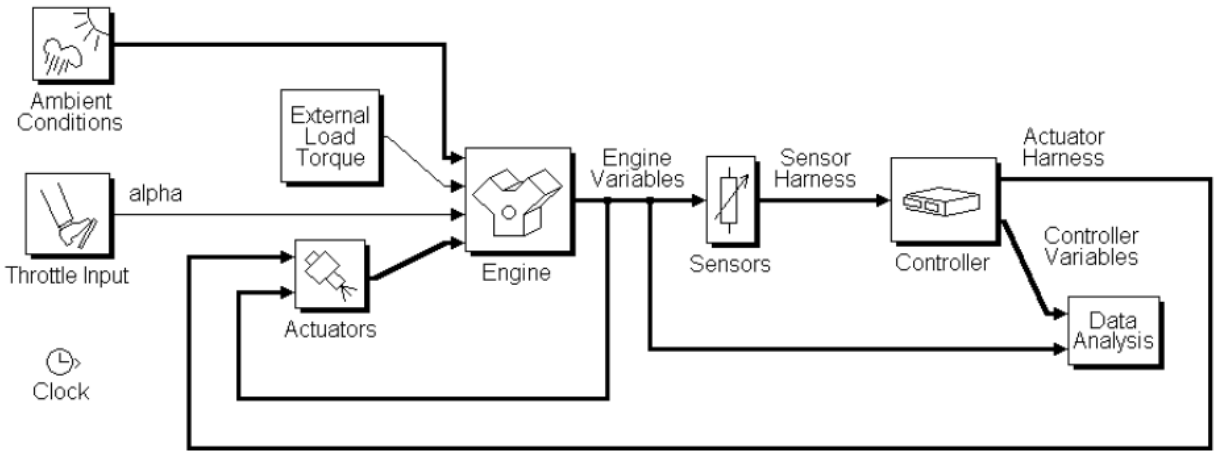

Fig.2.2. Overall simulink model of the engine and control system [54]

2.1. Engine

In internal combustion engines, the quality of the air-to-fuel ratio control depends directly on the accuracy of engine air charge which measured by manifold air flow and manifold air pressure sensors (MAF and MAP sensor). This factor also depends on the torque estimation and hence affects output performance of the engine. Air-to-fuel ratio decides not only the fuel economy, engine power, engine life but also the emission. Good air charge estimation accuracy is therefore necessary to meet ever more aggressive emission and drivability targets. Inaccurate air charge estimation may also negatively affect a fuel economy if the spark timing is not set to the best efficiency at given engine operating conditions. With the introduction of new technologies such as variable valve timing, continuously variable valve lift, cam profile switching, variable geometry intake manifold, cylinder deactivation, boost on demand, etc., a renewed interest is now paid to improving charge estimation algorithms to enable them to handle significant variations in volumetric

efficiency and intake manifold temperature that may occur during transient operation of advanced engines.

The inside of the Engine block (from the figure 2.2) is described more detail in figure 2.3. This structure decouples the strategic decisions from the low-level control tasks. In fact, all demands for engine torque such as engine start – up, idle speed control, engine speed limitation, engine protection, etc are collected and evaluated by the torque demand manager. Then, only one signal from torque demand manager is transferred to the torque conversion manager that issues the appropriate commands to the actuators such that the demanded torque can be realized as best as possible.

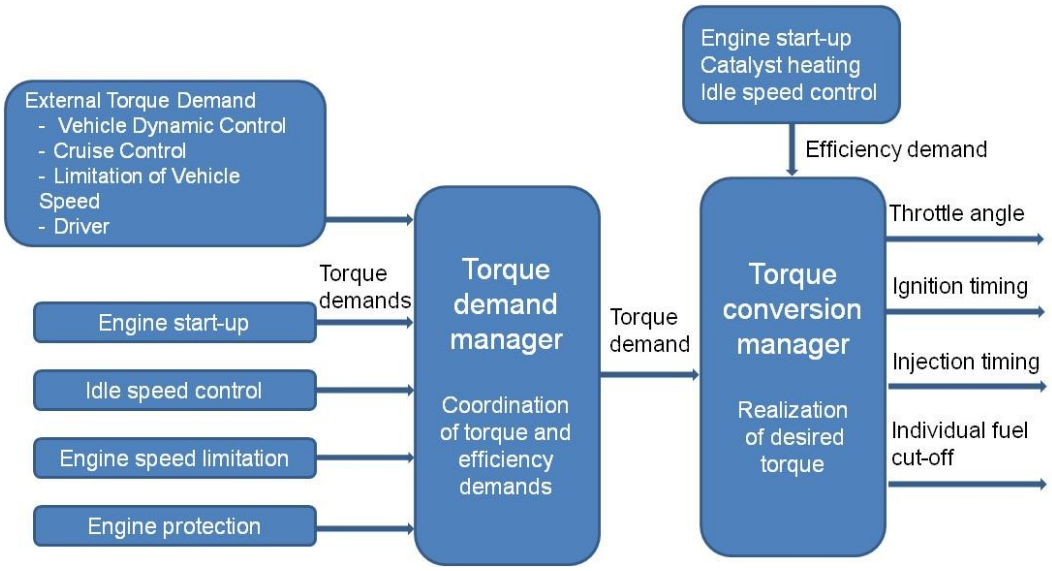

Fig.2.3. Engine torque control structure in a torque – based engine control unit [36]

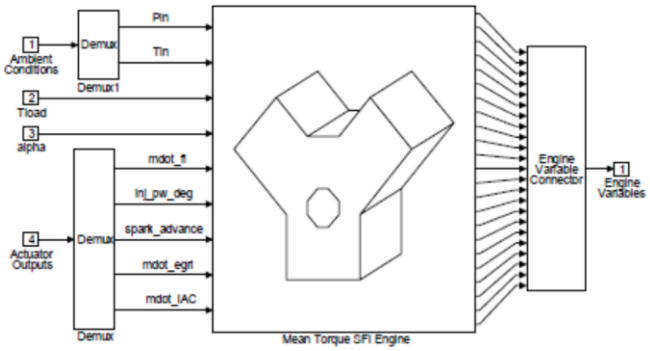

Fig.2.4. Engine block [54]

In order to build the model of the engine, first at all, the subsystem models of main elements in the engine must be created such as: throttle, intake manifold, mass flow rate, compression stroke, torque generation and acceleration, and then they are combined together.

2.1.1. Throttle body model

The first element of the simulation is the throttle body. In fuel injected engines, the throttle body is one of three main parts of the air intake system that controls the amount of air flowing into the engine, in response to driver accelerator pedal input in the main. The throttle body is usually located between the air filter box and the intake manifold, and it is usually attached to, or near the mass airflow sensor.

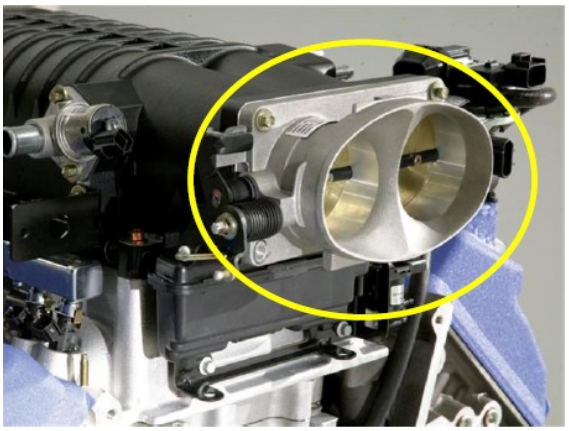

Fig.2.5. Throttle body

With the throttle body, the throttle plate angle and the pressure ratio pass through the device are the main components for modeling. These components will decide the mass airflow out of the throttle body and enter the cylinder $\dot{m}_{al}$. Moreover, $\dot{m}_{al}$ also depends on many other parameters which can be shown in the formula 2.1. In [30], the basis of the throttle body model is the one-dimensional compressible flow equation across an orifice.

$$\dot{m}_{al} = C_d . A_{th} . \frac{P_0}{\sqrt{R.T_0}} \left(\frac{P_t}{P_0}\right)^{\frac{1}{k}} \sqrt{\frac{2.k}{k-1}\left[1 - \left(\frac{P_t}{P_0}\right)^{\frac{k-1}{k}}\right]} \tag{2.1}$$

Airflow through the throttle plate depends on the minimum pressure in throttle body P_t and the pre-throttle body stagnation pressure P_0. The ratio between two parameters must be less or equal to $\left(\frac{2.k}{k-1}\right)^{\frac{k}{k-1}}$:

$$\frac{P_t}{P_0} \leq \left(\frac{2.k}{k-1}\right)^{\frac{k}{k-1}} \tag{2.2}$$

Substituting (2.2) to (2.1), we obtain:

$$\dot{m}_{al} = C_d . A_{th} . \frac{P_0}{\sqrt{R.T_0}} \sqrt{k} . \left(\frac{2}{k-1}\right)^{\frac{k+1}{2.(k-1)}} \tag{2.3}$$

If it is assumed that in the minimum area behind the throttle body, the difference of the intake air pressure is so small and can be omitted, then:

$$P_t \approx P_m \approx P$$

It is also assumed that the discharge coefficient C_d does not have any cross coupled terms between throttle area and pressure ratio. In this case, the discharge coefficient can be spitted into two uncoupled coefficients C_{d1} and C_{d2}, and the mass flow relation can be written as:

$$\dot{m}_{al} = (C_{d1} . A_{th}) . \left\{ C_{d2} . \frac{P_0}{\sqrt{R.T_0}} \left(\frac{P}{P_0}\right)^{\frac{1}{k}} \sqrt{\frac{2.k}{k-1}\left[1 - \left(\frac{P}{P_0}\right)^{\frac{k-1}{k}}\right]} \right\} \tag{2.4}$$

The equation 2.4 can be rewrite in the simple way as the follow equation:

$$\dot{m}_{al} = \text{MA.TC.PRI} \tag{2.5}$$

where:

- MA is the maximum mass air flow through the throttle body.

- TC is the throttle characteristic:

$$\text{TC} = \frac{C_{d1}(\alpha) . A_{th}(\alpha)}{C_{d1}(\alpha_{max}) . A_{th}(\alpha_{max})} \tag{2.6}$$

Normally, the throttle plate is of elliptical shape, so the cross-sectional flow area of throttle body A_{th} can be calculated as:

$$A_{th} = \frac{d.D}{2} . \sqrt{1 - \left(\frac{d.\cos(\alpha_0)}{D.\cos(\alpha_0 + \alpha)}\right)^2} - \frac{d.D}{2} \sqrt{\left(1 - \left(\frac{d}{D}\right)^2\right)}$$
$$+ \frac{D^2}{2} . \frac{1}{\sin \sqrt{\left(1 - \left(\frac{d}{D}\right)^2\right)}} - \frac{D^2.\cos(\alpha_0 + \alpha)}{2.\cos(\alpha_0)} . \frac{1}{\sin \sqrt{1 - \left(\frac{d.\cos(\alpha_0)}{D.\cos(\alpha_0 + \alpha)}\right)^2}} \tag{2.7}$$

In industrial manufacture, the term $cos\alpha_0^*$ is usually used instead of $cos\alpha_0$, where:

$$\cos\alpha_0^* = \cos\left(0{,}91.\alpha_0 - 2{,}59\right)$$

for α_0 measured in degrees.

- The third parameter PRI is given by:

$$PRI = \begin{cases} \dfrac{C_{d2}\left(\dfrac{P}{P_0}\right)}{C_{d2}(0)} \cdot \left(\dfrac{P}{P_0}\right)^{\frac{1}{k}} \cdot \left(\dfrac{2}{k+1}\right)^{\frac{k+1}{2.(1-k)}} \cdot \sqrt{\dfrac{2.k}{k-1}\left[1 - \left(\dfrac{P}{P_0}\right)^{\frac{k-1}{k}}\right]}, & \dfrac{P}{P_0} > \left(\dfrac{2}{k+1}\right)^{\frac{k+1}{(1-k)}} \\ \dfrac{C_{d2}\left(\dfrac{P}{P_0}\right)}{C_{d2}(0)}, & \dfrac{P}{P_0} \le \left(\dfrac{2}{k+1}\right)^{\frac{k+1}{(1-k)}} \end{cases} \tag{2.8}$$

By using data from the actual engine, α, $\frac{P}{P_0}$, and $\dot{m}_{al}$ can be measured, so that the discharge coefficient C_d can be calculated. Since, the cross-coupling of C_{d1} and C_{d2} and the validity of the no coupling assumption can be evaluated. Preliminary validation results indicate that there is a very little cross-coupling of C_{d1} and C_{d2}.

For further simplification in building the throttle body model, we assumed that the control input is the angle of the throttle plate. It means that, the air into the intake manifold is the product of two functions: the first function is the throttle plate angle and the second function is the atmospheric and manifold pressures. In case, if the pressure in the manifold is low (great vacuum), the mass flow rate through the throttle body increases and it only depends on the plate angle. The throttle body model for this low pressure behavior with a switching condition can be built based on the equations 2.10.

Based on published results in [85], mass flow rate into manifold (g/s) can be determined by equation:

$$\dot{m}_{al} = \mathrm{f}(\alpha)\mathrm{g}(P_m) \tag{2.9}$$

where, α is throttle angle (degree) and

$$\mathrm{f}(\alpha) = 2.821 - 0.05231\alpha + 0.10299\alpha^2 - 0.00063\alpha^3 \tag{2.10}$$

$$g(P_m) = \begin{cases} 1 & P_m \le \frac{P_{amb}}{2} \\ \frac{2}{P_{amb}}\sqrt{P_m P_{amb} - P_m^2} & \frac{P_{amb}}{2} < P_m < P_{amb} \\ -\frac{2}{P_{amb}}\sqrt{P_m P_{amb} - P_m^2} & P_{amb} < P_m < 2P_{amb} \\ -1 & P_m \ge 2P_{amb} \end{cases} \quad (2.11)$$

Here: P_m- manifold pressure (bar)

P_{amb}- ambient (atmospheric) pressure (bar)

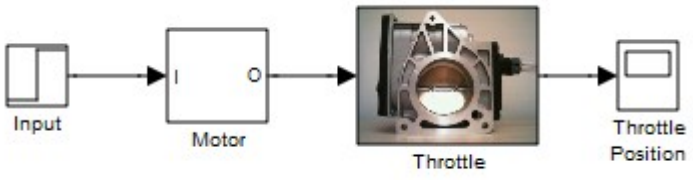

Fig.2.6. Throttle model

2.1.2. Intake manifold model

The intake manifold is one part of the air intake system of the engine. It includes the air box, air filter and mass air flow sensor. The role of the intake manifold is very important in the dynamic response of engine torque to distribute the necessary air for the cylinders to operate in the direct-injection engines. With the indirect-injection engines, the intake manifold allocates the air/fuel mixture throughout the combustion chambers in the engine. The shape and internal diameter of the intake manifold determines the rate and direction of the air or air/fuel mixture. In order to keep the pressure in the intake manifold always stable when the flow of air into each cylinder is unsteady, in this system is equipped a plenum which acts as accumulator. There are runners which connect the plenum with the cylinder head. Not only distribute air for the cylinders, the intake manifold is also used to mix air with small amount of exhaust to decrease NO_x emissions by using exhaust gas recirculation EGR. The introduction of EGR into the manifold can alter the intake manifold output and affect engine torque production.

As the function of the intake manifold, its model must determine the mass air flow out of the intake manifold and into the cylinder for fuel calculation.

Mass air flow out of intake manifold $\dot{m}_{ao}$ and mass flow of EGR out of intake manifold $\dot{m}_{egro}$ can be calculated as equations in [30]:

$$\dot{m}_{ao} = \dot{m}_{al} + \frac{P_a.V_m.M}{R.T^2}.\dot{T} - \frac{V_m.M}{R.T}.\dot{P}_a \tag{2.12}$$

$$\dot{m}_{egro} = \dot{m}_{egrl} + \frac{(P_m - P_a).V_m.M_{egr}}{R.T^2}.\dot{T} - \frac{V_m.M_{egr}}{R.T}.(P_m - P_a) \tag{2.13}$$

Combining two equations (2.12) and (2.13) with the volumetric efficiency relation then reduce, we obtain:

$$\dot{m}_{ao} = \frac{K.V_m.\dot{\theta}.\eta_v}{R.T}.\left[(M_a - M_{egr}).P_a + M_{egr}.P_m\right] - \dot{m}_{egro} \tag{2.14}$$

Differential equation in the partial pressure of air, the result will be:

$$\begin{aligned}\left(1 - \frac{M_{egr}}{M_a}\right).\frac{dP_a}{dt} &= \left[\left(1 - \frac{M_{egr}}{M_a}\right).\left(\frac{\dot{T}}{T} - K.\dot{\theta}.\eta_v\right)\right].P_a \\ -K.\eta_v.\frac{M_{egr}}{M_a}.\dot{\theta}.P_a &+ \frac{R.T}{M_a.V_m}\left(\dot{m}_{al} + \dot{m}_{egrl}\right) + \frac{M_{egr}}{M_a}.\left(\frac{P_m}{T}.\dot{T} - \dot{P}_m\right)\end{aligned} \tag{2.15}$$

From (2.15), it is easy to see that this equation depends on the ratio of molecular weights of air and EGR. The value of M_{egr} and M_a can be calculated from the chemical reactions:

$$C_7H_{13,16} + 10{,}29(O_2 + 3{,}773N_2) = 7CO_2 + 6{,}58H_2O + 38{,}82N_2 \tag{2.16}$$

Solving it, we obtain:

$$\begin{aligned}M_a &= \frac{\sum_{\text{air}} n_i M_i}{\sum_{\text{air}} n_i} = 28{,}838 \text{ g/mole} \\ M_{egr} &= \frac{\sum_{\text{products}} n_i M_i}{\sum_{\text{products}} n_i} = 28{,}884 \text{ g/mole}\end{aligned} \tag{2.17}$$

Consider the consequence of the complete mixing assumption:

$$\frac{\dot{m}_{egro}}{\dot{m}_{ao}} = \left(\frac{P_m - P_a}{P_a}\right).\left(\frac{M_{egr}}{M_a}\right) \tag{2.18}$$

Combining equations (2.12), (2.13), and (2.18) yields the differential equation in P_a:

$$\frac{dP_a}{dt} = \left[\frac{\dot{P}_m}{P_m} - \frac{R.T}{P_m.V_m.M}.(\dot{m}_{al} + \dot{m}_{egrl})\right].P_a + \frac{R.T}{V_m.M}.\dot{m}_{al} \quad (2.19)$$

The manifold pressure P_a can be esstimated:

$$\frac{dP_m}{dt} = \left(\frac{\dot{T}}{T} - K.\dot{\theta}.\eta_v\right).P_m + \frac{R.T}{V_m.M}.(\dot{m}_{al} + \dot{m}_{egrl}) \quad (2.20)$$

Volumetric efficiency η_v can be calculated as:

$$\eta_v = \frac{R.T}{V_m.M.K.\dot{\theta}.P_m}(\dot{m}_{al} + \dot{m}_{egrl}) + \frac{1}{K.\dot{\theta}}\left(\frac{\dot{T}}{T} - \frac{\dot{P}_m}{P_m}\right) \quad (1.21)$$

$$= \eta_v|_{\text{steady-state}} + \eta_v|_{\text{transient}}$$

The estimation of $\dot{m}_{ao}$ is very important to caculate the amount of fuel inject to the cylinder. The mass air flow through the intake valve of each cylinder can be summarized in the figure 2.7. In this case, the intake valve of the second cylinder is presented.

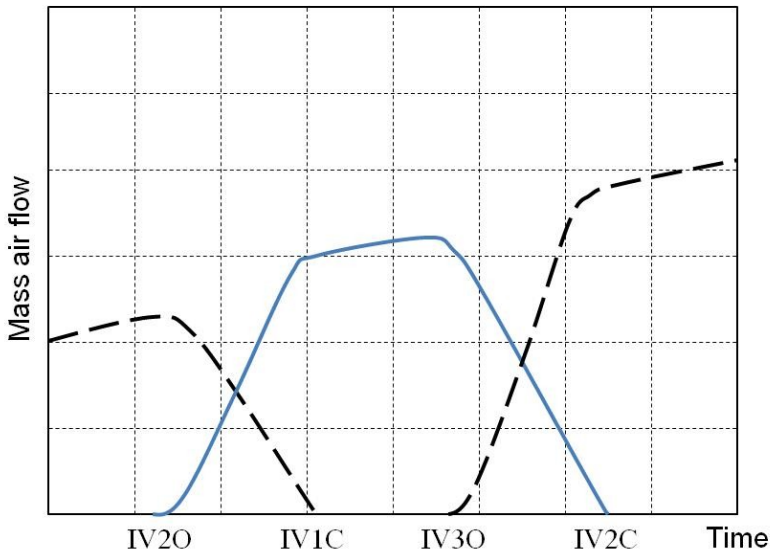

Fig.2.7 Idealized Air Flows

The figure 2.7 can be explained simply as follow: when the intake valve number 2 opens (IV2O), the intake flow starts enter the cylinder. Air flow increases gradually as a sinusoid function until it reaches rate a magnitude of $\dot{m}_{ao}$, at the same time, the previous intake valve closes (IV1C). The flow keeps the value around $\dot{m}_{ao}$ until the next intake valve opens (IV3O), then decreases as a sinusoid to zero when the intake valve closes (IV2C).

In order to build the model of the intake manifold, applying the equations above will be very hard because many parameters need to be determined. In this case, for further simplification, we assumed that the simulation model of the intake manifold is a differential equation of the manifold pressure. Then, the net rate of change of air mass is a function of time and depends on the difference between the incoming and outgoing mass flow rates in the intake manifold. This quantity, according to the ideal gas law, is proportional to the time derivative of the manifold pressure [84]. This model doesn't incorporate exhaust gas recirculation (EGR).

$$\dot{P}_m = \frac{RT}{V_m}(\dot{m}_{al} - \dot{m}_{ao}) \tag{2.22}$$

where, R - specific gas constant

T - temperature (^{0}K)

V_m - manifold volume (m^3)

$\dot{m}_{ao}$ - mass rate of air leaving the manifold and entering the combustion chamber (g/s)

$$\dot{m}_{ao} = -0.366 + 0.08979\dot{\theta}P_m - 0.0337\dot{\theta}P_m^2 + 0.0001\dot{\theta}^2P_m \tag{2.23}$$

$\dot{\theta}$ - engine speed (rad/s)

$\dot{m}_{al}$ - mass rate of air entering the manifold (g/s)

It is convenient to use the pressure ratio $\frac{P_m}{P_{amb}}$ as a state variable. The pressure ratio $\frac{P_m}{P_{amb}}$ in the intake manifold changes according to the following equation:

$$\frac{\dot{P_m}}{P_{amb}} = k_1(\dot{m}_{al} - \dot{m}_{ao}) \tag{2.24}$$

where

$$k_1 = \frac{T}{V_m T_0 \rho_0}$$

where ρ_0 is the atmospheric density and T_0 is the corresponding ambient temperature. The value of these factors can be chosen: $\rho_0 = 1.2\text{kg/m}^3$, $T_0 = 288^0$K.

Simulink models of throttle flow with valve angle and pressure and vacuum in the intake manifold are shown in figure 2.8 and figure 2.9, respectively. Throttle angle,

manifold pressure and ambient pressure are three inputs of the throttle flow model. The equation 2.10 is applied as function blocks to build model in simulink. Notice that, the throttle valve behaves in a nonlinear manner. The simulation results show the properties of a nonlinear equation with several variables. If the equation 2.10 is set to 0.5, by comparing the pressure ratio to its switch threshold, the switch block can determine whether the flowrate is sonic or not. In the sonic range, the flow rate is a function of the throttle position only.

Intake manifold pressure is a directly related to the engine load. It also demonstrates the engine condition and affects the volumetric efficiency, fuel consumption and performance of internal combustion engines. Manifold pressure is computed by the differential equation as described in equation 2.22. A Simulink function block also computes the mass flow rate into the cylinder, a function of manifold pressure and engine speed (Equation 2.23).

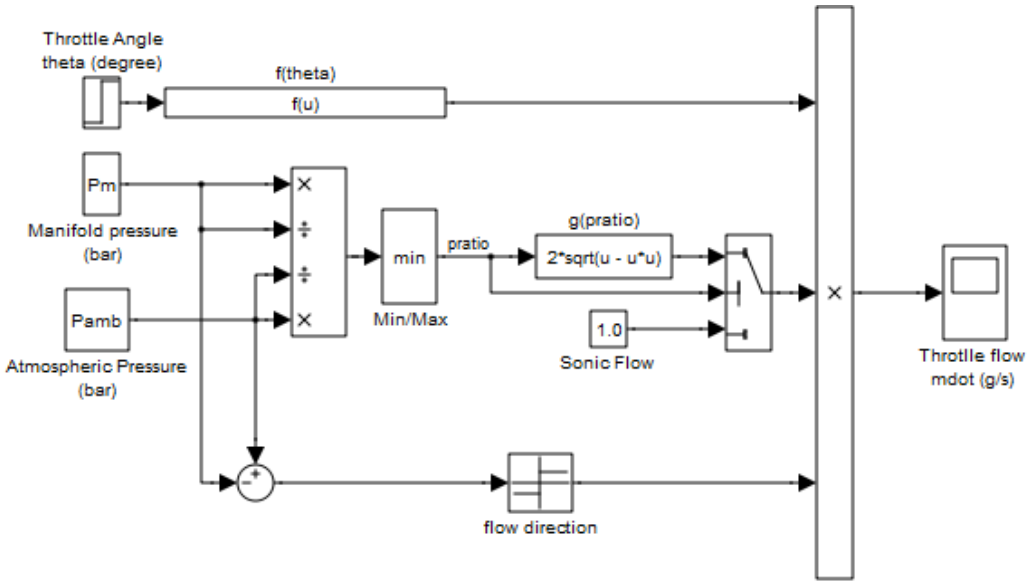

Fig.2.8. Throttle flow with valve angle and pressure

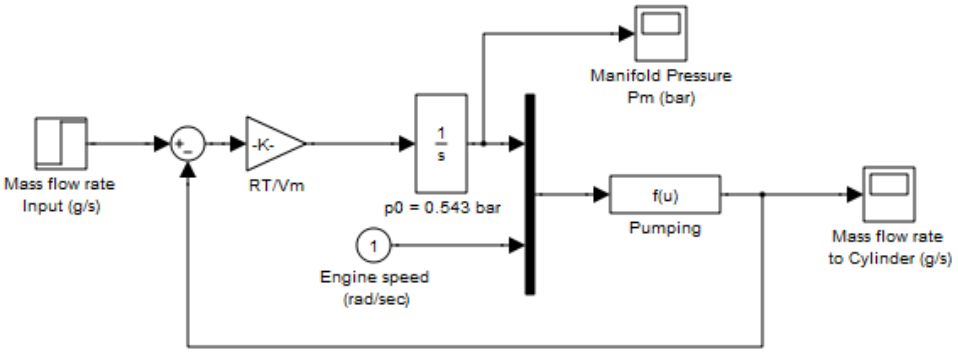

Fig.2.9. Mass flow rate into cylinder model

2.1.3. Intake system model

Before entering the cylinder for combustion, the air mass flow is accumulated in the intake block known as an integrator. The pulses issued from valve timing block which correspond to specific rotational positions are the important signals in order to calculate the intake and compression timing. Depending on the type of engine or manufacturer, the pulse is generated in each rotation of the camshaft, or every 180^0 of the crankshaft rotation. Each event shows a single implementation of the compression subsystem. Parameters of intake integrator are reset by using feedback signals from the trigger block within the compression subsystem. The signal from integrator will be processed immediately by the compression block before being reset, while triggers conceptually occur at the same instant of time. In order to present the delay between the intake and combustion of each air charge, a unit delay block is added into the compression subsystem. The value of the unit delay block is set by one event period of crankshaft rotation 180^0.

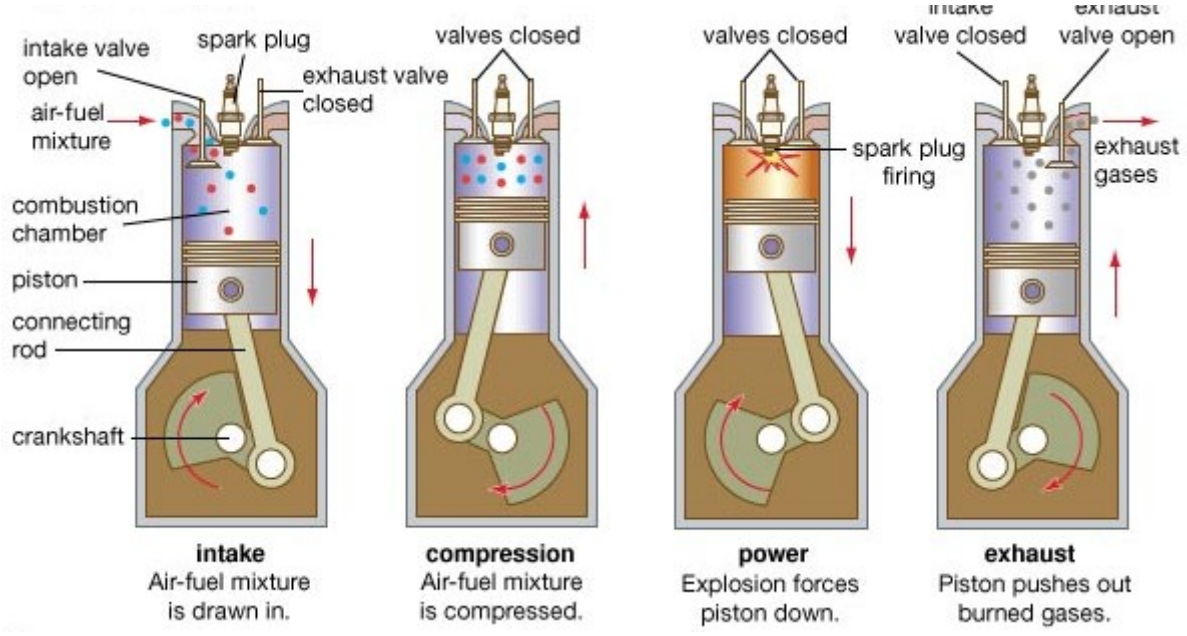

Fig.2.10. Four-stroke internal combustion engine [83]

In four-stroke internal combustion engines, the intake, compression, combustion and exhaust stroke complete in 720^0 or two complete revolutions of crankshaft. Now, we consider a complete four-stroke cycle for one cylinder as figure 2.10. When the piston moves from TDC (top dead center) to BDC (bottom dead center) in the intake stroke, the intake valves open for mixture of air and fuel enter the cylinder. In the intake manifold model, the mass flow rate from the manifold is integrated from the intake block. After rotation 180^0 of the crankshaft, when piston moves from BDC to TDC in compression

stroke, the intake valve closes and the unit delay block in the compression subsystem samples the integrator state. This value, the accumulated mass charge, is available at the output of the compression subsystem 180^0 later for using in combustion. During the combustion stroke, because the pressure in cylinder is very high, this pressure acts on the top of piston with a great force make the piston moves from TDC to BDC and the crankshaft accelerates due to the generated torque. The final 180^0, the exhaust stroke (piston moves from BDC to TDC), ends with a reset of the intake integrator, prepared for the next complete 720^0 cycle of this particular cylinder.

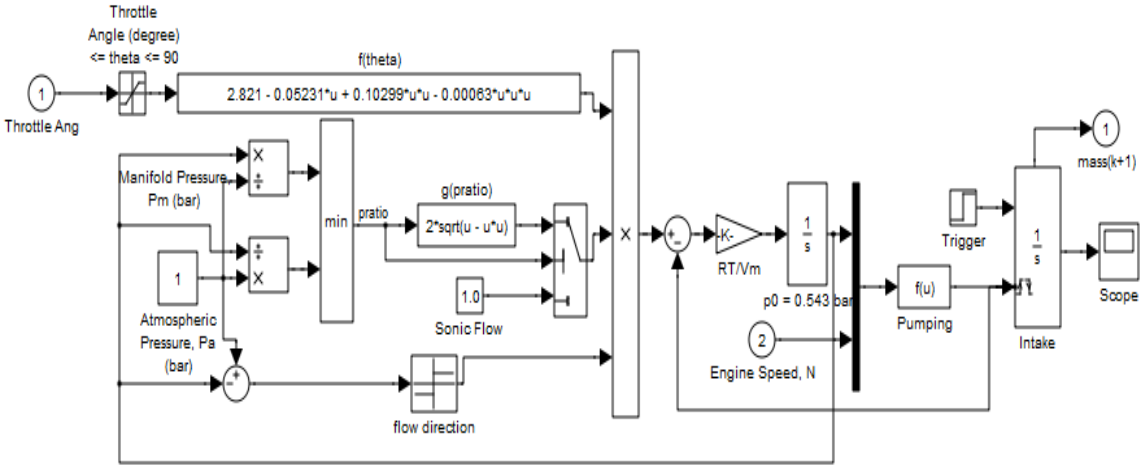

Fig.2.11. Intake manifold model

2.1.4. Torque generation model

To build the engine torque generation and acceleration model, the estimation function of the engine torque is very important. It is based on monitoring of the cylinder individual fluctuations of the high resolution engine speed signal. The engine speed signal is based on the measurements of a passage time between two subsequent teeth on a flywheel. The passage time decreases as the rotational speed increases thus the time interval errors increase. Moreover, low frequency oscillations from the powertrain and high frequency oscillations due to the crankshaft torsion, together with vibrations induced by the road, act as disturbances on the crankshaft . These disturbances influence directly the performance of the engine speed signal and consequently the torque monitoring function.

The engine torque of the internal combustion engine depends on many parameters. The effective parameters can be reflected through indicate torque T_{ind}, friction torque T_f, disturbance torque T_d and pump torque T_p. All of these torques are modeled as the rotational dynamics of the engine:

$$T_e = J_{crank}\ddot{\theta} = T_{ind} - T_f - T_d - T_p \quad (2.25)$$

❖ Indicated engine torque:

The indicated engine torque or torque due to combustion is the torque which generated in cylinder in the combustion stroke. Pressure in the cylinder increases because of the mixture burning and generates a force acts on the piston. The force creates an oscillating motion of the piston through the connecting rod and a rotating motion of the crankshaft, i.e… Hence, the relation between indicated torque and cylinder pressure is very close.

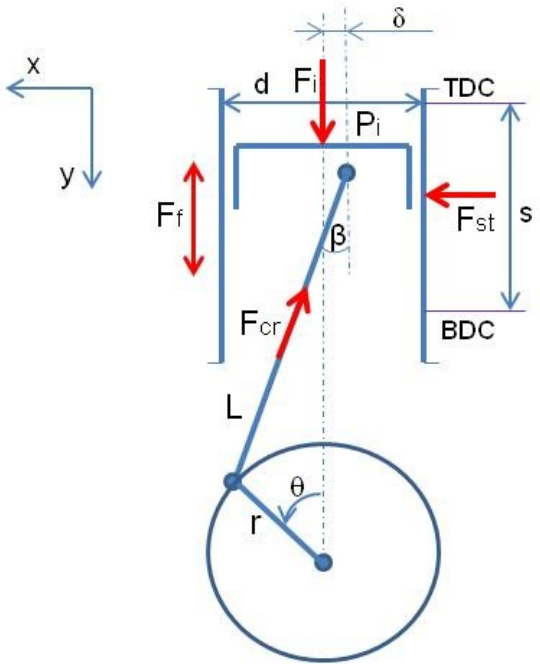

Fig 2.12. Forces and acceleration of the piston-crankshaft mechanism

In [1], the indicated torque is a function of many parameters and can be shown in the formula (2.26).

$$T_{ind} = a_1 \frac{\dot{m}_{ao}(t - t_d)}{\dot{\theta}(t - t_d)} a_{fi}(t - t_d) f_s(t - t_s) \quad (2.26)$$

where

$a_1 = 8{,}51.10^5 \mathrm{Nm/kg/rad}$: the maximum torque capacity

$a_{fi}(t - t_d)$: normalized air to fuel influence, $a_{fi}(t - t_d) = 1$

$f_s(t - t_s)$: a function of spark influence

t_d : intake to torque production delay: $t_d = \frac{5{,}48}{\dot{\theta}}$

t_s : spark to torque production delay: $t_s = \frac{1{,}3}{\dot{\theta}}$

The mass flow rate $\dot{m}_{ao}$ entering the combustion chamber satisfies the following equation which comes from the speed density calculation:

$$\dot{m}_{ao} = k\dot{\theta}\frac{P_m}{P_{amb}} \tag{2.27}$$

where

$$k = \frac{\rho_0 T_0 V_{1cyl}\eta_v . z}{4\pi T} \tag{2.28}$$

η_v is a volumetric efficiency (for simplicity the constant value of efficiency is taken i.e., $\eta_v = 0{,}8$).

V_{1cyl} is the volume of one cylinder (m^3) and z is the number of cylinders.

Substituting (2.27) into (2.26), we obtain:

$$T_{ind} = a_1 k\frac{P_m(t - t_d)}{P_{amb}} f_s(t - t_s) \tag{2.29}$$

From the equation 2.29, it is so easy to recognize that indicated torque depends on not only the pressure in the cylinder as mentioned above, but it also depends on many other factors. Spark advance, which affects directly to emission, partial burns, misfires, hence then the indicated torque, is a function of engine speed. At low engine speeds, the minimum spark advance for the best torque (MBT) is around 20 degrees before top dead center and it is possible to retard spark up to 10 degrees after top dead center. Figure 2.13 shows the spark advance according to engine speed.

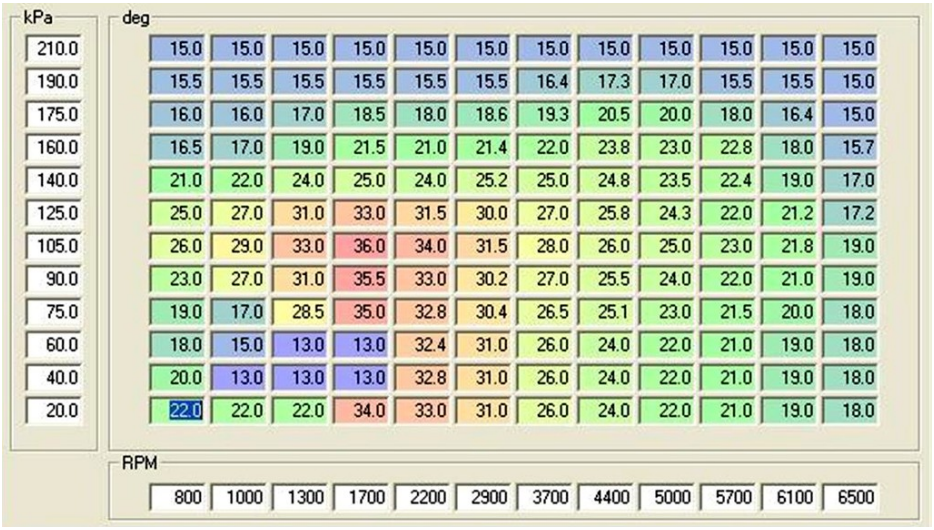

Fig.2.13. Spark advance table [80]

The spark influence can be calculated as the equation [86]:

$$f_s = [\cos(-b + u_2)]^{2,875} \tag{2.30}$$

where b is the position of OY axis from MBT, measured in radians, and u_2 is our control. The distance b can be fixed or adjusted within the interval [0, 15^0], thereby control action u_2 varies within the interval $[-b \;\; b]$. If b is fixed and $u_2 = 0$ then spark is retarded still from MBT.

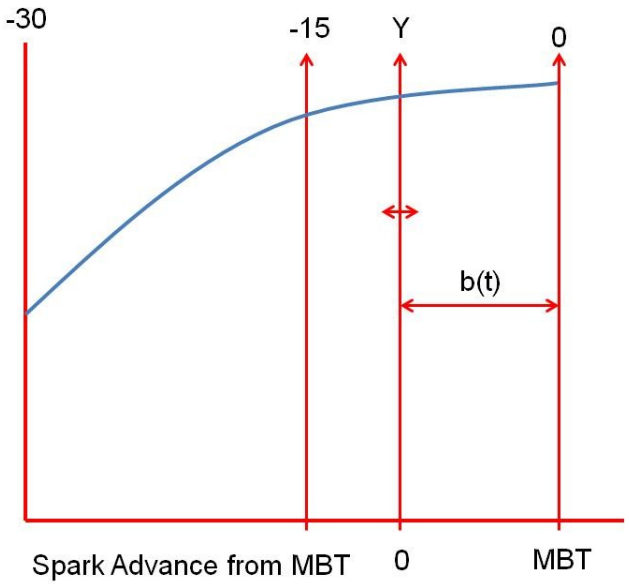

Fig.2.14. Spark advance from MBT

❖ Engine Friction Torque T_f:

In the internal combustion engine, the friction torque terms are subtracted from the

instantaneous indicated torque value to produce the brake torque at the crankshaft. It includes piston ring assembly, bearing, valve train, pumping losses and pumps.

The piston ring assembly friction torque may be responsible for 50 – 75 per cent of the entire engine friction. The components that contribute to friction are: compression rings, oil control ring, piston skirt and piston pin. The forces acting on the piston assembly include static ring tension, the gas pressure force and the inertia force.

Bearings friction contributions come from the journal bearings and their associated seals. Journal bearings are usually designed to provide the minimum film thickness of about 2 μm. The journal bearings operate under hydro-dynamic lubrication, which means a large load can be carried the journal bearing with low energy losses under normal operating conditions.

The valve train carries high load over the entire speed range of the engine. Loads acting on the valve train at lower speeds are due primarily to the spring forces, while at higher speeds the inertia forces of the component masses dominate.

Pumping losses torque is summation of the valve flow, which corresponds mainly to pressure losses in the inlet and exhaust valves and the restrictions outside the cylinder, in the inlet and exhaust systems, the air filter and intake manifold on the inlet side and the exhaust manifold, muffler and tail pipe on the exhaust side.

Pump friction torque are employed to circulate the oil, water and fuel.

Engine friction torque T_f can be calculated as the simple formula [1]:

$$T_f = \left(a_{1f} + \dot{\theta} a_{2f} + \dot{\theta}^2 a_{3f}\right) \frac{V_{1cyl}.1000.z}{4\pi} \tag{2.31}$$

where: $a_{1f} = 97[\frac{\mathrm{N}}{\mathrm{m}^2}], a_{2f} = 0{,}1432[\frac{\mathrm{N}}{\mathrm{m}^2}\frac{\mathrm{s}}{\mathrm{rad}}],\ a_{3f} = 2{,}74.10^{-4}[\frac{\mathrm{N}}{\mathrm{m}^2}\frac{\mathrm{s}^2}{\mathrm{rad}^2}]$

❖ Engine Pump Torque T_p

$$T_p = (P_{amb} - P_m) \frac{V_{1cyl}.z}{4\pi} \tag{2.32}$$

❖ Engine Disturbance Torque T_d [1]:

The value of T_d can be presented, for the idle control problem, by a class of bounded functions with bounded derivatives, i.e.

$$|T_d(t)| \le c, \qquad |\dot{T}_d(t)| \le c_1 \tag{2.33}$$

where c and c_1 are positive constants. Typical value for c is $20Nm$.

Substituting (2.29), (2.31), (2.32) and (2.33) to (2.25), we obtain:

$$J_{crank}\ddot{\theta} = a_1 k \frac{P_m(t-t_d)}{P_{amb}} f_s(t-t_s) - \left(a_{1f} + \dot{\theta}a_{2f} + \dot{\theta}^2 a_{3f}\right)\frac{V_{1cyl}.1000.z}{4\pi} - (P_{amb} - P_m)\frac{V_{1cyl}.z}{4\pi} - 20 \tag{2.34}$$

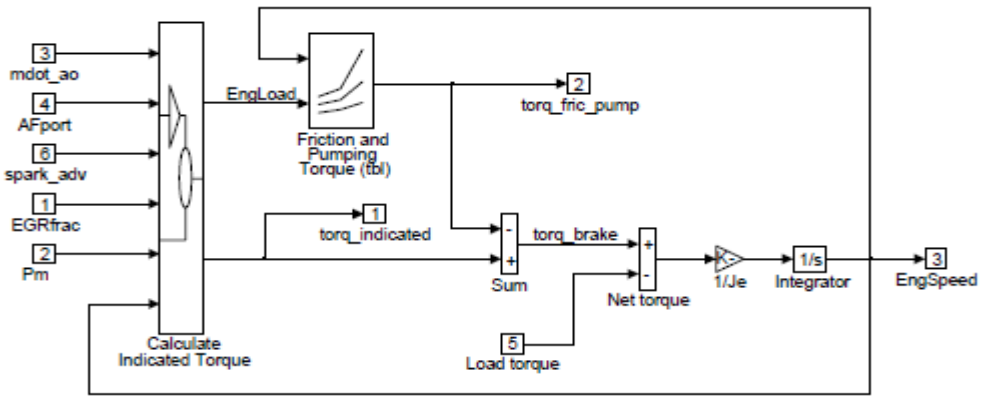

Fig.2.15. Torque Generation block

The figure 2.16 is an example plot of engine brake torque as a function of the average engine speed and the average amplitude of six cylinder engine.

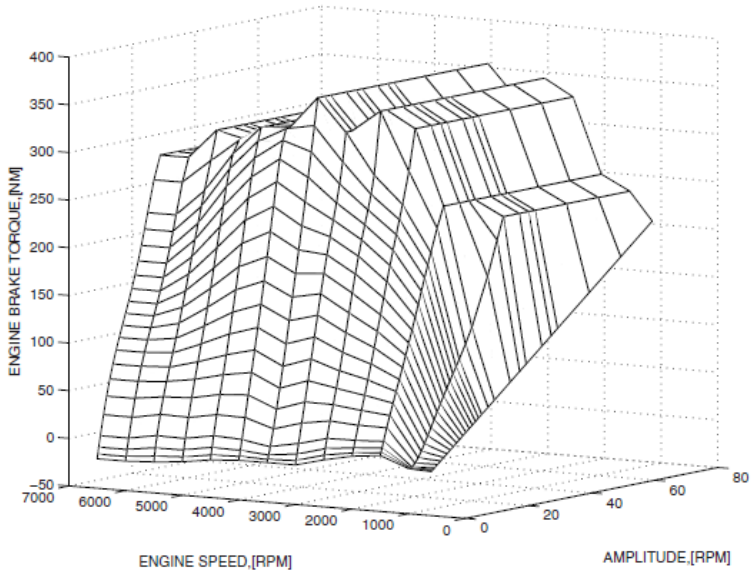

Fig.2.16. The engine brake torque as a function of the engine speed and average amplitude [1]

2.1.5. Mass moment of inertia

In the crankshaft-rod-piston group, all oscillating masses and all rotating masses are summed into one oscillating and one rotating mass. The piston rod mass is represented with one oscillating and one rotating mass and the crankshaft mass is seen as strict rotating and the piston mass as strict oscillating.

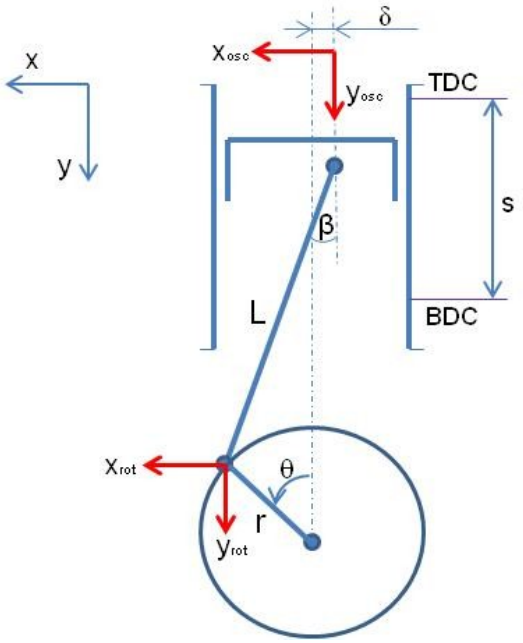

Fig.2.17. Mass effect on the piston rod coordination

Applying the second Newton's law to calculate the kinetic energy of the engine:

$$\int T_{mass} d\theta = \frac{1}{2} m_{rot} v_{rot}^2 + \frac{1}{2} m_{osc} v_{osc}^2 \tag{2.35}$$

Differentiation of the equation (2.35), yields:

$$T_{mass} \dot{\theta} = m_{rot} v_{rot} \dot{v}_{rot} + m_{osc} v_{osc} \dot{v}_{osc} \tag{2.36}$$

Here: $m_{rot}, v_{rot}, m_{osc}, v_{osc}$ are the masses and velocity of rotating and oscillating masses, respectively.

$$v_{rot}^2 = \dot{y}_{rot}^2 + \dot{x}_{rot}^2$$

$$\Longrightarrow v_{rot} = \sqrt{\dot{y}_{rot}^2 + \dot{x}_{rot}^2} \Longrightarrow \dot{v}_{rot} = \frac{\dot{y}_{rot}\ddot{y}_{rot} + \dot{x}_{rot}\ddot{x}_{rot}}{\sqrt{\dot{y}_{rot}^2 + \dot{x}_{rot}^2}} \tag{2.37}$$

$$v_{osc} = \dot{x}_{osc} \implies \dot{v}_{osc} = \ddot{x}_{osc} \tag{2.38}$$

Substituting (2.37) and (2.38) to (2.36):

$$T_{mass}\dot{\theta} = m_{rot}(\dot{y}_{rot}\ddot{y}_{rot} + \dot{x}_{rot}\ddot{x}_{rot}) + m_{osc}\dot{x}_{osc}\ddot{x}_{osc} \tag{2.39}$$

On the other hand, from figure 2.17, we have:

$$y_{rot} = r(1 - \cos(\theta)) \Rightarrow \dot{y}_{rot} = r\dot{\theta}\sin(\theta)$$
$$\Rightarrow \ddot{y}_{rot} = r(\ddot{\theta}\sin(\theta) + \dot{\theta}^2\cos(\theta)) \tag{2.40}$$

$$x_{rot} = r\sin(\theta) \Rightarrow \dot{x}_{rot} = r\dot{\theta}\cos(\theta) \Rightarrow \ddot{x}_{rot} = r(\ddot{\theta}\cos(\theta) - \dot{\theta}^2\sin(\theta)) \tag{2.41}$$

If τ is defined as the piston distance ratio, we have: $\tau = \frac{l}{r}$ where l is the piston distance measured from the TDC. The first and second derivatives of τ according to the crankshaft angular θ are known as crankshaft angular velocity and crankshaft angular acceleration ratio.

$$\dot{\tau} = \frac{d\tau}{d\theta} \text{ and } \ddot{\tau} = \frac{d\tau^2}{d^2\theta}$$

$$y_{osc} = r\tau \implies \dot{y}_{osc} = r\dot{\tau}\dot{\theta} \implies \ddot{y}_{osc} = r(\dot{\tau}\ddot{\theta} + \ddot{\tau}\dot{\theta}^2) \tag{2.42}$$

$$x_{osc} = 0 \tag{2.43}$$

Substituting (2.40), (2.41), (2.42) and (2.43) to (2.39):

$$T_{mass} = \ddot{\theta}(r^2 m_{rot} + m_{osc}r^2\dot{\tau}^2) + \dot{\theta}^2(m_{osc}r^2\dot{\tau}\ddot{\tau}) \tag{2.44}$$

The mass torque can be calculated from the kinetic energy of the masses in motion. The kinetic energy can be expressed as:

$$E_{mass} = \int_0^{2\pi} T_{mass}\, d\theta = \frac{1}{2}\Theta\dot{\theta}^2 \tag{2.45}$$

Here: Θ is the mass moment of inertia with respect to the crankshaft angular.

Differentiation the equation (2.45) to obtain the mass torque:

$$T_{mass} = \frac{dE_{mass}}{d\theta} = \Theta\ddot{\theta} + \frac{1}{2}\dot{\Theta}\dot{\theta}^2 \tag{2.46}$$

From (2.44) and (2.46), the moment of inertia for a one cylinder engine is identified:

$$\Theta = r^2 m_{rot} + m_{osc} r^2 \dot{\tau}^2 \tag{2.47}$$

The piston distance measured from the TDC l can be calculated from the figure 2.17:

$$l = \sqrt{L^2 - \delta^2} + r - L\cos(\beta) - r\cos(\theta)$$

$$\tau = \frac{l}{r} = \frac{\sqrt{L^2 - \delta^2} + r - L\cos(\beta) - r\cos(\theta)}{r}$$

$$\Rightarrow \tau = 1 + \frac{L}{r}\sqrt{1 - \frac{\delta^2}{r^2}} - \frac{L}{r}\cos(\beta) - \cos(\theta) \tag{2.48}$$

Other hand:

$$r\sin(\theta) = \delta + L\sin(\beta)$$

$$\Rightarrow r^2\sin^2(\theta) = \delta^2 + 2\delta L\sin(\beta) + L^2\sin^2(\beta) \tag{2.49}$$

Since the trigonometric identity:

$$\sin^2(\beta) = 1 - \cos^2(\beta)$$

Substituting to (2.49):

$$r^2\sin^2(\theta) = \delta^2 + 2\delta L\sin(\beta) + L^2(1 - \cos^2(\beta))$$

$$\Rightarrow \cos^2(\beta) = 1 + \frac{\delta^2}{L^2} + \frac{2\delta}{L}\sin(\beta) - \frac{r^2}{L^2}\sin^2(\theta) \tag{2.50}$$

The piston distance is defined:

$$\tau = 1 + \frac{1}{\xi}\sqrt{1 - \mu^2} - \frac{1}{\xi}\sqrt{1 - \mu^2 + 2\mu\xi\sin(\theta) - \xi^2\sin^2(\theta)} - \cos(\theta) \tag{2.51}$$

Here: $\xi = \frac{r}{L}$ and $\mu = \frac{\delta}{L}$

The first and second derivatives of the piston distance with the respect of the crankshaft angular will be obtained the velocity and acceleration angular ratio for one

cylinder engine, respectively:

$$\dot{\tau} = \frac{d\tau}{d\theta} = \sin(\theta) + \frac{\xi \sin(\theta)\cos(\theta) - \mu\cos(\theta)}{\sqrt{1 - \mu^2 + 2\mu\xi\sin(\theta) - \xi^2\sin^2(\theta)}} \tag{2.52}$$

$$\ddot{\tau} = \frac{d^2\tau}{d\theta^2} = \cos(\theta) + \frac{\xi\cos^2(\theta) - \xi\sin^2(\theta) + \xi^3\sin^4(\theta) + 3\xi\mu^2\sin^2(\theta)}{\left(\sqrt{1 - \mu^2 + 2\mu\xi\sin(\theta) - \xi^2\sin^2(\theta)}\right)^3} - \frac{3\xi^2\mu\sin^3(\theta) + \mu\sin(\theta) - \mu^3\sin(\theta)}{\left(\sqrt{1 - \mu^2 + 2\mu\xi\sin(\theta) - \xi^2\sin^2(\theta)}\right)^3} \tag{2.53}$$

Combining all submodels above, we have the engine model as the figure 2.18:

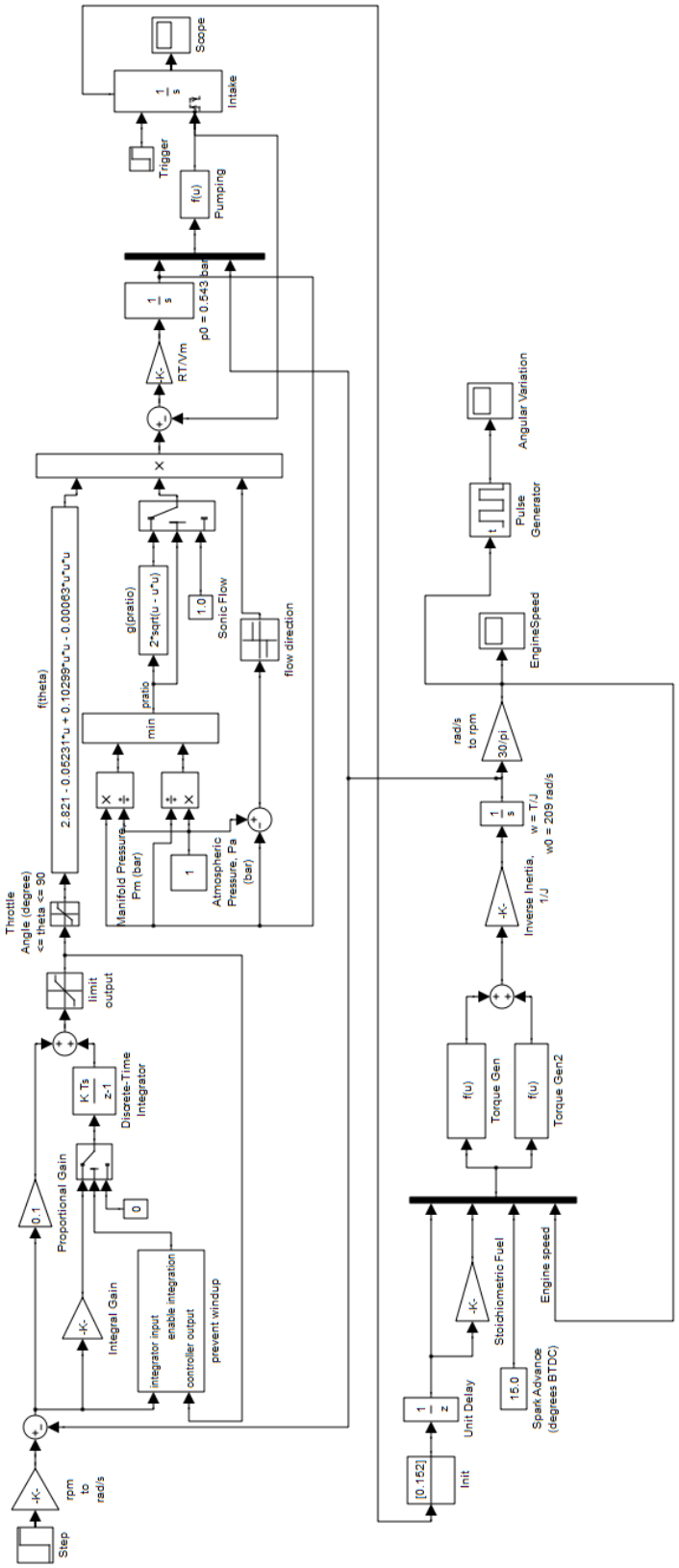

Fig.2.18. Simulink engine model

2.2. Sensors

2.2.1. Lambda sensor

Lambda sensors in automotive applications are used to measure the air fuel (A/F) ratio of engine exhaust gases and to control the optimum A/F ratio for perfect exhaust gas after-treatment by catalytic converters. Therefore, they are also known as oxygen or A/F ratio sensors.

In stoichiometric engine operation, emission levels heavily depend on how accurate the air-fuel ratio can be kept at $\lambda = 1$. Due to measurement and computational tolerances, sufficiently accurate stochiometric operation requires a closed loop control.

λ can be defined as formula:

$$\lambda = \frac{(m_{air}/m_{fuel})_{\text{current}}}{(m_{air}/m_{fuel})_{\text{stoichiometric}}} \tag{2.54}$$

For stoichiometric combustion approximately 17.4 kg of air are necessary for 1 kg gasoline. However, even with stoichiometric mixtures the combustion will be never perfect. Beside the main reaction products CO_2 and H_2O, we find significant concentrations of H_2, CO, and HC as rich components, as well as NO_x as lean components. To keep the harmful CO, HC, and NO_x below the legal limits at the end of the exhaust pipe the exhaust gas undergoes an after-treatment in a catalytic converter.

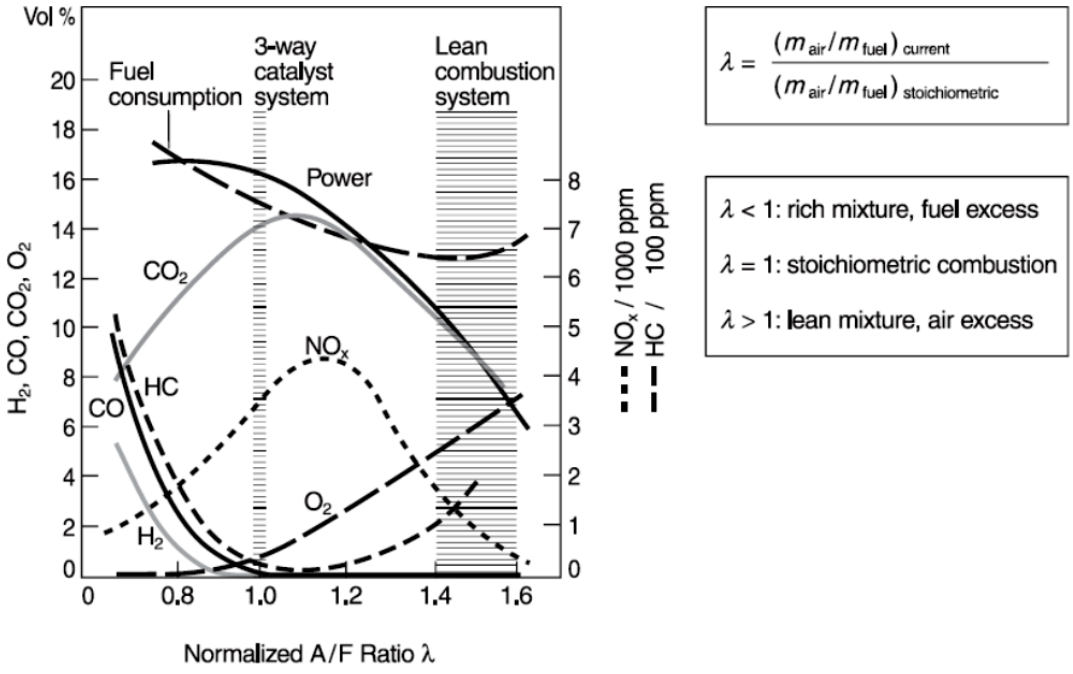

Fig.2.19. Engine exhaust gases and normalized A/F ratio λ [14]

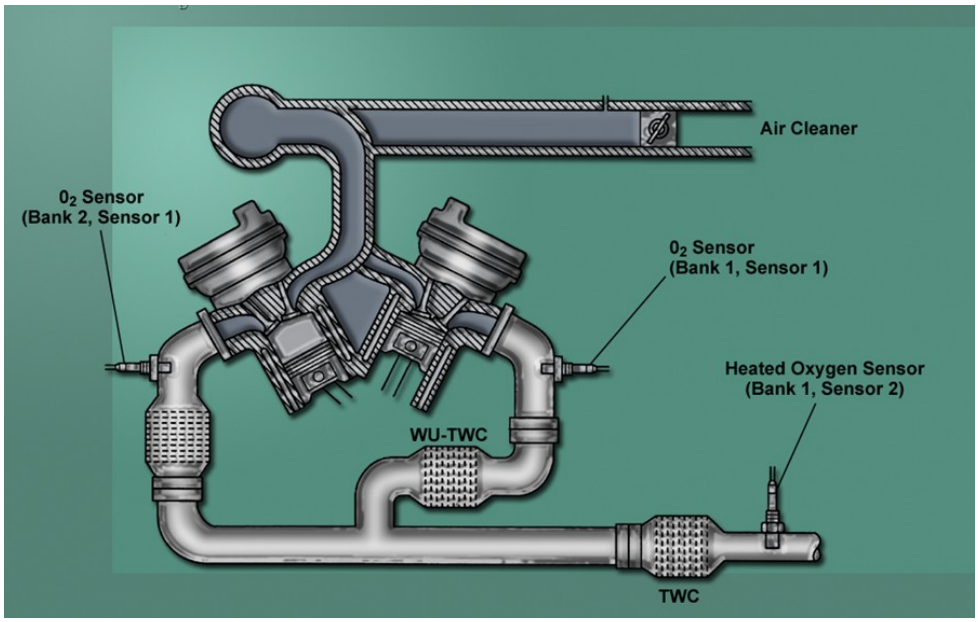

Fig.2.20. Oxygen sensor location [84]

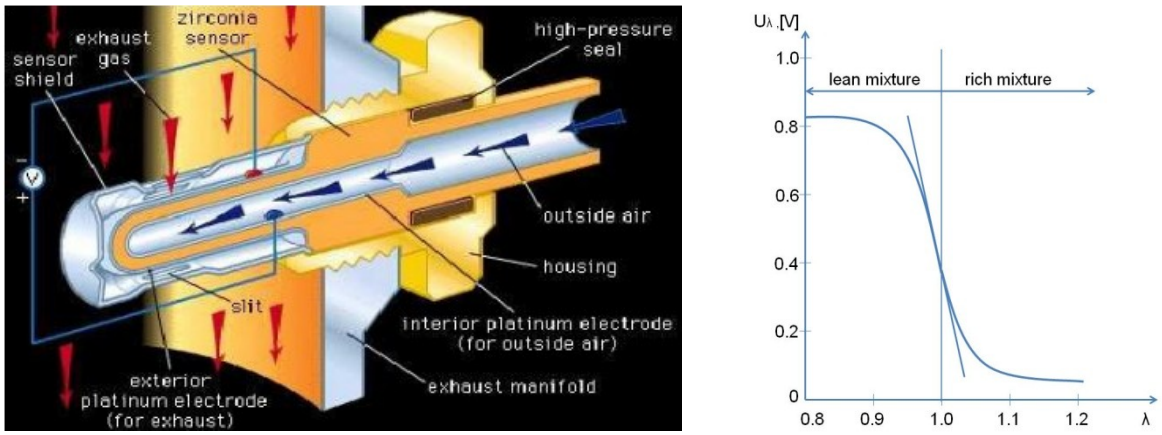

Fig.2.21. Zirconium dioxide sensor [84] and its output voltage

Figure 2.22 shows the results of λ obtained when the engine coolant temperature changes in two very different values. In the first case, the engine temperature is about 85^0C and operates with low speed and load. At this value, the engine has fully warmed up, torque of engine reaches to the maximum. In the second case, temperature of engine is decreased around 35^0C by removing the thermostat in the coolant system. This results in a large coolant flow through the engine, which prevents the engine from warming up.

2.2.2. Throttle position sensor

The throttle position sensor (TPS) is one of the most important sensors for controlling the engine. The signal from the TPS is used for calculation many parameters such as amount of fuel will be injected into the cylinder or intake system; determine the working mode of

the

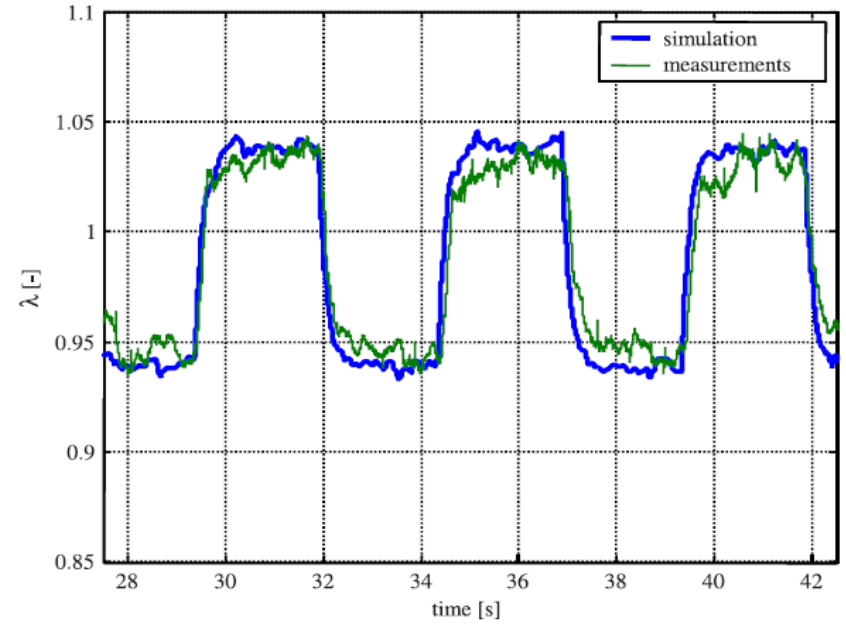

(a)

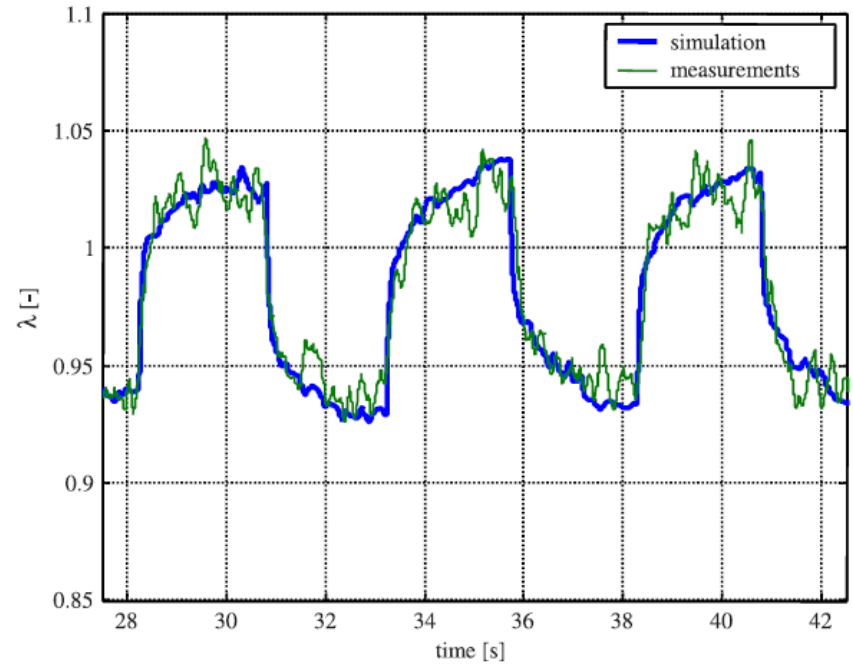

(b)

Fig. 2.22. Air/fuel ratio for engine, fuel injection modulation [36]

a. warmed engine (85^0C), b. cold engine (35^0C)

engine. It usually located at the throttle body, on the plate spindle so that it can directly monitor the position of the throttle plate. Potentiometer is the most popular used in automotive engine. The resistance in the potentiometer varies as a function of the throttle

plate position (and hence throttle position). TPS converts the throttle valve angle into an electrical signal. As the throttle open, the signal voltage increases.

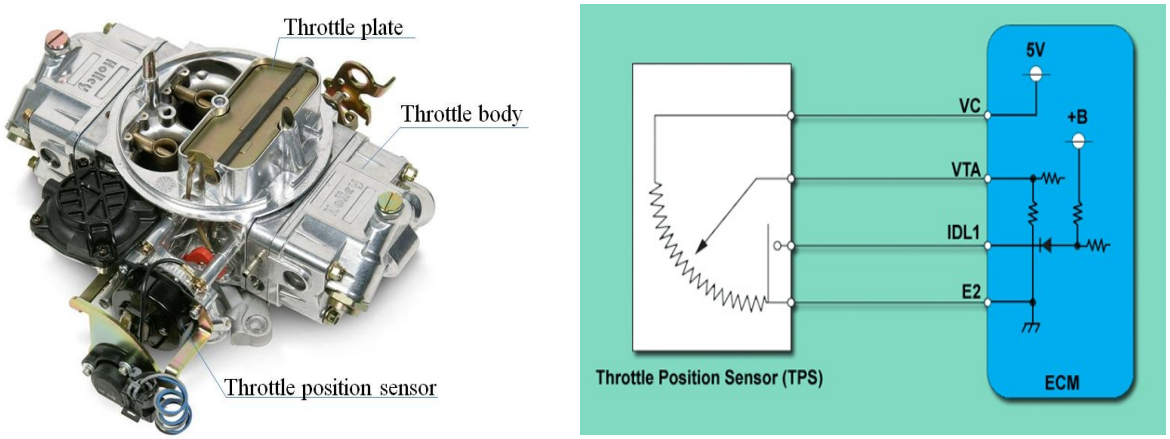

Fig.2.23. Throttle position sensor [84]

The ECU uses throttle plate position information to know:

- Engine mode: idle, part throttle, wide open throttle
- Switch off AC and emission controls at wide open throttle
- Air-fuel ratio correction
- Fuel cut control

The output voltage depends on the engine speed. At idle speed, voltage is approximately 0.6-0.9V on the signal wire. At this voltage, the ECU knows the throttle plate is closed. At widely open throttle, signal voltage is approximately equal to 3.5-4.7 volts.

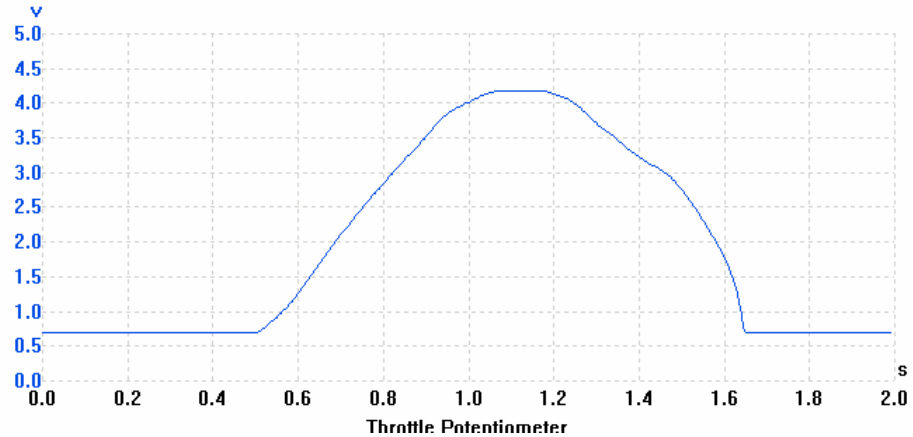

Fig.2.24. Output voltage of throttle position sensor [23]

2.2.3. Engine speed sensor

In order to measure the engine speed, crankshaft position sensor which located at the flywheel, or camshaft position sensor which is located at the camshaft, can be used. In modern automotive engine, crankshaft position sensor is more popular applied because of its advantages. It is an electronic device used in an engine to record the rate at which the crankshaft is rotating. This information will be sent to the ECM to control ignition and fuel injection. In this thesis, the signal from the crankshaft position sensor will be also used for diagnostic the health of cylinders by evaluating this signal to the angular acceleration. The sensor system consists of a rotating part, typically a disc, as well as a static part, the actual sensor. The Hall Effect sensor is used typically as the static part requiring a magnet to be mounted somewhere in the periphery of the rotating disc, but other detection principles can also be employed i.e optical or inductive.

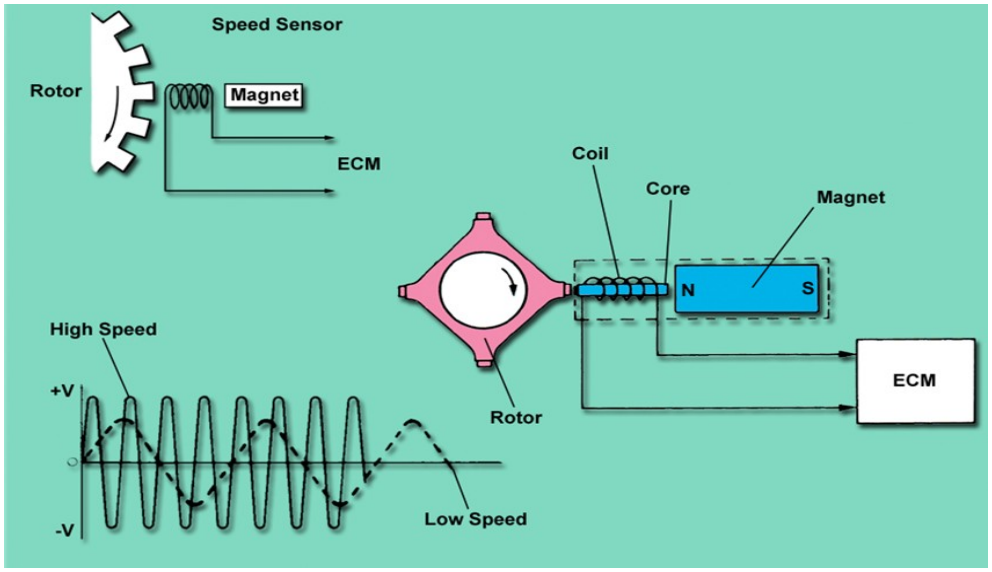

Fig.2.25. Engine speed sensor [84]

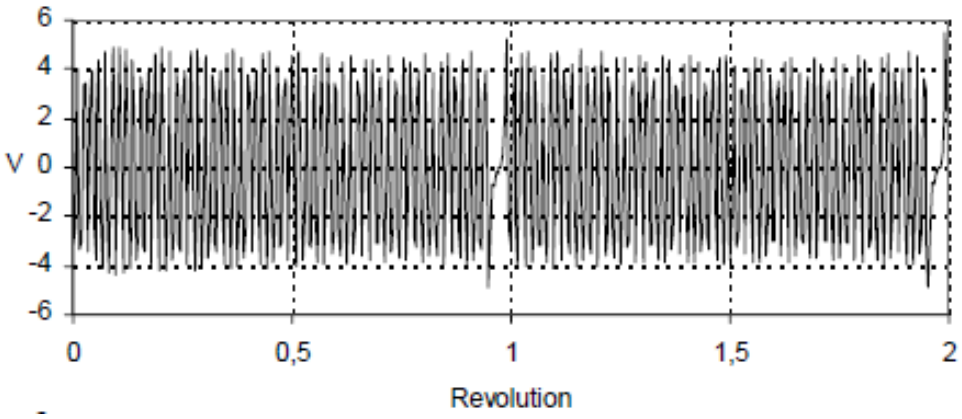

Fig.2.26. The waveform of engine speed sensor during two complete revolution [68]

Figure 2.26 shows the particular waveform of output voltage from the engine speed sensor. It is Alternating Current (AC) and can be changed depends on the manufacturers, proximity and engine speed. The gap in the picture is due to the "missing tooth" in the flywheel or reflector and is used as a reference point for the ECM to ascertain the engines position. Some systems use two reference points per revolution. The output voltage of the crankshaft sensor increases when the engine speed increases and contrary. The minimum voltage requirement is crucial as while a small AC voltage may be present, it may be insufficient to trigger the primary circuit. The main reason for evaluating this waveform is to monitor the output when the engine fails to start due to a loss of primary triggering.

2.2.4. Mass air flow sensor

The mass airflow sensors (MAF), which are used to measure the air entering the engine (include the volume and density). The ECU processes the signal from MAF sensor to calculate the amount of fuel to maintain the correct air/fuel mixture. MAF sensors are widely used in multiport fuel injection systems with two basic types: hot wire and hot film. In automotive engine, the hot wire type is used more popular.

Mass airflow sensors use electrical current to measure airflow. The platinum wire (hot wire) or nickel foil grid (hot film) are the sensing element, which is heated by alternating current source. The temperature of sensing elements are always kept in a certain value that hotter than the intake air. It is 75^0C and 100^0C above ambient temperature with the hot film and hot wire MAFs, respectively. When the air flow through the MAF sensor, as its temperature is lower than hot sensing element, it cools the element. In order to keep the temperature of the sensing element constantly, the supplied electric current must be increased. Because the cooling effect varies directly with the temperature, density and humidity of the incoming air, the amount of current needed to keep the element hot is directly proportional to the air massflow entering the engine.

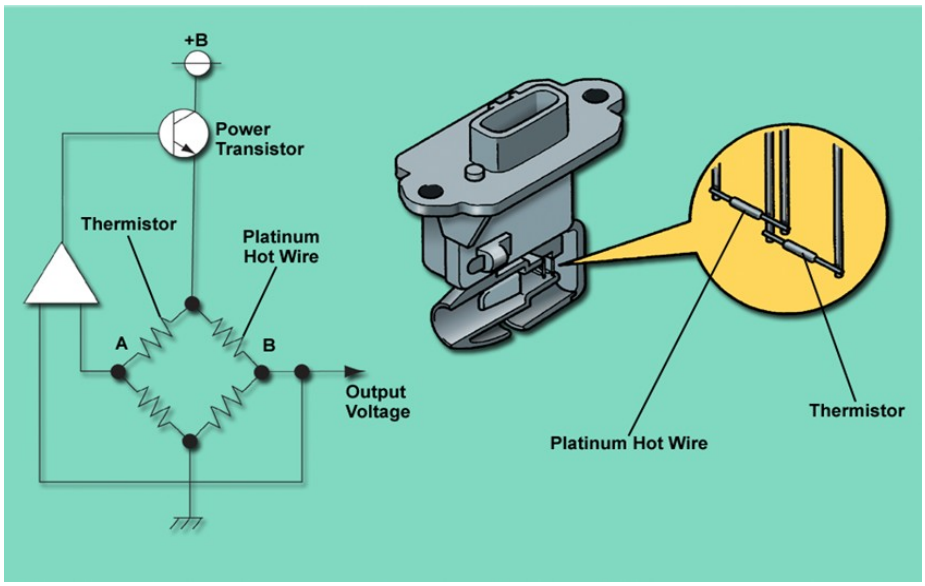

Fig.2.27. Hot wire MAF sensor [84]

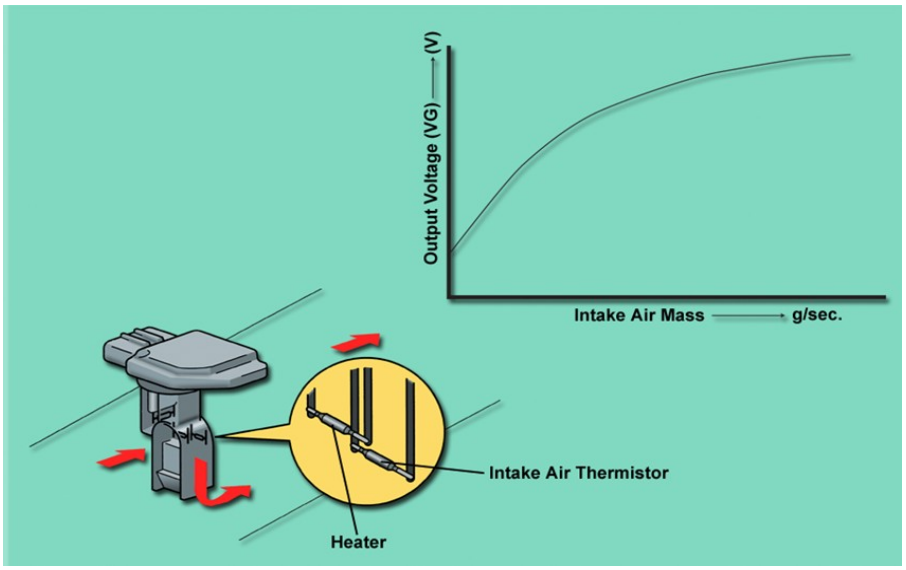

Fig.2.28. MAF sensor signal voltage [84]

Low airflow = low voltage; High airflow = high voltage

2.2.5. Manifold absolute pressure sensor (MAP sensor)

A MAP sensor is used to measure the absolute pressure in the intake manifold, and then compare with a reference vacuum. The signal from the MAP sensor and others such as the barometric pressure sensor; engine speed sensor and the throttle position sensor are sent to ECU to determine the engine load. Fuel ratio and spark timing are then fine tuned by the computer using additional sensors, this also helps to control fuel economy and emissions. MAP is a micromechanical pressure sensor. The measuring element, which is composed of a silicon chip, is at the heart of the micromechanical pressure sensor. The output of the MAP

sensor is an analog variable voltage. One side of a silicon wafer is exposed to engine vacuum and the other side is exposed to a perfect vacuum.

Four deformation resistors are attached to the silicon layer which changes in resistance when strain is applied to the wafer. The resistors are electrically connected to a Wheatstone bridge circuit and then to a differential amplifier, which creates a voltage that is proportional to the vacuum applied. Their electrical resistance changes when mechanical force is applied as Piezo-resistivity. The measuring element is surrounded on the component side by a cap which is at the same time encloses the reference vacuum. They are extremely robust and insensitive to aggressive media such as oils, fuels, brake fluids, saline fog and industrial climate. The pressure sensor case can also incorporate an integral temperature sensor, whose signals can be evaluated independently. This means that at any point a single sensor case suffices to measure temperature and pressure.

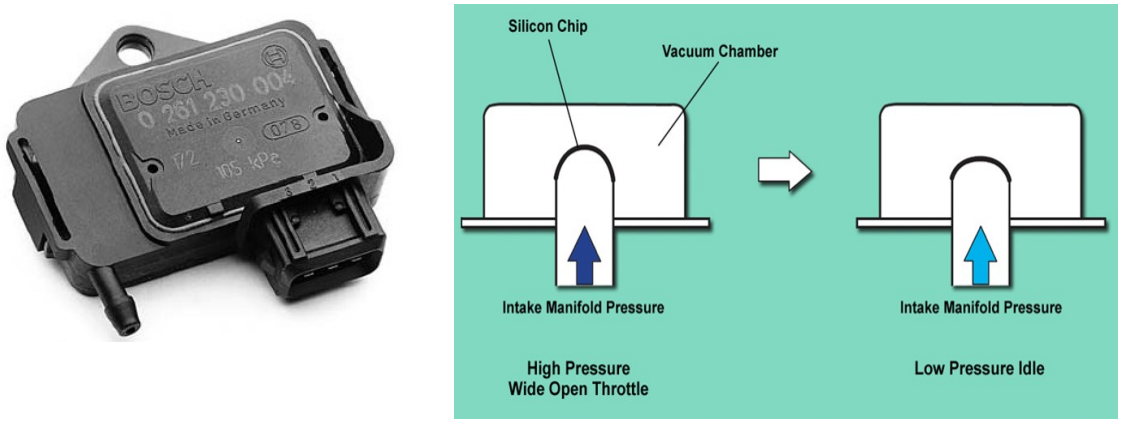

Fig.2.29. MAP sensor

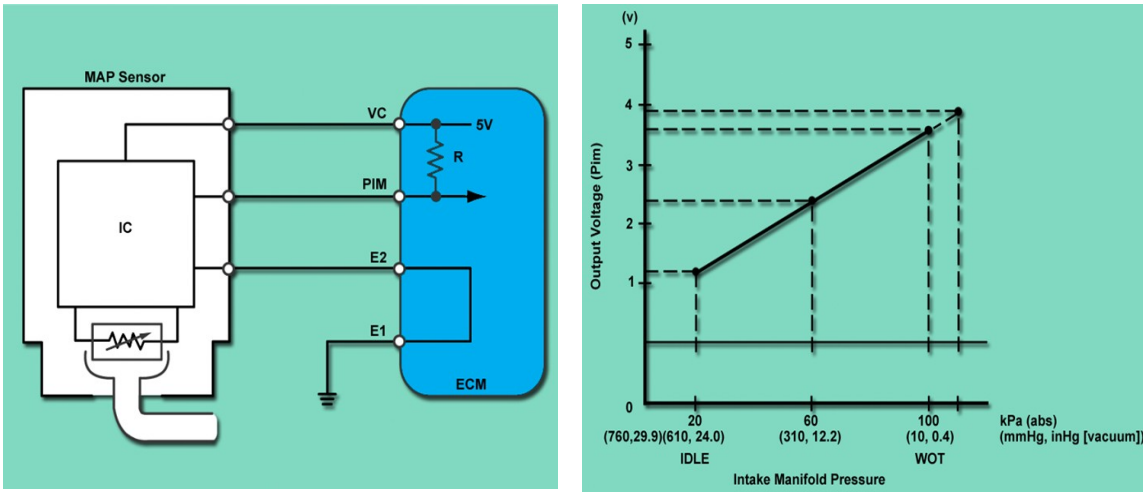

Fig.2.30. MAP sensor circuit and output voltage [84]

2.3. Electronic Control Unit

The electronic Control Unit (ECU) is a microprocessor, which is used for controlling the automotive engine. It receives the signal from engine sensors, exhaust emission sensors, temperature sensors and a throttle-pedal position sensor,… and then process these signals with an optimized program to control the amount of fuel injection, the injection timing, the ignition timing, and any other features the engine may have such as an electronically controlled throttle, variable valve timing/lift or exhaust-gas recirculation, etc.

The discrete time control algorithms are placed inside the Control Algorithms blocks which is "wired" between the input and output signal conditioning block. The input signal conditioning block performs the conditioning necessary to convert the simulated sensor outputs to the engineering units typically used by the control algorithms block. This often involves analog-to-digital converter models and conversion tables. The output signal conditioning block converts control signals to the type of signal necessary for the engine's control actuators, such as a pulse width modulated signal, a desired stepper motor position, etc.

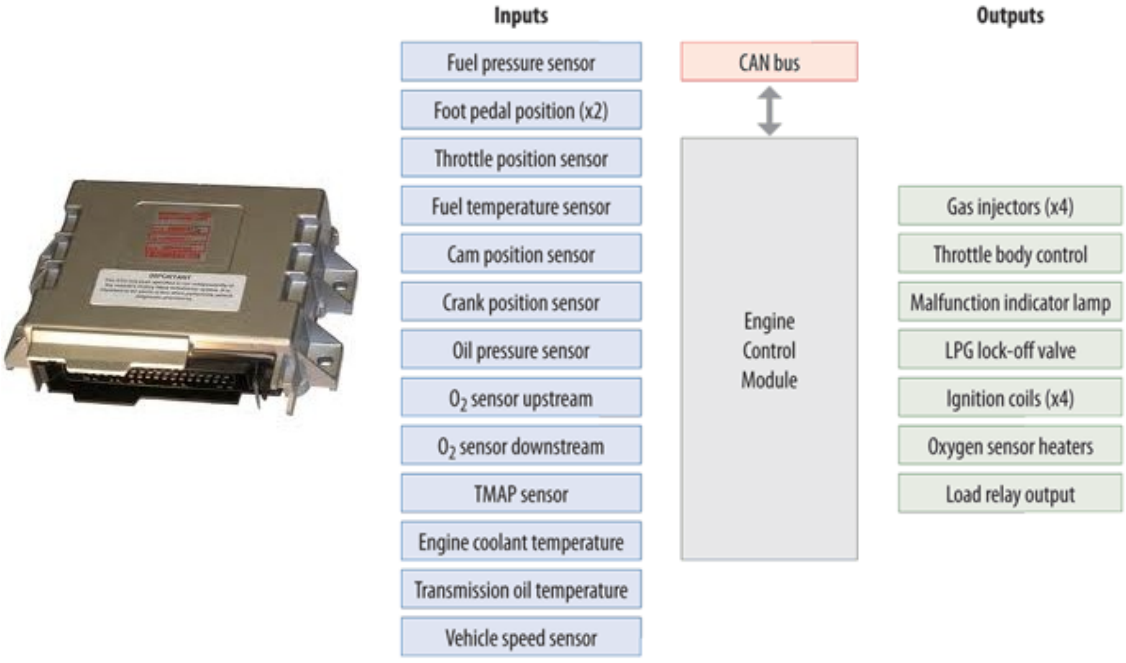

Fig.2.31. ECU and its inputs, outputs

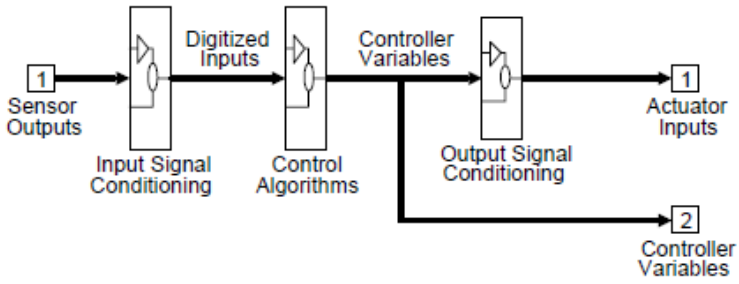

Fig.2.32. Electronic control unit block

2.4. Actuators

Four actuators are used for this engine control system, including fuel injectors, an ignition system, an EGR (exhaust gas recirculation) valve and an idle air control valve. These actuators are controlled by the controller.

2.4.1. Fuel injector

The fuel injectors, which directly control fuel metering to the intake manifold, as pulsed by the ECU. The ECU completes the injector ground circuit for a calculated amount of time referred to as injection duration or injection pulse width. The ECU determines which air/fuel ratio the engine runs at based upon engine conditions monitored by the input sensors and a program stored in its memory.

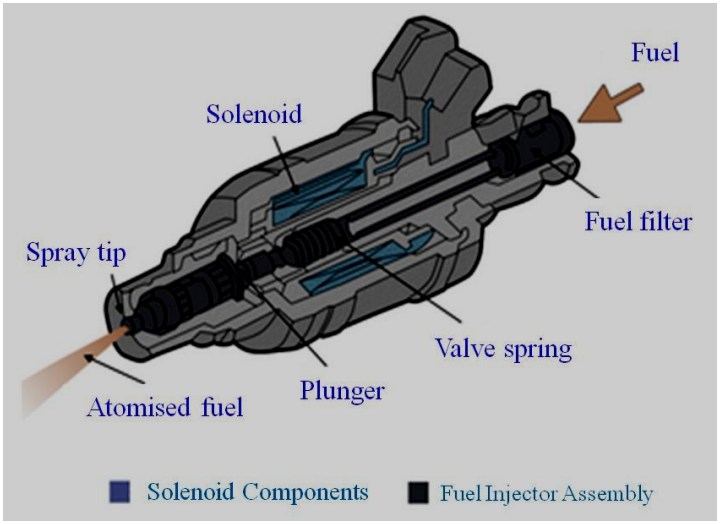

Fig.2.33. Fuel injector [80]

The amount of fuel injection into the cylinder m_f depends on the open time of the injector valve t_{inj}. If it is assumed that mass flow rate of air out of the manifold doesn't change $\dot{m}_{ao} = \text{const}$, then m_f can be calculated [70].

$$m_f = \frac{m_{ao}}{L_{st}\lambda} = \frac{1}{L_{st}\lambda}\frac{\dot{m}_{ao}}{\omega}\frac{2}{z} \tag{2.55}$$

where

$$L_{st} = \frac{m_{ao,th}}{m_{f,th}} = 14{,}66$$

Here: $m_{ao,th}$ and $m_{f,th}$ are the theoretical air and fuel mass. $m_{f,th}$ is equivalent to the mass of fuel needed for an ideal stoichiometric combustion with the oxygen.

The amount of the injected fuel m_f is also calculated as approximately formula:

$$m_f = Q_f . A_{eff} . \sqrt{2\frac{\Delta p}{Q_f}} . t_{inj} \tag{2.56}$$

Q_f, A_{eff} are the fuel density and the effective opening area of the valve, respectively and assumed to be constant.

Δp is the pressure difference between fuel rail and manifold at manifold injection or between fuel rail and combustion chamber at direct in – cylinder injection. At manifold injection, the pressure difference Δp is around 5 bar. At direct in-cylinder injection, the pressure difference Δp is up to 400 bar.

The injection time at stationary engine operation is proportional to

$$t_{inj} \sim \frac{1}{\lambda}\frac{m_{ao}}{\omega}\frac{2}{z}$$

For a reference air-fuel ratio λ_0, the reference injection time t_0 is proportional to

$$t_0 \sim \frac{1}{\lambda_0}\frac{m_{ao}}{\omega}\frac{2}{z}$$

For arbitrary air – fuel ratios λ, we have

$$t_{inj} \sim \frac{\lambda_0}{\lambda} t_0$$

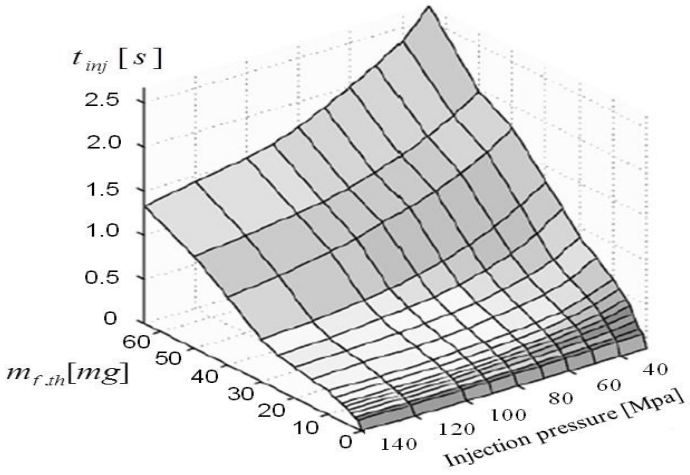

Fig.2.34. An example of piezoelectric injector map [70]

2.4.2. Exhaust gas recirculation valve (EGR)

The EGR valve recirculates exhaust into the intake stream. Exhaust gases have already combusted, so they do not burn again when they are recirculated. These gases displace some of the normal intake charge. This chemically slows and cools the combustion process by several hundred degrees, thus reducing NO_x formation.

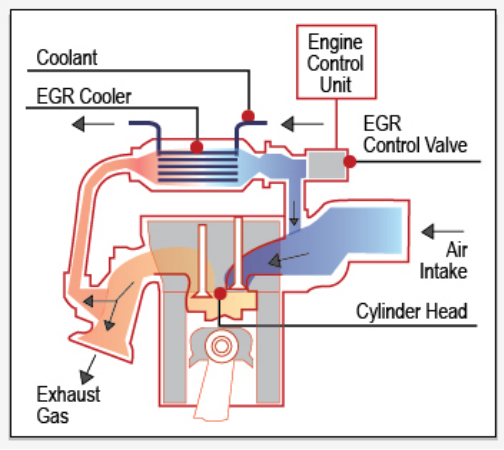

Fig.2.35. EGR system [80]

The actuators bock is shown in figure 2.36. The actuator commands (from the controller) come in through in port 1. A signal select block was created to split the actuator signal vector and route the signals to the appropriate actuator models. Each of the actuators has a mass flow rate for its output, except for the ignition system block where the output is simply a value for the current spark advance. The fuel injectors' block also determines the injector pulse width in degrees of crank rotation. This is used in the engine model to determine if a portion of the fuel pulse is injected after the intake valve closes.

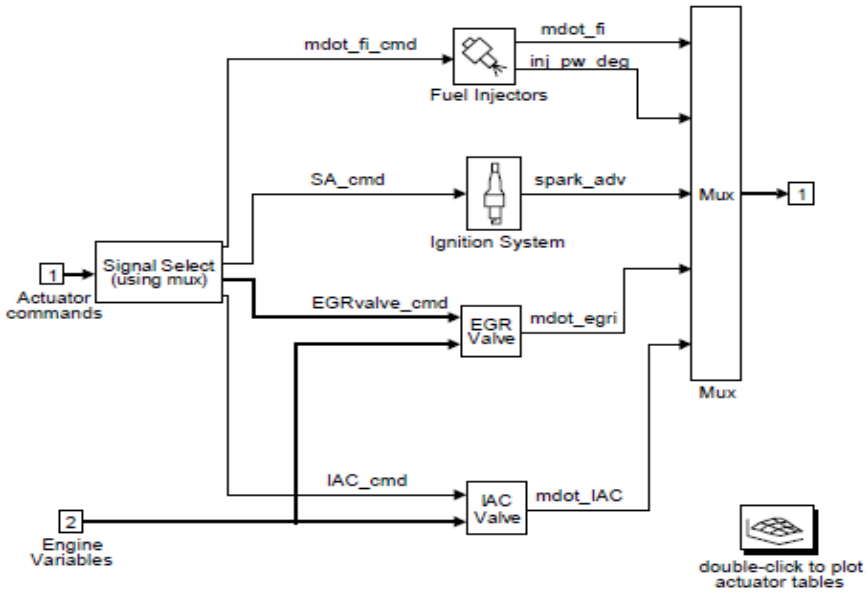

Fig.2.36. Actuators block

3. CONNECTING ENGINE MODEL TO dSPACE

3.1. Fundamental of dSPACE and Hardware-in-the-loop (HIL) simulation

The dSPACE prototyping systems, developed by dSPACE Inc., allow the user to optimize control designs of the real controlled system flexibly without manual programming. Design faults can be found and corrected on the spot immediately. The user's design is realized automatically on dSPACE prototyping systems from a Matlab/Simulink block diagram and calculated in real time. In addition, dSPACE provides sufficient I/O interfaces for connection between the user's design and the real world.

Fig.3.1. The dSPACE simulation and its connector panel [58]

The dSPACE single-board hardware provides fast processors and comprehensive I/O interfaces–all on single boards that are installed directly in the PC. The dSPACE Real-Time Interface allows the user to automatically implement Matlab/ Simulink models on dSPACE hardware via a code generated by Real-Time Workshop (RTW). In summary, the dSPACE prototyping systems have the following advantages: Quick and reliable real-time testing and optimization of control functions, in-vehicle capable and high-speed hardware, wide range of I/O interfaces, easy integration of CAN, LIN, and FlexRay bus systems and automatic realization of Matlab/Simulink models on dSPACE hardware.

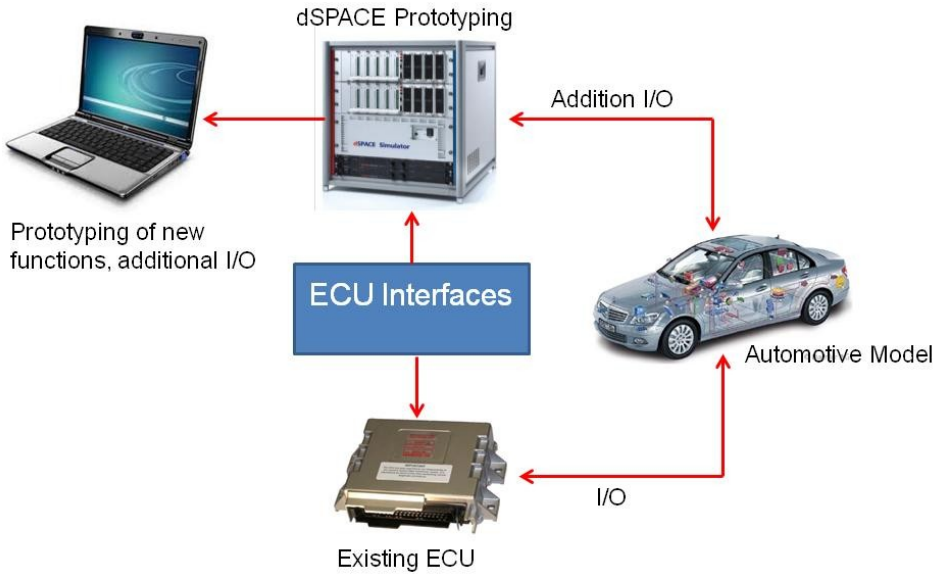

Fig.3.2. dSPACE prototyping system

Hardware-in-the-loop (HIL) simulation is a method used in the product development cycle in which one or more real components interact with components that are simulated in real time (dynamic models). HIL simulation has been used in testing electronic vehicle ECUs with great success for many years now. One important application area for HIL simulation is testing ECU diagnostics. This is not surprising, in view of the fact that diagnostics software has increased in complexity and grown immensely in importance over the last few years. To make diagnostic tests easier to handle on the HIL simulator, dSPACE now offers test automation and diagnostic tools, and integration of these two, from a single vendor. It has become an integral component in the electronic development process for testing control functions in the automotive industry. All of this can be summarized in Fig.3.3.

HIL simulation involves operating mechatronic systems, particularly electronic control units (ECUs), in a closed loop with components that are simulated in real time to test them intensively in this virtual environment. The simulated subsystem has to perform the following actions within one simulation step:

- Read the measurement signals (actuator controlled by the ECU)
- Calculate and perform numeric integration (simulate the entire dynamic model of the real system)
- Output the results (sensor simulation for the ECU)

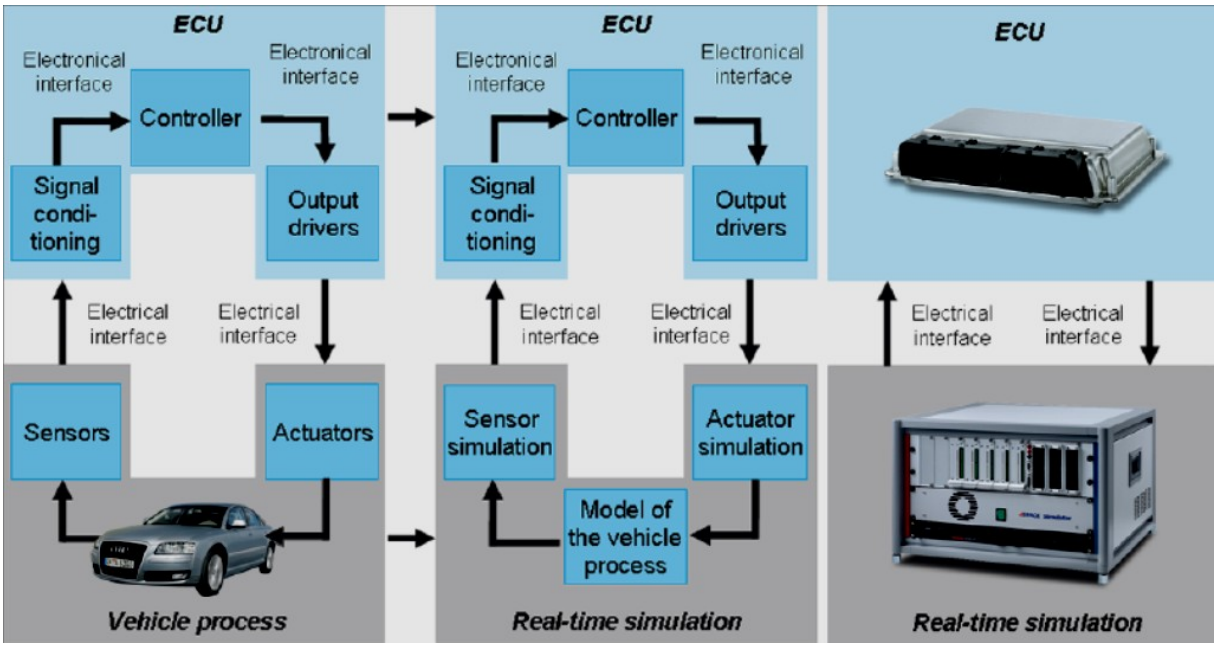

Fig.3.3. Signal flows in a real system and HIL simulation [48]

The structure of an HIL simulator equipped with all the components needed for testing ECU diagnostics is shown in Fig.3.2.

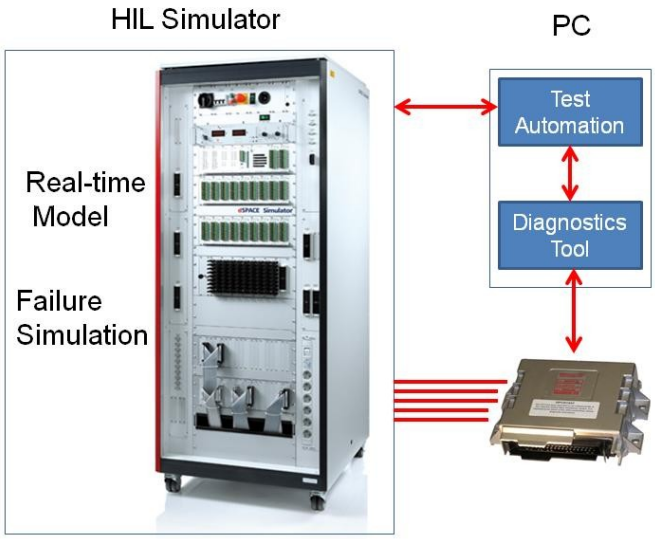

Fig.3.4. Structure of an HIL simulator with integrated diagnostics

In hardware-in-the-loop tests, the electronic control unit (ECU) to be tested is not installed in the real vehicle, but connected to a simulation system that simulates the ECU's environment (vehicle, sensors, actuators) in real time. This means that comprehensive, automated tests can be run in a simulated environment at any time. HIL simulation is used in various spheres – from testing single ECUs to whole ECU networks, right through to release tests on the entire electronic system. One objective is to ensure correct functionality. In other

cases, HIL simulation is used to test communication between ECUs, the energy and vehicle electrical system management, and network management. One important application area for HIL simulation is testing the diagnostics software of vehicle ECUs. One basic reason for this is that the proportion of ECU software devoted to diagnostics has increased constantly over the last few years. In modern engine ECUs, for example, diagnostics account for between 40% and 50% of typical statistics such as the number of calibration parameters, functions, and code lines, as well as processor run time. This is also reflected on the testing side. For example, tests on diagnostic functionality already constitute up to a quarter of the total testing costs for an ECU.

3.2. HIL Systems: Basics and Components

3.2.1. Basics of HIL System

HIL systems can vary considerably from application to application. Even so, it is possible to identify numerous components that are always present in a similar form.

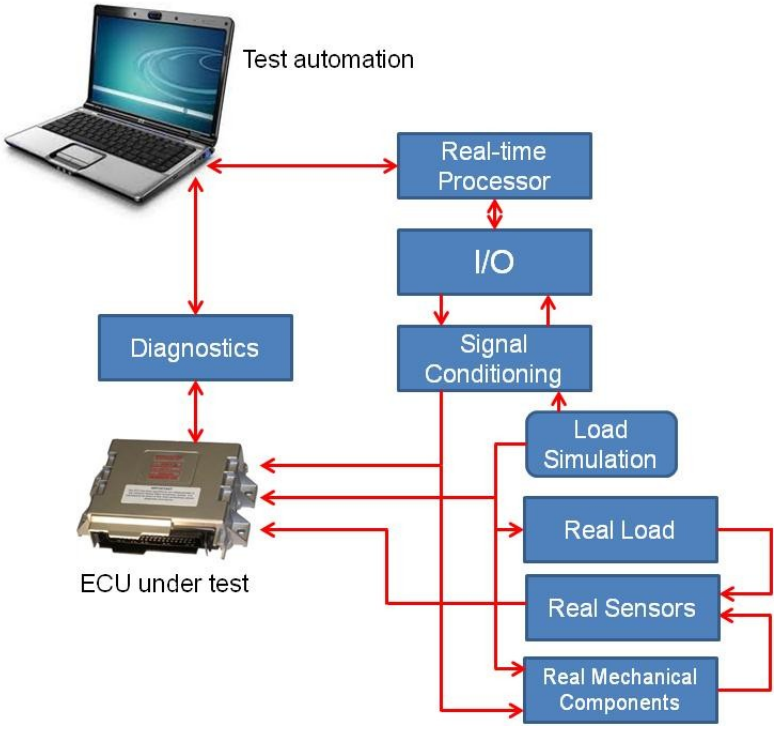

Fig.3.5. Components of an HIL system

3.2.2. Components of the HIL System

Host PC: An off-the-shelf Windows® PC is generally used as the user interface to the real-time processor (experiment software) and for executing the modeling and implementation software. To ensure high data rates and low latencies in communication

with the real-time hardware, specially optimized interface cards are used, and sometimes also Gigabit Ethernet.

Real-time processor system: Standard server PCs with a real-time operating system have now almost caught up with special real-time processor boards in terms of pure processor performance, which is particularly important for model calculation. However, connection to the I/O cards is problematic, as server PCs are frequently not optimized for this. Thus, processor boards with optimized I/O interfaces are used for high-end applications to achieve an optimum overall system consisting of a processor and I/O.

I/O boards and signal conditioning: Automotive HIL applications require boards for simple analog and digital signals, and also special boards for fast, engine-angle-synchronous signals for fast sensor simulation (signal from crankshaft rotation sensor, camshaft signals) or actuator measurement. Some of these I/O boards already possess the necessary protection circuits and signal adaptations to specific automotive electrical system voltages (12 V, 24 V, etc.); otherwise, separate signal conditioning is used (e.g. for current interfaces, lambda probes, etc.).

Bus systems: The ECUs form networks and communicate via various bus systems in the vehicle (CAN, LIN, FlexRay, MOST). When parts of the network are operated in HIL, the bus behavior of all the missing ECUs has to be appropriately simulated. Thus, the HIL simulator must be able to generate messages (this is called restbus simulation) and to read all the messages coming from the ECU. Here too, special I/O boards are used, frequently with intelligent subprocessors or FPGAs and suitable bus transceivers.

Electrical loads and load simulation: ECUs control electrical actuators (called loads), e.g. valves, electric motors, relays, current-controlled actuators and piezo injectors. Either the real loads or electrically equivalent circuits can be used in an HIL system. The ECU's diagnostic system monitors these actuators so that it can take appropriate action if a fault occurs (short circuit, open circuit) or at least inform the driver. Quite often, it is sufficient to connect a substitute resistance to the ECU as a load. However, if the load itself has dynamic behavior (variable resistance such as in a headlamp) and the ECU performs diagnostics on this, either a real load is integrated into the HIL system or an electronic (= dynamic) load simulation controlled by the real-time system is used.

Electrical fault simulation: To generate the electrical fault states mentioned above, failure simulation units are often integrated into the HIL system. These can simulate hard

short circuits and open circuits, and also leakage resistance and loose contacts. Relays or semiconductor switches are used for this depending on requirements. The failure system is programmed and activated either interactively or via test automation.

Real components: To treat ECUs realistically, real components are often necessary. These might be loads that are not easy to simulate, or that can only be simulated with a lot of effort, and sometimes smaller setups or even complex test benches are used.

Power supply: Simulating the vehicle electrical system and the battery vehicle also requires power supplies whose voltages can be specified dynamically by the simulator. This is especially important for undervoltage and overvoltage tests (e.g. in jumpstarts by trucks) and for simulating voltage drops when starting the engine.

3.3. Testing Diagnostic Functions with HIL

The central element is the test automation tool, which holds the complete test sequence. The test automation tool therefore takes on the task of controlling the entire system. It begins by accessing the real-time model of the simulator to ensure that the operating point used for testing the diagnostic function is correct one. This is necessary because not all diagnostic functions are active at all the operating points.

In the validation of onboard diagnostics (OBD), electrical failures are generated by failure simulation to test that they are correctly detected. Then ECU's fault memory is read out via the connected diagnostics tool, and the result is compared with the expected trouble codes. This procedure can be repeated in automated form for all ECU pins and all type of failure, such as sort circuits, line breaks, and leakage and contact resistances. Finally, the test results are documented in an automatically generated test report.

The detection of limit violations in the ECU can be tested in a similar way. Operating points that violate maximum limits (from the ECU's point of view) are set in the HIL simulator. It is then possible to check whether the ECU's diagnostic function correctly detected the violations by reading out the fault memory. Similarly, HIL simulation can be used to test the detection of communication errors, for example, by omitting or corrupting specific messages from the rest bus simulation. Finally, tests on correct implementation of the diagnostics protocol can also be performed in this way.

Diagnostics also perform another function with respect to HIL simulation: They are often used as an aid to ECU testing. For example, the following actions can be performed automatically during an HIL test:

- Reading and clearing the fault memory to detect unexpected errors or to produce a defined initial state for a test.
- Reading out the variant coding and setting new variants.
- Performing read and write access to ECU-internal calibration and measurement variables, particularly where no calibration interface is available
- Flashing a new software version to the ECU

ECUs for the combustion engines generally have time-based and crankshaft-angle-based function and subsystems. The main task of engine control consists in high precision capture of the engine angle (reading crankshaft and camshaft signals) and the output of injection and ignition signals.

While the ECU's normal I/O can be simulated sufficiently well with a typical sampling rate of 1ms, special fast subsystems are used for the crankshaft-synchronous signals.

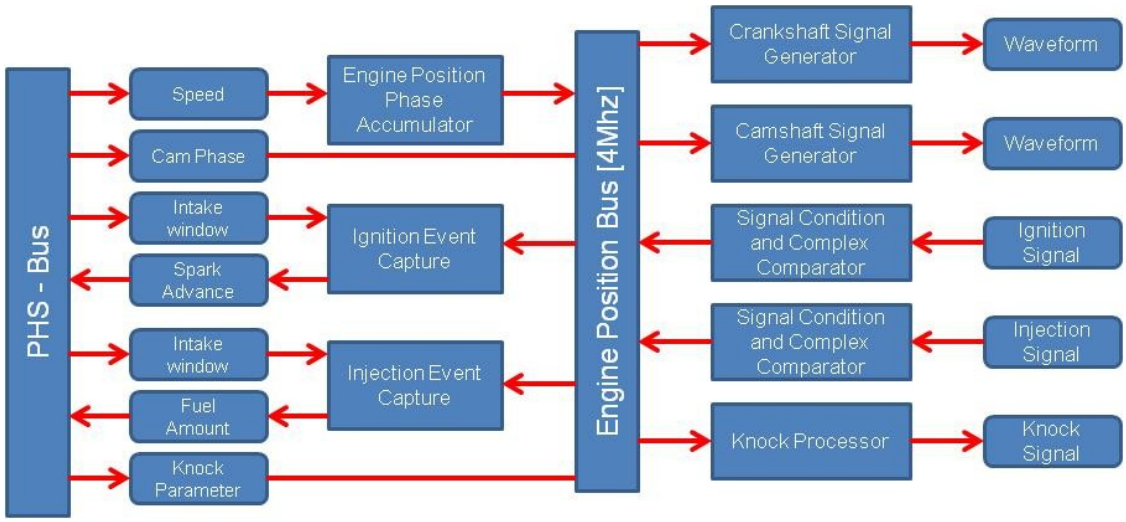

Fig.3.6. Angular processing unit for the crank-angle-synchronous generation of crankshaft signals and knock signals and for capturing injection and ignition signal [58]

4. SIMULATION RESULTS

4.1. Mass flow rate

Depend on the working mode of the engine, the throttle valve is controlled by acceleration pedal or lever via a direct mechanical linkage. In modern engines with electronic throttle control, throttle valve is controlled by a motor which receives the signal control from ECU. As described in the equations (2.9), (2.10) and (2.11) in the section 2, the mass flow rate into the manifold is a function of throttle angle α and manifold pressure P_m. In this case, for further simple, we assumed the manifold pressure P_m less than one half of ambient pressure P_{amb} ($P_m \leq \frac{P_{amb}}{2}$), so $g(P_m) = 1$. Mass flow rate into the manifold obtained by simulate the equation (2.10) in Matlab program. The result of simulation is shown in the figure 4.1.

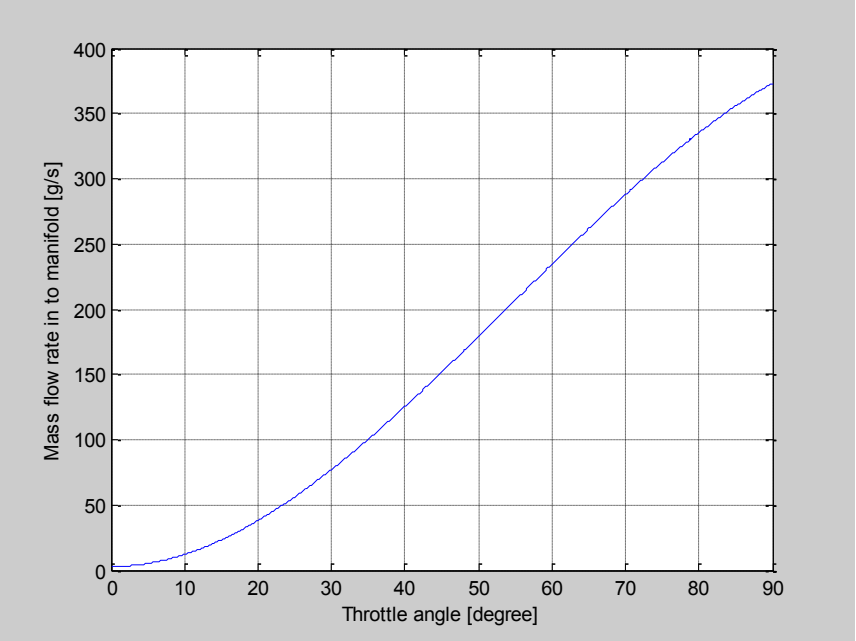

Fig.4.1. Mass flow rate into the manifold

When the throttle is wide opened (approximate 90 degree) at full acceleration mode, the pressure in the intake manifold is almost equal to the ambient atmospheric pressure and the mass flow rate pass the throttle into the cylinder reaches to maximum amount. And when the throttle is partially closed (almost 0 degree), the manifold vacuum develops as the intake drops below ambient pressure.

Manifold pressure is a function of many parameters. It is described as the equation (2.22), (2.23) and (2.24) in Section 2 and simulated by simulink as the figure 2.8 and 2.9.

The parameters are chosen: $R = 278.9$[Nm/Kg/^{0}K]; $T = 318$ [^{0}K]; $V_m = 5.10^{-3}$ [m^3]; $\rho_0 = 1.2$ [$\frac{\text{kg}}{\text{m}^3}$] and $T_0 = 288$ [^{0}K].

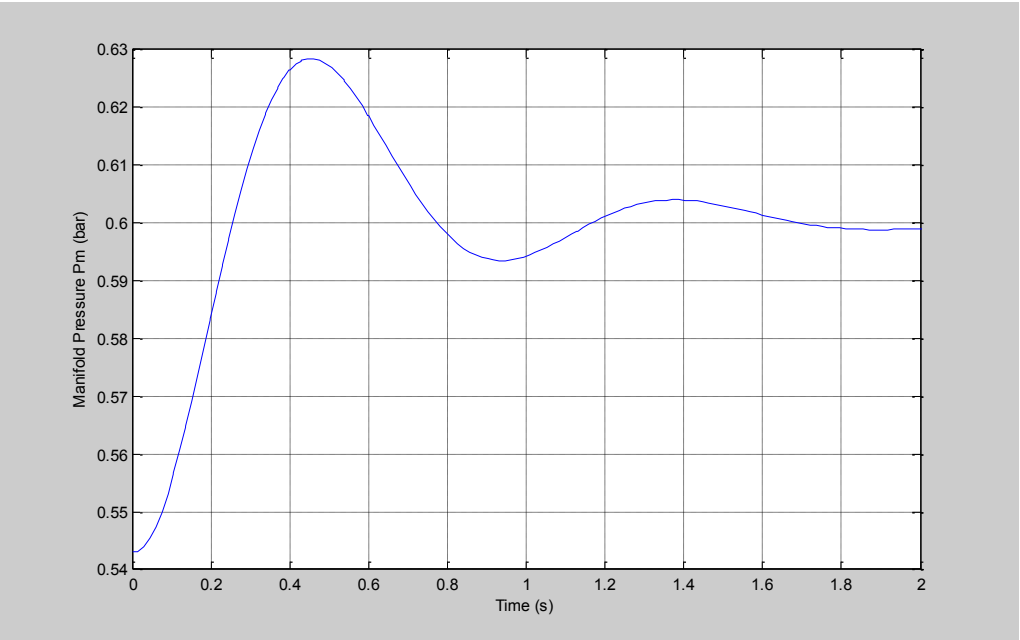

Fig.4.2. Simulation result of manifold pressure in intake system

From the result of simulation, it is seen that the pressure in the manifold is lower than ambient pressure (it is called the vacuum). When the throttle is opened wider (increasing the throttle angle), the pressure increases very. This can be explained that in one moment, when the intake valves are not opened and the air fill fully the manifold, so the pressure increases. In the next phase, the piston moves from top dead center to the bottom dead center in the intake stroke, the cylinder volume rises and pressure drops, the intake valves are opened. Because of the pressure difference in and out the cylinder, the air mass flowrate moves into the cylinder and the manifold pressure drops.

The mass flow rate out of the manifold and entering the cylinder for combustion is directly proportional to the open rate of the throttle valve. In the combustion internal engine, as more amount of air into the cylinder as possible for burning the fuel and then for increasing the engine power. The mass flow rate of air is measured by a sensor. The signal from this sensor is sent to the engine control unit to balance and deliver the correct fuel mass supply for the engine.

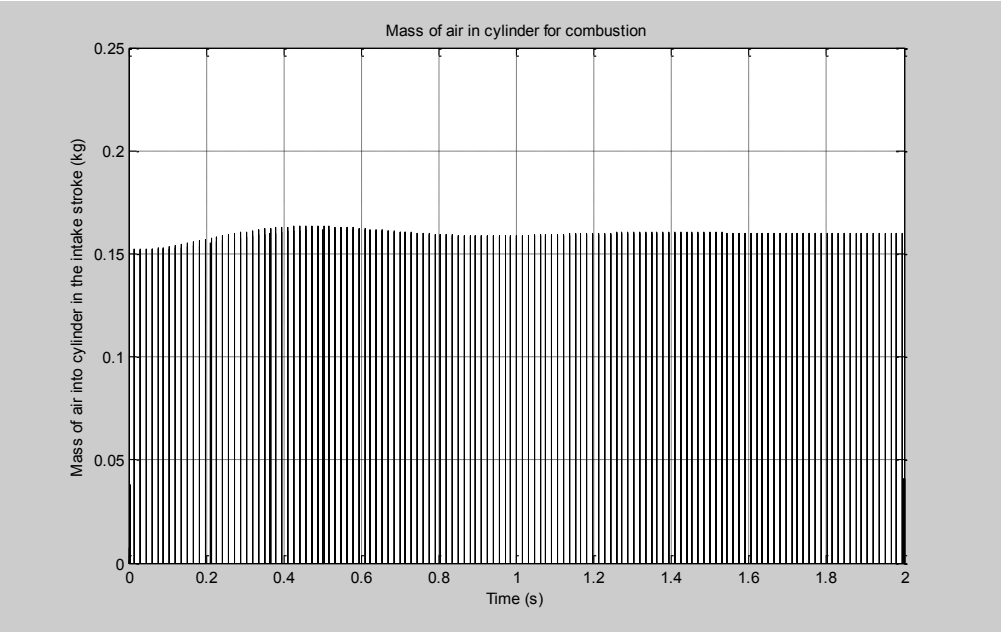

Fig.4.3. Simulation result of mass flow rate in cylinder for combustion

4.2. Engine torque

In spark-ignition (SI) engines, fuel and air mixture is prepared in advance and the mixture is ignited by the spark discharge. The spark initiates a small flame kernel that develops into a turbulent flame which propagates through the cylinder. The combustion increases the temperature and pressure which produces work on the piston. The main goal for the spark is to ignite the fuel and initiate a stable combustion, at a position that meets demands of maximizing the efficiency, fulfilling emission requirements, and preventing the engine from being destroyed. The demands are sometimes conflicting; for example at high engine loads the ignition timing for maximum efficiency has to be abandoned in favor of prevention of engine destruction by way of engine knock.

Two essential parameters are controlled with the ignition system: Ignition energy and ignition timing. The control of ignition energy is an important topic for assuring combustion initiation but the focus in this thesis is on the ignition timing that maximizes the engine torque.

The diagram of ignition system can be shown in the figure 4.4. The calculation of the spark advance must be done considering the available information on engine speed, air mass in cylinder, knock onset during the last combustion event, etc. Since the dwell-time is rather short and the ignition takes place during the compression of the gases in the cylinder, the ignition has a smaller inherent delay than the injection. The ignition is thus the fastest

actuator for a port-fuel injected SI engine.

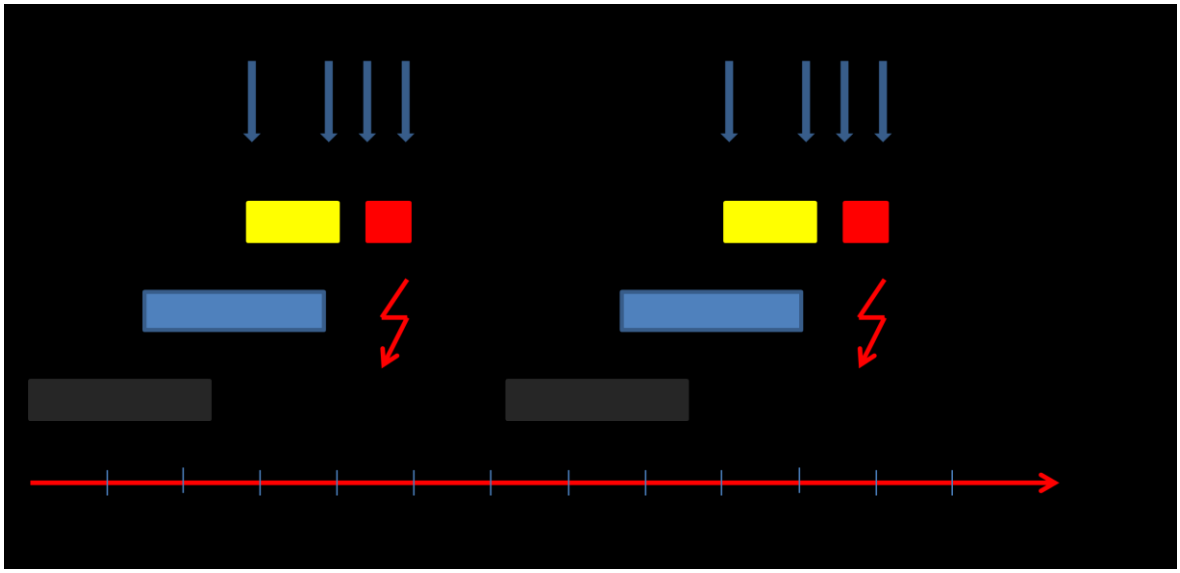

Fig.4.4. Timing diagram for the ignition [36]

- At the point a, start point for the determination of the ignition timing. The calculation is conducted by the ECU and updated continuously the ignition events and finished at the point b, then the calculated values are sent to the time – processing unit.
- The ignition delay time always occurs in the engines. This is important parameter when modeling the SI engines. In figure 4.4, the coil is connected to the battery terminals at the point c and finishes at the point d. The time between c and d is known as the dwell angle.
- At the point d, the circuit breaker is opened causing the spark to start. Normally, it happens before TDC depend on the engine speed. The early ignition is called spark advance angle. Both variables are chosen such that the thermodynamic conditions of combustion are optimized.

Changing the spark advance between c and d is possible within small limits. The case of missing a spark event must be strictly avoided because such misfires can cause severe damage to the TWC. Accordingly, increasing the spark advance is always more critical.

Misfiring is a common fault of the engine. The reasons of misfiring are bad spark plug or bad plug wires; worn distributor cap; or even a burned valve. When the misfiring occurs in one or more cylinders, the engine is not firing correctly then creates excessive engine vibration. Air/fuel mixture in that cylinder either burns incompletely or not at all, this

causes the pressure in the cylinder cannot reach the maximum value, then the engine power decreases. Figure 4.5 shows the pressure difference in the cylinder when firing and misfire.

As mentioned above, spark advance is one of the most important factor affect engine torque. Optimal ignition timing depends on how the flame propagates through the combustion chamber and the losses such as heat transfer to the wall and piston, flows into and out of crevices, and piston blow by. The flame propagation is a function of many parameters such as engine speed, engine load, engine temperature, intake air temperature, fuel quality, air/fuel ratio, and humidity. Optimal ignition timing thus depends on many engine parameters. Some of the parameters that are measured and accounted for, in today's systems, are: engine speed, engine load, coolant temperature, and intake air temperature.

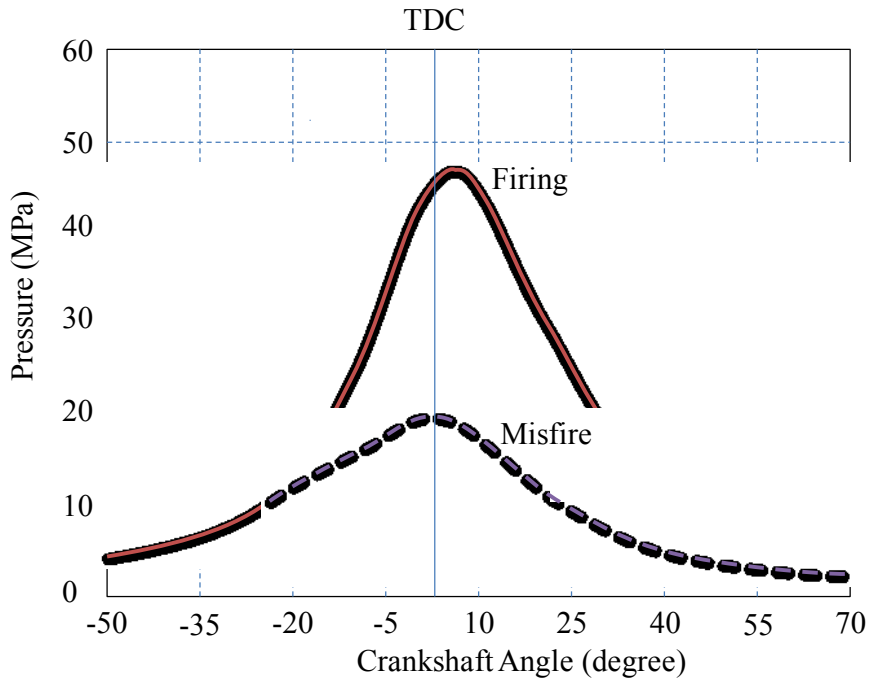

Fig.4.5. Difference of firing and misfire pressure in cylinder

Engine torque is reflected generally in the equation (2.25) in section 2. It is a function of indicate torque, friction torque, disturbance torque and pump torque.

The indicate torque T_{ind} is determined as the equations (2.26), (2.27), (2.28) and (2.29). The spark advance for maximum brake torque can be chosen from the table in figure 2.13 or can be calculated in the equation (2.30).

The friction torque T_f, which is contributed by compression rings, oil control ring, piston skirt and piston pin, and so on can be calculated by the equation (2.31). The values of

a_{1f}, a_{2f}, a_{3f} are chosen in [1] to obtain the minimum T_f.

Engine pump torque T_p and disturbance torque T_d are determined by (2.32) and (2.33), respectively.

Finally, the engine torque is obtained by substituting all the torques, which is generated in the engine into the equation (2.25). The simulation model was created as the figure 2.15. For further simply, the parameters such as air mass flow rate, air/fuel ratio, exhaust gas return (EGR) and manifold pressure are kept constant value. In this case, the simulation results show the response of the engine torque when the spark advance changes as the figure 4.6.

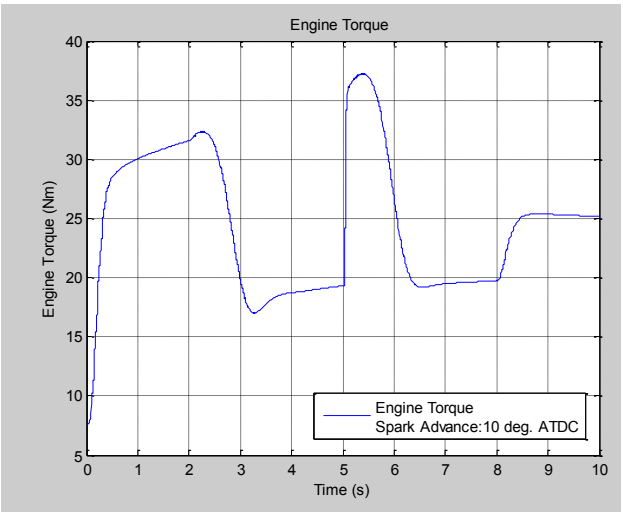

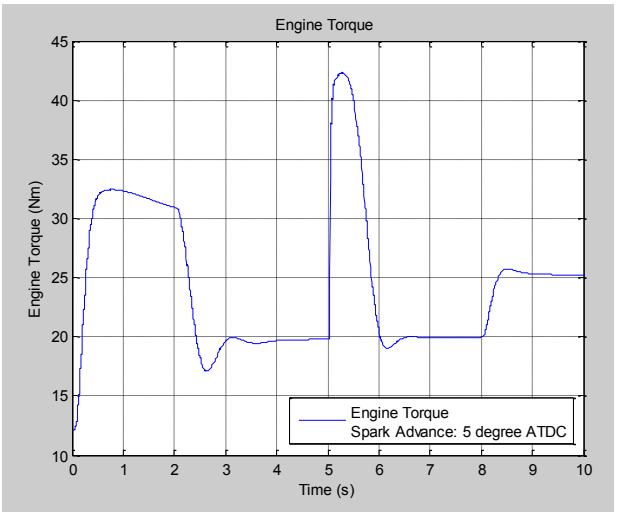

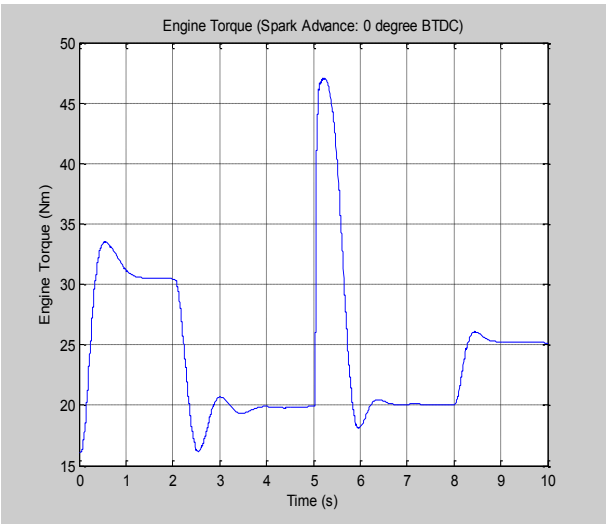

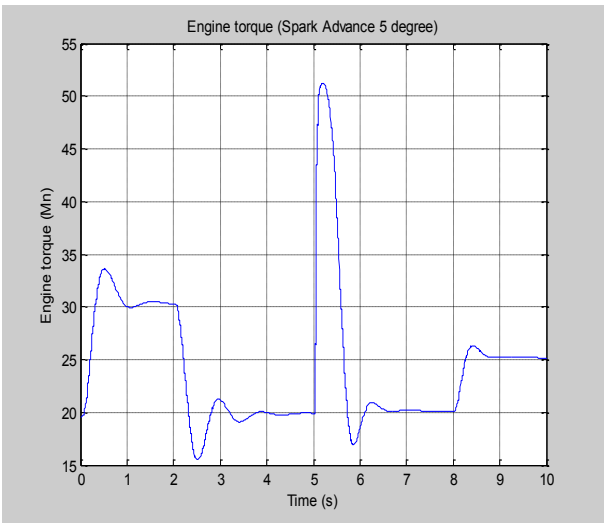

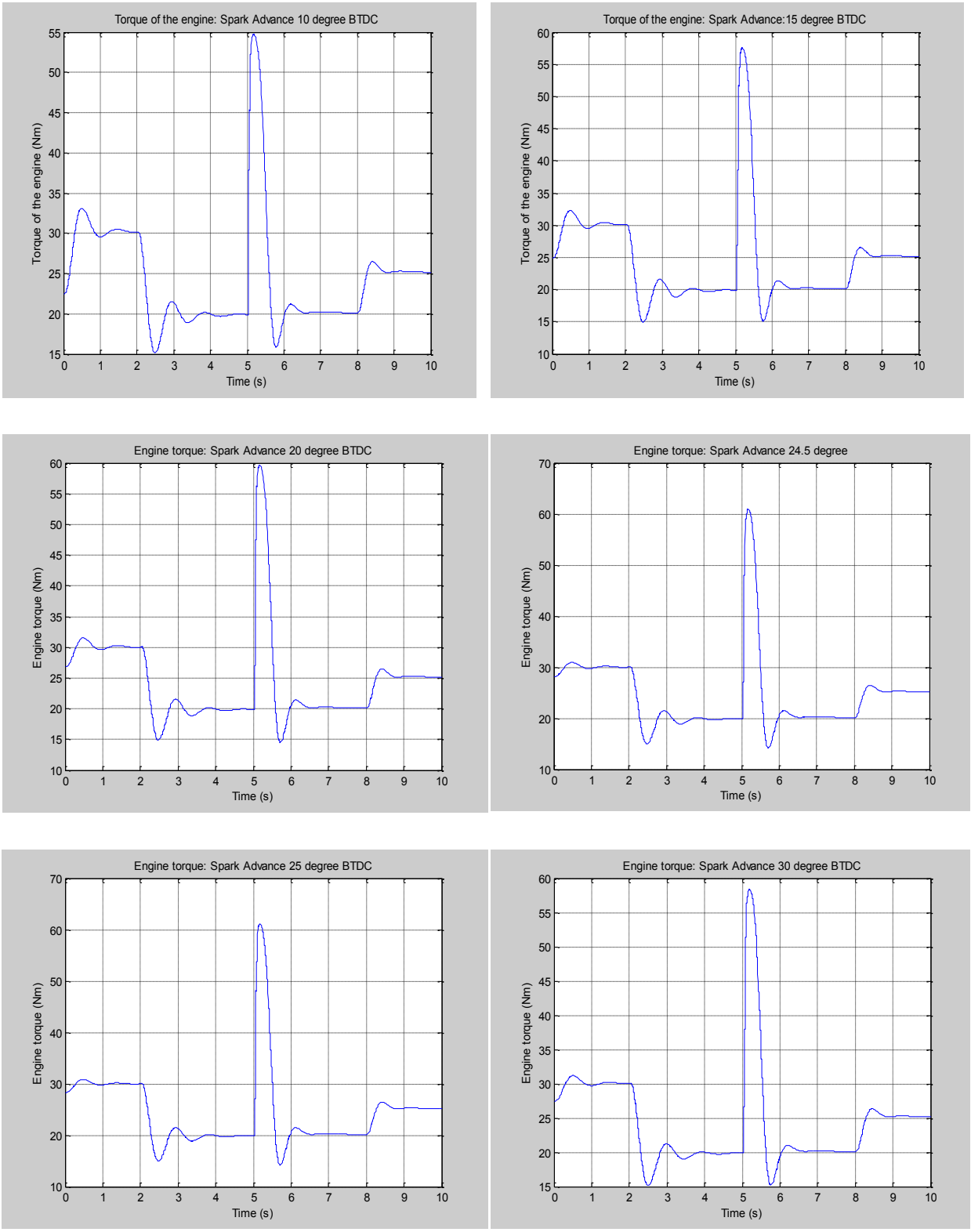

Fig.4.6. Engine torque via spark advance

From the results of simulation, it is easy to recognize that the engine torque when the plug sparks firing to burnt the mixture in the cylinders after top dead center (ATDC) is very low and out of the normal shape. It means that the engine operates with unstable state. If the

spark advance increases, the peak of engine torque also increases. But if the spark advance is greater 25 degree before top dead center, the engine torque will be decreases. Synthesis all the simulation results at many different value of spark advance, we obtain the graph as the figure 4.7.

From the simulation results of engine torque at the rotation approximately 3000 RPM and the spark advance is changed, the position for maximum brake torque (MBT) is marked, and MBT timing is approximately 24.5^0 before top dead center (TDC). This simulation results is almost the same with the real engine. The spark is positioned to the right of the MBT timing, rather than the opposite, since it reduces NOx emissions and increases the margin to knock.

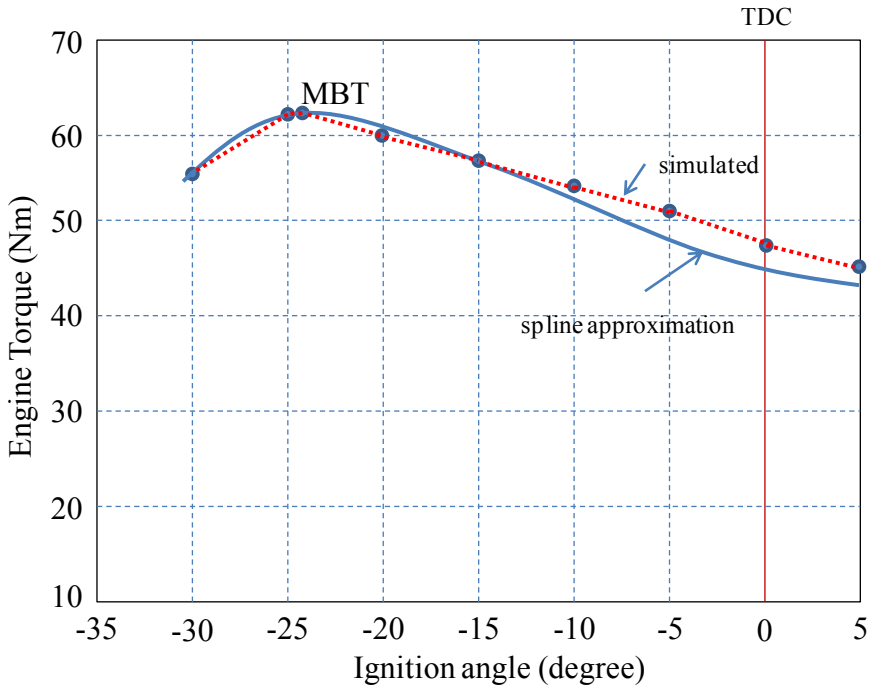

Fig.4.7. Engine brake torque as function of ignition angle

4.3. Engine speed

In spark–ignition engines, the synthesis of a control strategy at idle speed is one of the most challenging problems. The goal is to maintain the engine speed as close as possible to a reference constant engine speed despite load torque disturbances (due to e.g. the air conditioning system, the steering wheel servo-mechanism) and engagements and disengagements of the transmission occurring when the driver operates on the clutch. In order to achieve the best fuel economy, the reference engine speed is chosen at the minimum value that yields acceptable combustion and emission quality, and noise, vibration and

harshness characteristics.

Nowadays, in modern automotive engines, the hybrid system techniques have been applied to the idle speed control problem. The hybrid nature of the problem of engine control comes not only from the digital controllers used to manage an analog plant, but also from the behavior of the plant to be controlled.

The engine speed is simulated from engine model in the figure 2.18, which is combined from many submodels. The simulations were conducted at two working mode of the engine: idle speed and load. The results of simulation can be seen in the figure 4.8 and 4.9, respectively.

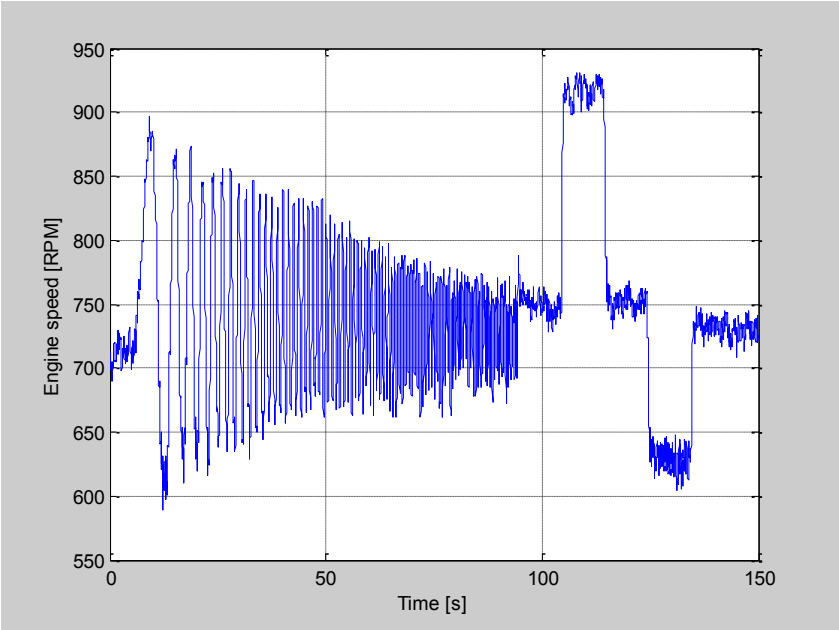

Fig.4.8. Simulation result of engine idle speed as a function of time

In fact, an accurate model of a four–stroke gasoline engine has a "natural" hybrid representation because: pistons have four modes of operation corresponding to the stroke they are in, while power–train and air dynamics are continuous–time processes. In addition, these processes interact tightly. In fact, the timing of the transitions between two phases of the pistons is determined by the continuous motion of the power–train, which, in turn, depends on the torque produced by each piston.

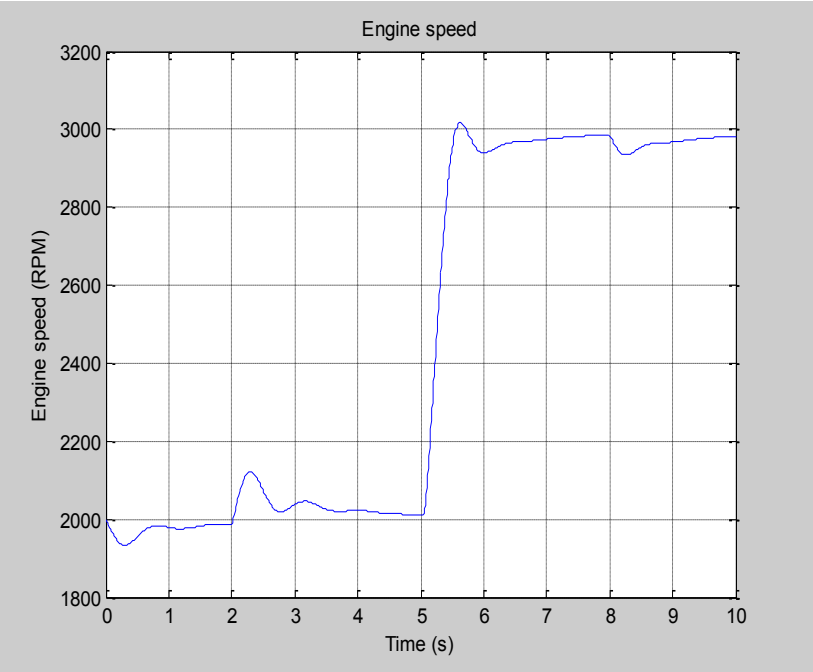

Fig.4.9. Simulation result of engine speed with load mode as a function of time

4.4. Moment of Inertia

In IC engines, moment of inertia is a very important parameter, especially in the one cylinder engine. It is the inertia of a rotating body respect to its rotation. The moment of inertia plays much the same role in rotational dynamics as mass does in linear dynamics, describing the relationship between angular momentum and angular velocity, torque and angular acceleration, and several other quantities. The flywheel in IC engine is designed to have very large moment of inertia. A large moment of inertia will require a large driving torque. The flywheel is set in rotation when the vehicle is started. It stores energy given to it as energy of rotation. Because of its large moment of inertia, it prevents the engine from stopping when the pistons are not supplying energy. The flywheel prevents the engine from accelerating too much when energy is supplied to it. In this way, it keeps the engine turning through its cycles even when the piston is not supplying power (pistons supply power for only a fraction of the total cycle time). The function of the flywheel is to make the motion of the vehicle smooth and jerk-free.

Moment of inertia of the one cylinder engine is determined by the equation (2.47) in the Section 2.1.5. It is simulated by using the Matlab program. The moment of inertia simulation result is shown in the figure 4.10

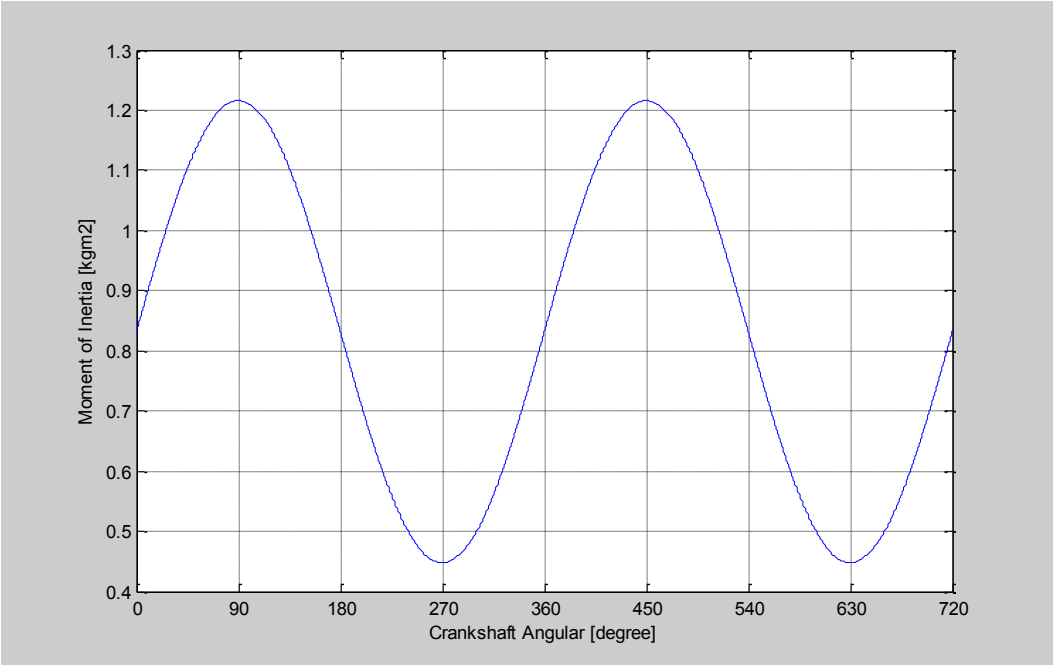

Fig.4.10. Moment of inertia of the one cylinder engine vs. angle of rotation

4.5. Crankshaft angular variation, velocity and acceleration

As stated in the targets of the thesis, acceleration of the crankshaft is the main parameter for diagnostic the IC engine. It is evaluated from the first derivative of angular velocity or second derivative of the angular variation with respect to time.

In the four stroke internal combustion engines, the piston move upward from bottom dead center (BTC) to top dead center (TDC) in the compression stroke, the intake and exhaust valves are closed and hence, the pressure increases as the gas in the cylinder is compressed. When the piston reaches near the TDC, the spark plug ignites to burn the air/fuel mixture. The combustion process of SI engines can be divided into three broad regions: ignition and flame development, flame propagation, and flame termination. Flame development is generally considered the consumption of the first 5% of the air-fuel mixture (some sources use the first 10%). During the flame development period, ignition occurs and the combustion process starts, but very little pressure rise is noticeable and little or no useful work is produced. Just about all useful work produced in an engine cycle is the result of the flame propagation period of the combustion process. This is the period when the bulk of the fuel and air mass is burned (about 80-90%). During this time, pressure in the cylinder is greatly increased, and this provides the force to produce work in the expansion stroke. The final 5% (some sources use 10%) of the air-fuel mass which burns is classified as flame termination. During this time, pressure quickly decreases and combustion stops.

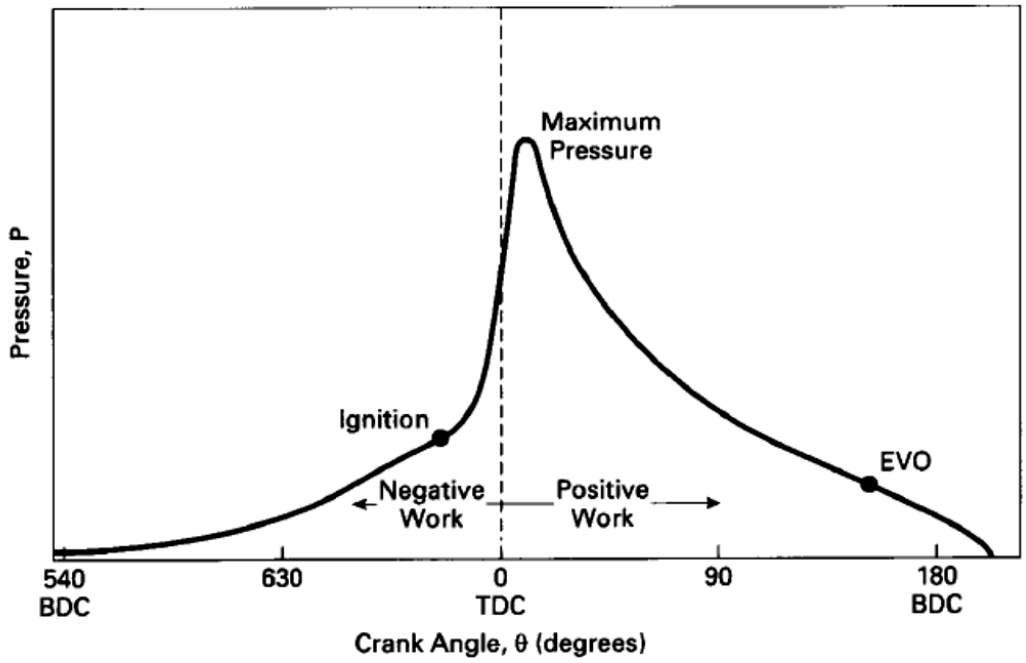

Fig.4.11. Cylinder pressure in the combustion chamber [72]

The high pressure of the gases acting on the face of the piston causes the piston to move to the BDC. The force on the piston is transmitted by the piston rod to the crankshaft, where the motion of the piston is converted to angular motion of the crankshaft (figure 2.12 in section 2). So, the crankshaft angular acceleration is the result of the force, which is caused by pressure in the cylinder acts on the top of piston in the power stroke. The higher pressure in cylinder, the greater force acting on the top of the piston and hence the crankshaft angular acceleration getting higher. It means that the state of applying work and current pressure in the cylinder can be directly reflected through the crankshaft angular acceleration.

The angular variation, angular velocity and angular acceleration of the crankshaft were described in the equations (2.51), (2.52) and (2.53) in section 2.1.5. These parameters are simulated in Matlab and the result of simulation is shown in the figure 4.12. The simulation is conducted in two revolutions to complete one working cycle of the engine. From the result of simulation, it is easy to see that the angular variation start from zero, corresponding to the position of the piston at the bottom dead center in compression stroke. It means that the angular velocity must start from zero, too. When the piston moves from bottom dead center to top dead center in compression stroke, both intake and exhaust valves are closed, so the pressure in the cylinder increases because of decreasing volume. In this case, the angular acceleration will become deceleration. In the power stroke, the air/fuel

mixture is fired and the pressure in cylinder increases rapidly. The high pressure generates the force acting on the top of piston and pushes the piston move to the bottom dead center. In this stroke, the angular velocity increases very fast, hence the angular acceleration is also increases. The process is similar in the two next strokes: exhaust and intake.

Thus, the power contribution from each cylinder can be determined by observing crankshaft acceleration and deceleration.

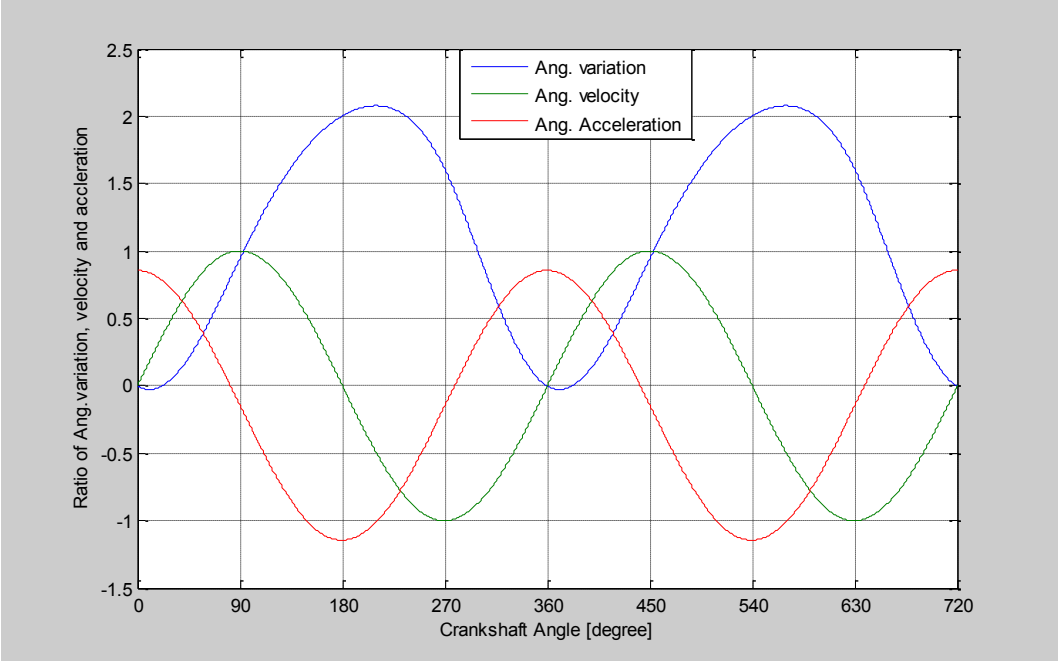

Fig.4.12. Crankshaft angular variation, velocity and acceleration

The signals from the simulation contain information about a significant number of engine parameters. By observing and analyzing these signals allow us to diagnose the engine, such as:

- Evaluate the static and dynamic compression for each cylinder
- Identify faults in the ignition system
- Evaluate the condition of the injectors
- Obtain information about the ignition timing
- Identify the rotational characteristics of the flywheel
- Identify missing and bent teeth of the flywheel

More detail explanations will be described in the section 5.

5. DIAGNOSTICS INTERNAL COMBUSTION ENGINE

Diagnostics of engines is a very important field in manufacturing, operating, and developing automotive engines and it has a long history. In the past, the engine diagnostics was performed manually and off-board. By the time, when the field of the automotive engine control develops and becomes very important because it yields benefits on several ways such as fuel efficiency, exhaust emission reduction, better delivery, and so that, on-board diagnosis also develops very quickly. Many methods of fault diagnostics for gasoline engine have been found such as vibration spectrum analyzing, vibration wavelet theory, instantaneous rotary speed analyzing, lubrication oil iron-microparticle and copper-microparticle spectrum analyzing, etc. However, fault diagnostics model-wise, there are many advantage controlling theory and algorithm models, such as neural network, expert system, heredity algorithm, fuzzy algorithm, etc.

Gas pressure in the cylinder of an engine varies throughout the Otto four-stroke engine cycle. Work is produced and consumed by acting of gas pressure at the piston during expansion and compression stroke, respectively. The gases produce energy through the combustion process. These changes in energy combined with changes in the volume of the cylinder lead to fluctuations in gas pressure. The ability to accurately predict the pressure allows for better understanding of the processes taking place in the cylinder such as the interactions between the gases, oil film, piston and liner. Cylinder pressure that is generated by engine combustion contains much information related to engine performance such as fuel burning rate, combustion heat release rate, and fuel-air ratio. Not only this, in the gasoline engine, the angle of spark ignition advanced is also a very important factor. It was estimated to be at the angle ranging from 25 to 5 degrees before top dead center (BTDC) and the burn duration is approximately ranging between 60 and 80 degree of the crankshaft rotation. Generally, the burn duration angle increases with load and, with the exception of the quarter load data, the angle spark firing becomes later with increasing load. The delay in spark firing as the inlet pressure increases is expected, however, the increase in burn duration goes against the predicted trend.

Cylinder pressure can be measured directly or indirectly. Many types of pressure transducers have been developed for the purpose of direct measurement; these provide a very high degree of precision. However, if they are installed in the engines of on-road vehicles to perform control or diagnostic duties, several problems arise. The first is the high

cost of the transducer hardware, which prohibits their use in most production on-road vehicles. Although one manufacturer has placed pressure transducers in medium-class commercial vehicles, the installation is only in the first cylinder of the SI engine. A second problem is that the poor durability of current cylinder pressure transducers makes them unfit for production vehicle use. In addition, there is little room in a vehicular engine to install transducers and associated equipment. For these reasons, the alternative of indirect methods to obtain cylinder pressures becomes attractive.

In this thesis, the engine fault diagnostics technique based on instantaneous crankshaft angular acceleration measurements will be used. Many faults caused by faulty combustion and mechanics in multicylinder engines can be detected through measurement and analysis of the crankshaft's angular acceleration. Using a low-cost magnetic sensor near the flywheel teeth, this method is easily applicable for production, service and on-board diagnosis. Errors in angular acceleration signal due to noise and limitations of the measurement procedure can be minimized by appropriate digital signal processing. The measured waveforms are interpreted based on a model describing the relationship between input variable (pressure in the combustion chamber) and output (angular acceleration).

5.1. Description of the diagnostic method

In some literatures, the signal of the crankshaft instantaneous rotating speed is utilized in SI engine fault diagnosis. In fact, the instantaneous angular acceleration and rotating speed have something in common; they both are on the basis of the rotating speed of the crankshaft. However, the instantaneous angular acceleration can reflect the state of applying work of the SI engine more powerfully than the instantaneous rotating speed does. According to Newton’s Second Law, the angular acceleration of a rotating body is proportional to the moment of couple which is acted on. It’s well known that the course of working of the SI engine is that each cylinder fires according to the ignition order at the interval of a certain crankshaft rotation angle, and each cylinder intermittently in the power stroke acts to the piston and simultaneously to the crankshaft and supplies moment of couple to drive the crankshaft, then the crankshaft gain energy and angular acceleration. So the instantaneous angular acceleration can directly reflect the state of applying work and current pressure in each cylinder. By means of analyzing the angular acceleration signal, the instantaneous engine running state and a lot of related faults can be discovered. Under the normal working conditions, the motive force performance of each cylinder is unanimous

basically, the gasoline engine operates steadily. Its angular acceleration always fluctuates in a normal range and presents certain regularity. The operation when a certain cylinder is working abnormally, the consistency of motive force is destroyed, the engine becomes bad to the stationary of operation, and the angular acceleration signal will be out of shape. By observing its fluctuation, the working process in each cylinder can be evaluated.

5.2. The relation between volume and pressure in the cylinder of SI engine

As mentioned above, pressure in the compression and power stroke in each cylinder influences directly to the instantaneous angular acceleration and depend on the volume of cylinder. This relation can be displayed by a pressure–volume diagram which represents the dependence of pressure on volume at different stages of the process of power and compression according to the Boyle's law [3].

$$p_1 V_1^n = p_2 V_2^n = C \text{ or } pV^n = C \tag{4.1}$$

Work done during the power stroke [3]:

$$W = \frac{p_1 V_1 - p_2 V_2}{n - 1} \tag{4.2}$$

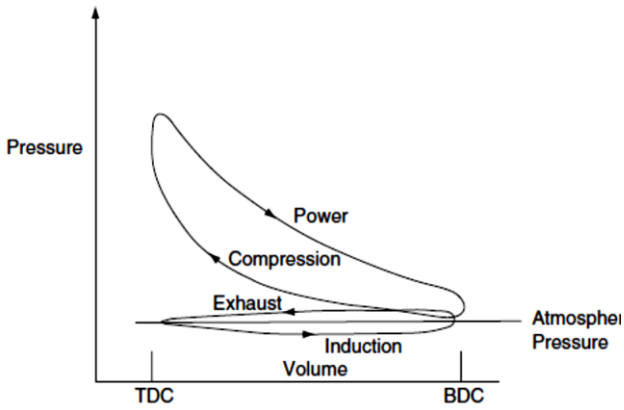

Fig.5.1. Indicator diagram for a 4-stroke engine [3]

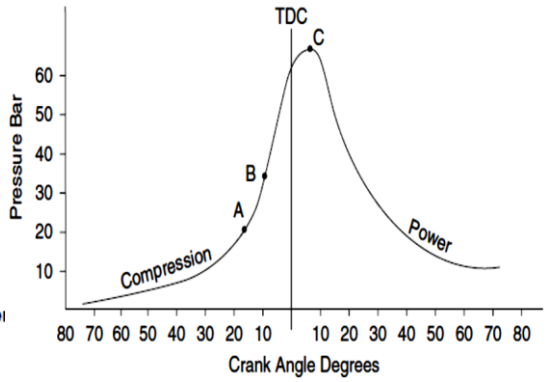

Fig.5.2. Cylinder pressure vs. crankshaft angle [3]

The peak value time of the pressure and also the angular acceleration of a SI engine is almost overlapped with the beginning of the power stroke, by the right of this; the peak of the wave of angular acceleration can be associated with the top dead center of a certain cylinder's power stroke, so the state of applying work can be directly known. In fact, the peak value time would lag behind the top dead center by a certain amount of angular degrees. According to the kinematics of the SI engine, when the piston is on the top dead

center, the arm of force acting at crankshaft is small, so the moment of couple is consequently small as well. Only after the beginning of the power stroke, the corresponding wave peak would occur.

5.3. Effect of the missing pulses in the signal from crankshaft on the frequency spectrum

As stated one time in section 2.2.3 at chapter 2, the waveform of crankshaft signal was plot as the figure 2.26. In this section, the signal will be described more detail by comparing the autospectrum of crankshaft signal in two cases.

Firstly, the measurement is conducted when flywheel has enough 60 teeth. In this case, 60 pulses are generated in one revolution of the flywheel as it is shown in figure 5.3. The horizontal axis scale is in the nominal number of revolutions what assumes the rotation at the steady state angular velocity. For the 4-stroke and 4-cylinder engine there are two revolutions corresponding to a complete period of the engine operation. The corresponding order spectrum is shown in figure 5.4. The frequency axis is not in Hertzs but in orders as a multiple of the rotational frequency. The frequency 60 ord means that during a revolution the pulse string contains 60 waves. As it was assumed that the signal is sinusoidal the order spectrum contains a single component.

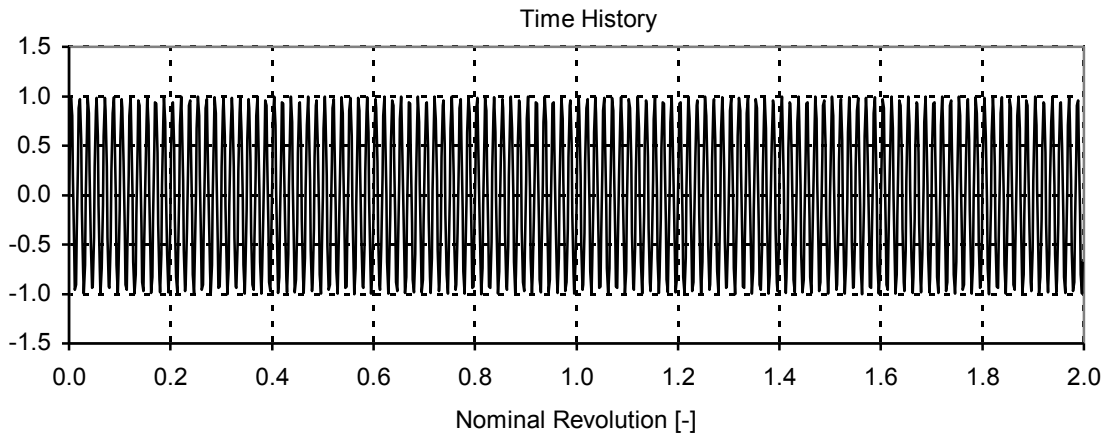

Fig.5.3. The crankshaft signal when the flywheel has enough 60 teeth

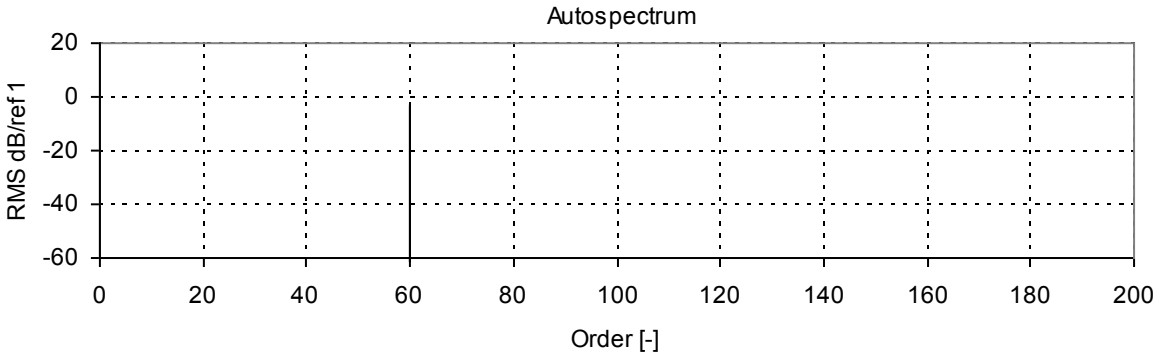

Fig.5.4. The autospectrum of crankshaft signal

In the second case, two teeth are removed from the flywheel. It means that, two pulses will be disappeared in each of the two revolutions of the crankshaft signal. Moreover, the autospectrum plot isn't a line, but it contains sidebands. The figure 5.5 and 5.6 are the plots of time history and autospectrum when two teeth are removed from the flywheel, respectively.

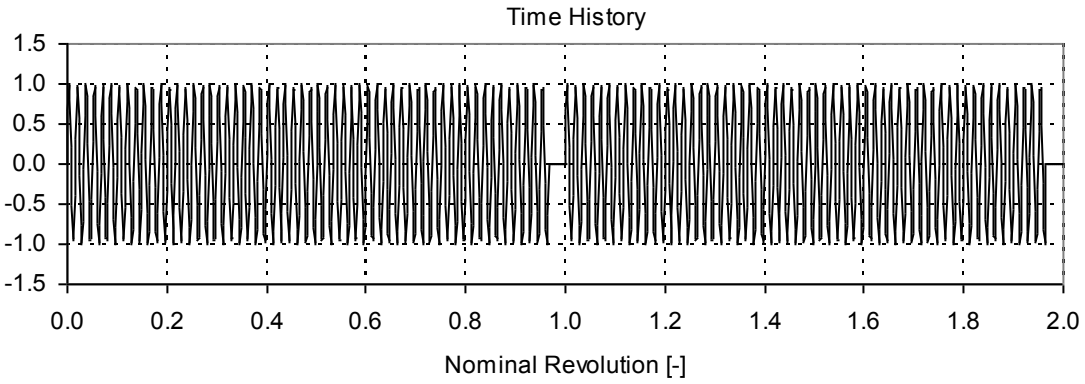

Fig.5.5. The crankshaft signal when two teeth are removed

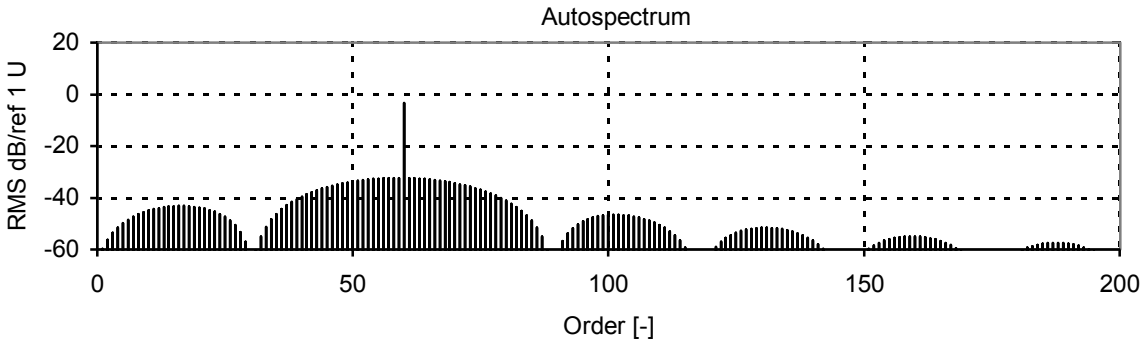

Fig.5.6. The autospectrum of crankshaft signal

The example in figure 5.5 shows that some correction of acquired row time signal is

needed. Two missing pulses have to be added as two waves of sinusoidal signal by approximation based on estimation of the pulse frequency.

5.4. Phase Demodulation using Hilbert Transform

The non-uniform rotation of the crankshaft produces a phase modulated impulse signal. The angular variation of engine crankshaft can be measured by a transducer measuring pulses generated by teeth on the engine crankshaft for the engine electronic control units (see figure 5.20). The procedure of the phase demodulation will be demonstrated on an example of a harmonic signal with a phase which is modulated by another harmonic signal. It is assumed that the signal is without missing pulses and that its frequency considered as a carrying frequency of 60 ord is modulated by a signal of 2 ord. The time record of the two engine revolution length is shown in figure 5.7. The four sections of increased density of the waves may be distinguished in this time record. This simulation corresponds to four increasing and the same number of decreasing of angular velocity due to the four firing and compression strokes.

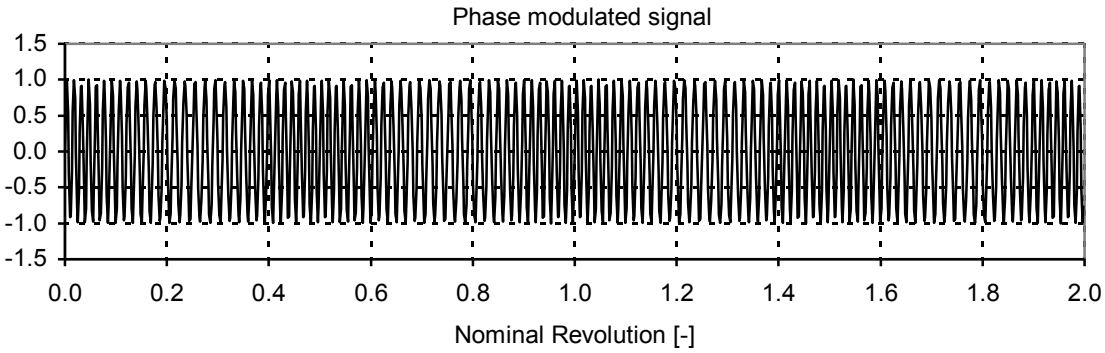

Fig.5.7. Phase-modulated signal

As the output of the crankshaft transducer is not a sinusoidal signal and therefore contains several harmonics of the basic impulse frequency the first step in phase demodulation procedure is to separate the frequency band containing a carrier component and with sideband components by using a band-pass filter.

The phase modulation signal can be calculated using an analytical signal which is created by adding an imaginary part to the measured signal. The imaginary part is the Hilbert Transform of the real part. To compare the original signal with its Hilbert transform the phase modulated signal is zoomed out at 0.1 revolutions as the figure 5.8.

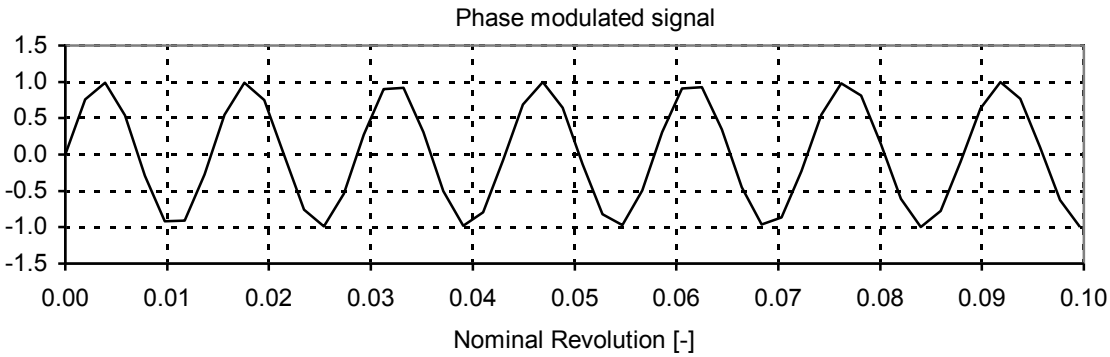

Fig.5.8. Zoom of phase-modulated signal

The modulated signal $x(t)$ in figure 5.7 is determined by the equation [69]:

$$x(t) = A\cos(\omega_0 t + \beta\cos(\omega t + \varphi(t))) \quad (4.3)$$

where:

A - amplitude. In this case, $A = 1$

$\omega_0 = 2\pi f_0$ - carrying frequency. f_0 in this example is 60 pulses (one revolution of crankshaft).

t- interval time: $t: 0 \rightarrow 2$.

β- modulation index. $\beta = 5$

ω- modulation frequency. $\omega = 2\pi.2$

So, the equation (4.3) can be rewrite:

$$x(t) = c\cos(2\pi.60.t + \beta\cos(2\pi.2.t + \varphi)) \quad (4.4)$$

The order spectrum can be seen as the figure 5.9. The carrying component is of 60 ord frequency. Note the sidebands components of the amplitude greater than the amplitude of the carrying frequency.

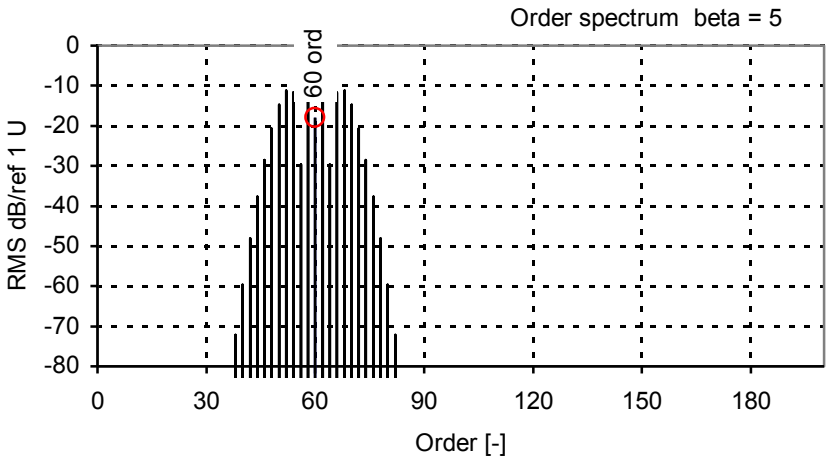

Fig.5.9. Order spectrum when $\beta = 5$

My example is $\beta = 5$, but in fact, it is much smaller. Compare the record in figure 2.26 with the record in figure 5.7. It is evident that the variation of the number of the waves in figure 2.26 cannot be distinguished. In figure 5.10 is one example when $\beta = 0.1$. The order spectrum contains only a pair of the sideband components.

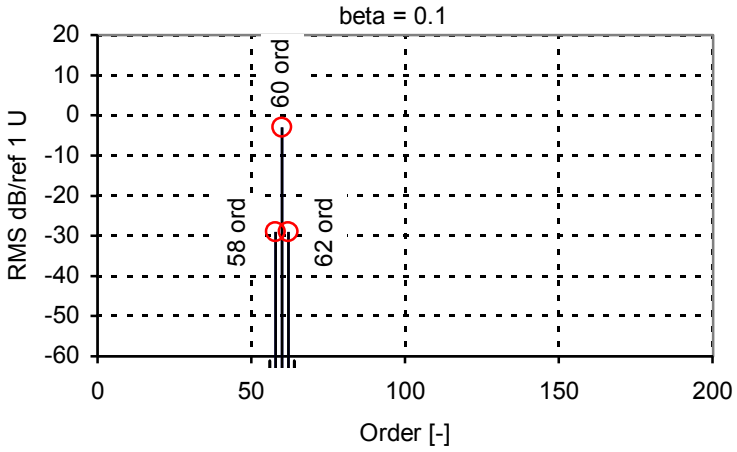

Fig.5.10. Order spectrum when $\beta = 0.1$

To compound the complex analytical signal $z(t)$, the real sampled signal $x(t)$ must be extended by an imaginary part $y(t)$ that is the mentioned Hilbert Transform of the real signal.

$$z(t) = x(t) + jy(t) = |z(t)|\exp(j\varphi(t)) \tag{4.5}$$

The relation between the FFT of $y(t)$ and $x(t)$ with the length N can be determined:

$$N_i = j\text{sign}\left(\frac{N}{2} - i\right)X_i \tag{4.6}$$

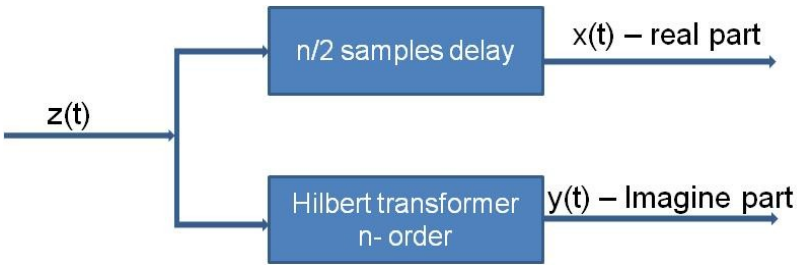

Fig.5.11. Evaluation of the analytical complex signal in real time

The original signal of Hilbert Transform with 4 period of the modulation signal can be seen in the figure 5.12.

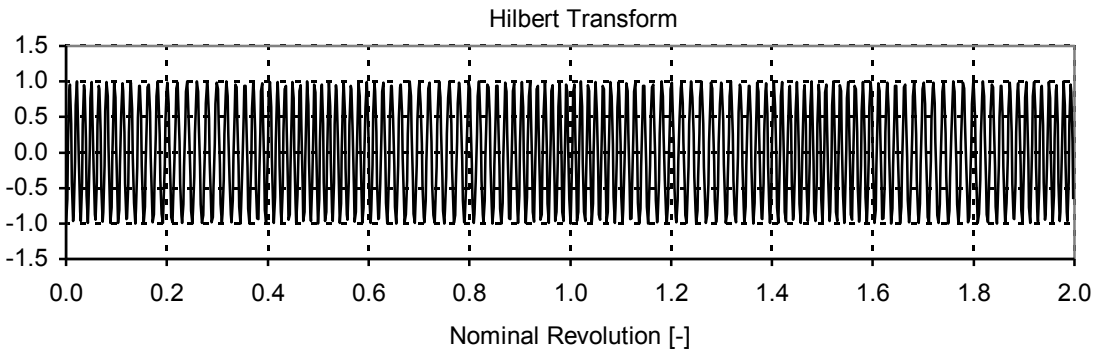

Fig.5.12. The Hilbert Transform signal

Similar to the phase modulated signal, the Hilbert Transform signal is also zoomed out at 0.1 revolutions to be observed easier as the figure 5.13.

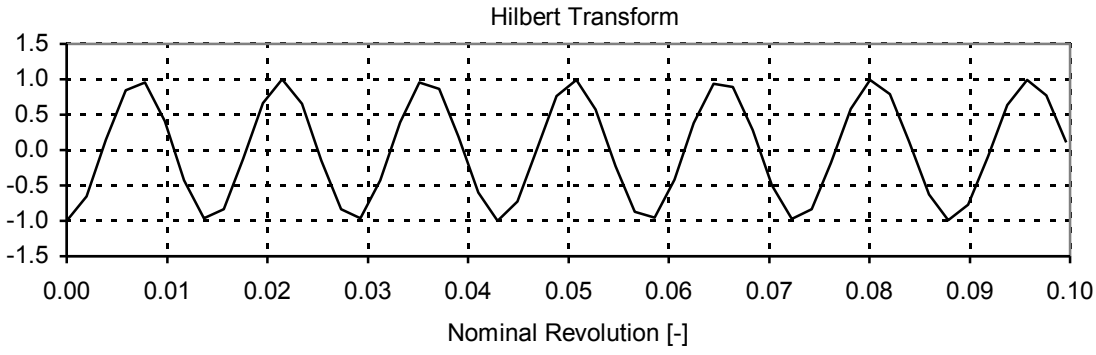

Fig.5.13. Zoom of the Hilbert Transform signal

The relation between the phase of the analytical signal and the phase of the modulation signal $\Delta\varphi(t)$ is as follows:

$$\varphi(t) = \arctan\left(\frac{y(t)}{x(t)}\right) = \omega_0 t + \Delta\varphi(t) \tag{4.7}$$

where: ω_0 is angular frequency of the carrier component. The modulation signal $\Delta\varphi(t)$ is shown in figure 5.14.

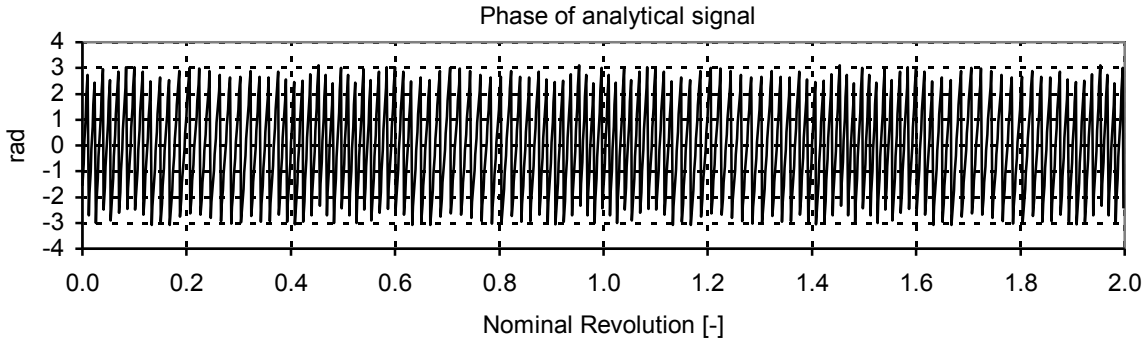

Fig.5.14. Phase of analytical signal

The ZOOM of the wrapped phase $\Delta\varphi(t)$ is shown in figure 5.15. The range of the phase is limited by 2π radians.

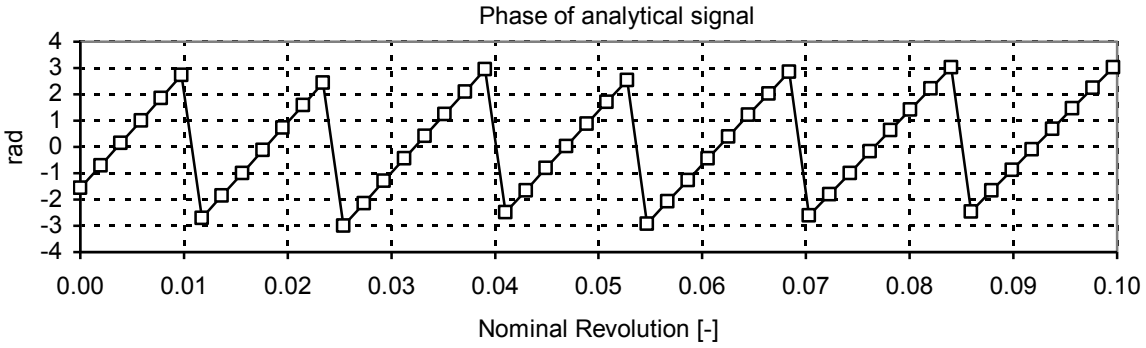

Fig.5.15. Zoom of phase of analytical signal

The angle range of the complex values from 0 to 720 angular degrees, the true angle of the analytical signal as the function with jumps at 0 to 720, must be obtained by unwrapping which is based on the fact that the absolute value of the difference between two consecutive angles is less than π radians. The unwrapped phase is shown in figure 5.16.

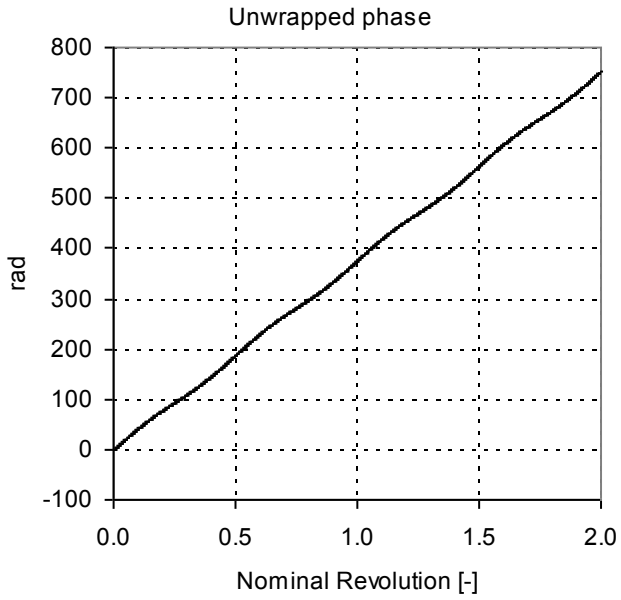

Fig.5.16. Unwrapped phase of analytical signal

The detrended phase is shown in figure 5.17. Note that the amplitude of modulation signal is the same with the modulation index in figure 5.15.

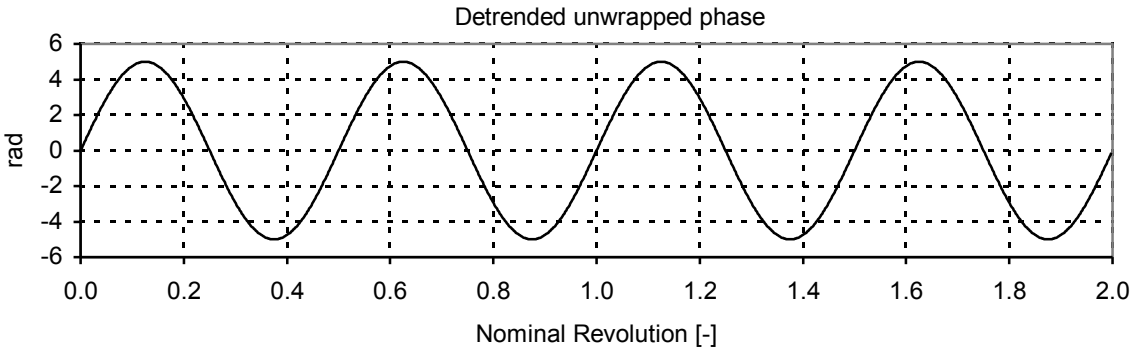

Fig.5.17. Detrended unwrapped phase of analytical signal

The phase normalization results in the diagram phase scale that corresponds to an angle of the complete revolution. The corresponding angle of rotation is a function composed from a linear term and phase modulation signal. The linear term corresponds to the steady-state rotational speed.

The phase modulation signal is the fluctuation of the rotation angle around the linear term $\omega_0 t$.

Normalized detrended unwapped phase is obtained by dividing the detrended

unwwapped phase for 60 (the number of pulses per revolution) and can be seen as the figure 5.18.

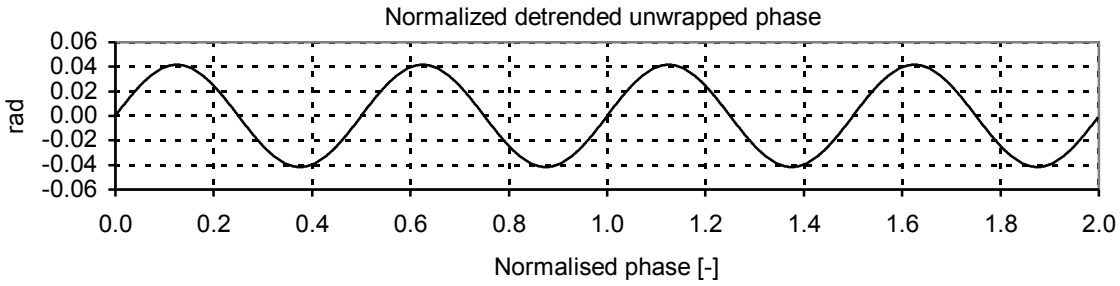

Fig.5.18. Normalized detrended unwrapped phase of analytical signal

The first derivative of the linear term with respect to time corresponds to the steady – state rotational speed, while the first derivative of the modulation signal gives the fluctuation of the rotational speed around the zero value. The second derivative of the analytical signal phase with respect to time is the same as the first derivative of the fluctuation part of the rotational speed, which is known as the angular acceleration.

5.5. Crankshaft variation measurement and evaluate the acceleration

Rotational speed of the 4-stroke / 4-cylinder spark engines running at idle varies in a certain range at the average level of 800. The purpose of measurements is to explain the source of the rotational speed non-uniformity. The first step of analysis is to identify the rotational speed variation not only in term of the complete revolutions but in terms of the basic operational stages of the engine under test. This goal of tests requires the measurement of the instantaneous rotational speed and angular acceleration.

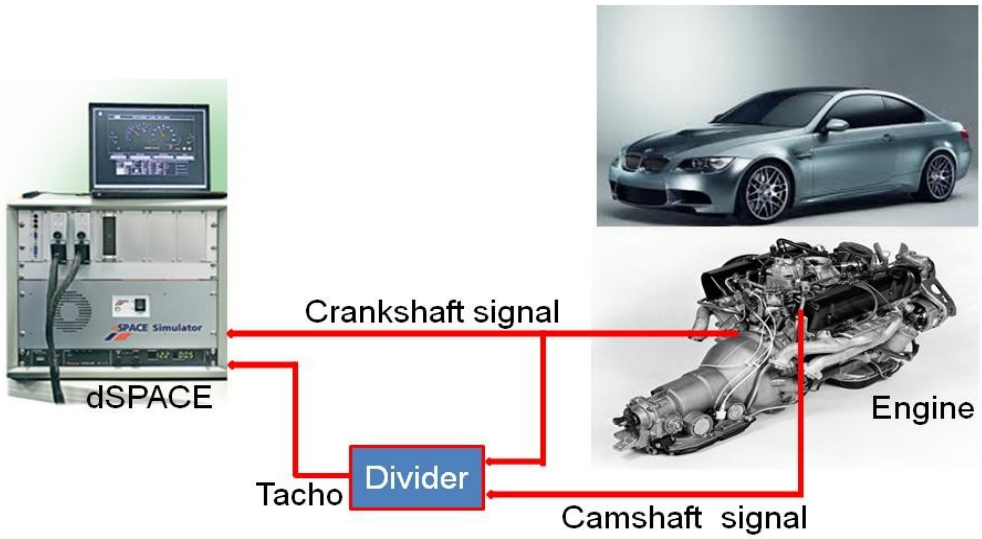

Fig.5.19. Crankshaft variation measurement

Measurements were restricted only to the time history of a pulse train that is generated by a transducer that is connected to the engine control unit. Any special device or encoder is not supposed to attach to the engine crankshaft. The transducer that is a part of engine generates 58 pulses between the gaps of 2 missing pulses. All the 58 pulses are distributed in the period of a revolution uniformly in 60 positions situated proportionally to the rotational angle. To improve accuracy of the modulation signal evaluation a computer program incorporates the missing pulses.

Simulation results of the crankshaft angular variation when the engine operates in the idle speed mode. Then, crankshaft angular acceleration is evaluated from crankshaft angular variation. In this case, engine speeds are kept around 800 RPM and changed the spark advance.

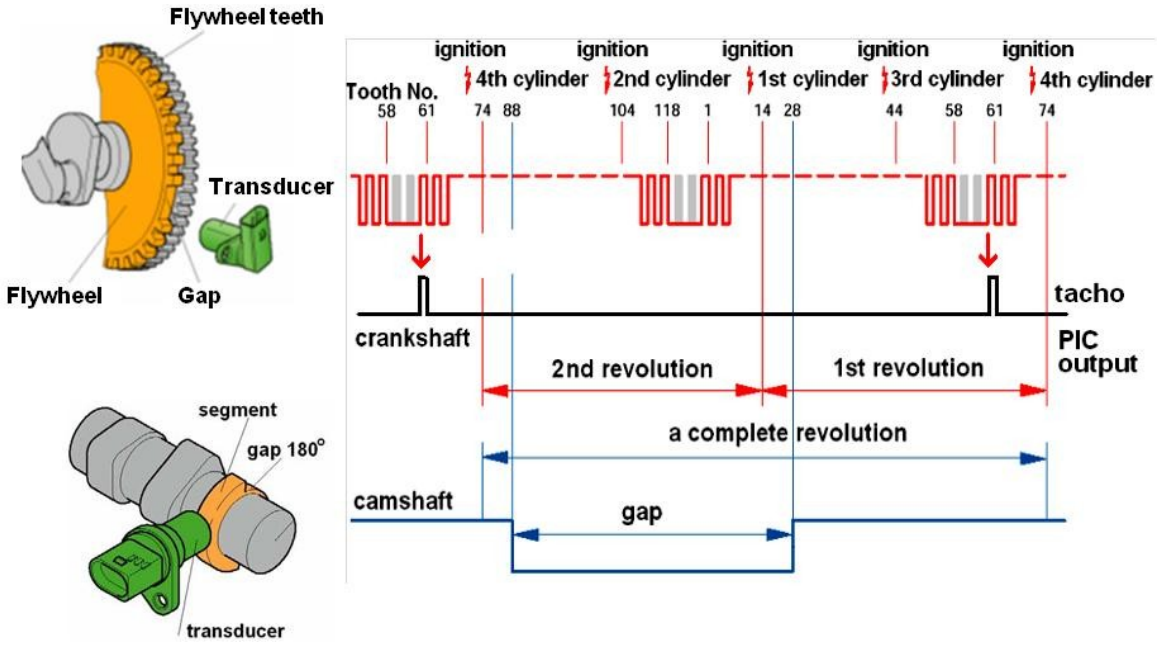

Fig.5.20. Rotational pulse signal [68]

The impulses generated by the sensor identifying the revolution of the camshaft are set to limit record to two complete revolutions.

- The angular velocity of the engine can be obtained by the first derivative of angular variation.

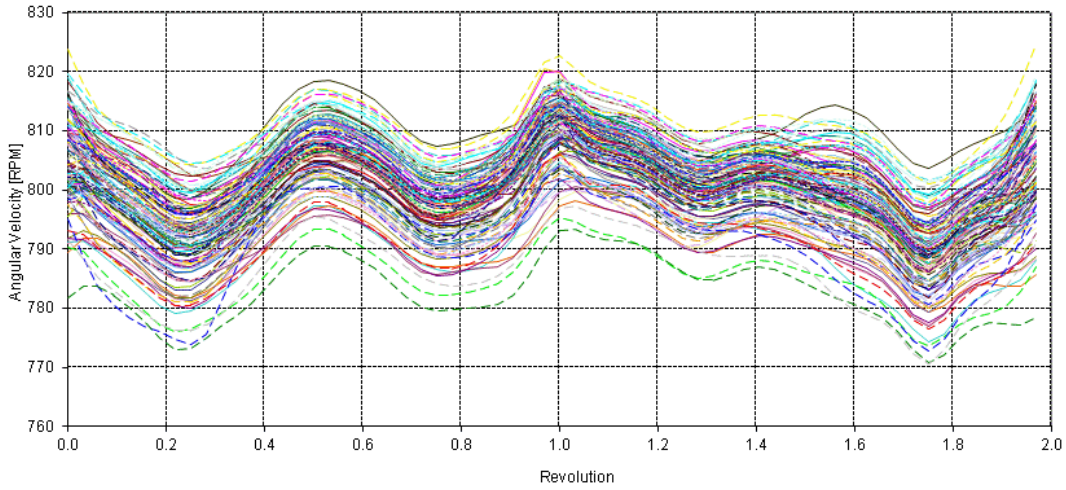

❖ The angular acceleration of the engine is obtained by the second derivative of angular variation. The phase and magnitude of angular acceleration of the engine are more harmonious between the cylinders.

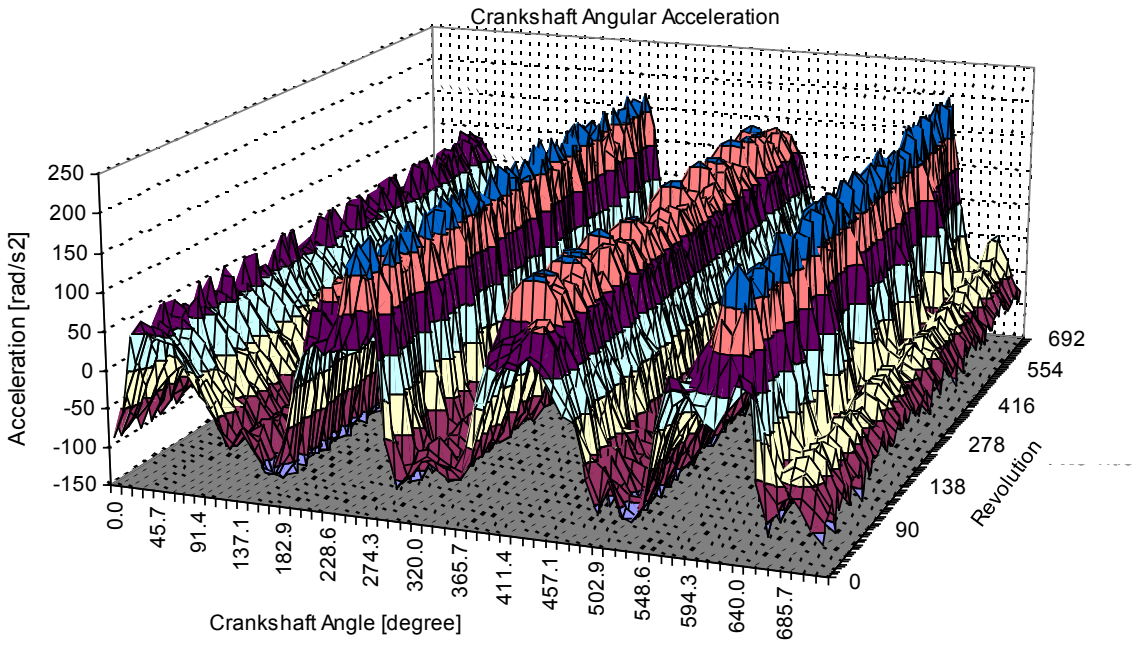

The engine was simulated and evaluated in this thesis is four cylinders spark internal combustion engine, with the fire order 1-3-4-2. From the evaluation results, it is so easy to recognize that the value of crankshaft angular acceleration of the first cylinder is less than the others. This means that, there are some faults exist in the first cylinder.

As mentioned above, the signal from crankshaft angular acceleration fluctuation reflects the state working of the engine as well as the current pressure in each cylinder. In this case, the increase rate of pressure of the first cylinder in the combustion (power) stroke

is lower than three other cylinders. The main reason of the problem is misfires. This problem causes by not only the incomplete combustion occurs and unburned fuel is followed the exhaust which burns in the hot catalytic converter, but also increases the friction, compression occurring in other cylinders, and the presence of an external engine load combine to produce a net deceleration during the power stroke. The power output usually losses 25%, the engine shakes so badly at idle speed, hard to start and may even stall at idle, depending on the accessory load (air conditioning, headlights and electric rear defroster, etc). When misfire occurs, performance suffers along with fuel economy, emissions and idle quality. Normally, when a misfiring engine is subjected to an emissions test, it will usually fail because of the unusually high levels of hydrocarbons (*HC*) in the exhaust.

Which the diagnosed engine, three problems may cause the engine misfire: loss or weak of spark; the air/fuel mixture is too lean; or loss of compression.

- The reasons of loss or weak spark are anything that prevents coil voltage from jumping the electrode gap at the end of the spark plug. Causes include worn, fouled or damaged spark plugs, bad spark plug wises or even a cracked distributor cap. A weak coil or excessive rotor gas inside a distributor would affect all cylinders, not just a single cylinder.
- The lean misfire problem can occur only when the air/fuel mixture is too lean (not enough gasoline in the mixture or the A/F ratio is greater than 1 for burning. Many reasons can be caused such as: dirty, clogged or inoperative fuel injector; air leaks; or low fuel pressure because of a weak pump, restricted filter or leaky pressure regulator. Low fuel pressure would affect all cylinders rather than an individual cylinder, as would most air leaks. The effect of the exhaust gas return (EGR) leaky is similar the air.
- When the cylinder loses most of its air/fuel mixture before be ignited, it is called loss of compression. These cases may be caused when the exhaust valve is burned or the head gasket is blown. If two adjacent cylinders are misfiring, it's likely the head gasket between them has failed. Also, if an engine is overheating or losing coolant, it's likely the head gasket is the culprit.

Misfire of the gasoline internal combustion engine is a hard fault to diagnose because it changes depending on engine load or operating conditions. It seems to occur for no clear reason. The engine may only misfire and run rough when cold but then smooth out as it

warms up. Or, it may start and idle fine but then misfire or hesitate when it comes under load. Also, it may run fine most of the time but suddenly misfire or cut out for no apparent reason.

By using the signal from crankshaft, the operating condition of the engine always under the controlled. The signal can be used not only for controlling the engine to reach the optimal power, but also for diagnostics engine. In fact, rotation speed, the instantaneous angular velocity and instantaneous angular acceleration have something in common because they are on the basic of the rotating speed of crankshaft. However, the instantaneous angular acceleration can reflect the state of applying work more powerfully than rotation speed, the instantaneous angular velocity, so it is applied in this thesis to diagnose the engine with many advantages.

6. CONCLUSION

Automotive industry has long development history. Along with the development, besides the improvement of technological factors, diagnostic also constantly developing and has gained important achievements. It is a very important field in manufacturing, operating, and developing automotive engines because it yields benefits on several ways such as fuel efficiency, exhaust emission reduction, better delivery and so on. Many diagnostic methods have been discovered and still an attractive field for the scientists.

Due to the increasing requirements, the overall demands on a modern automotive engine are that it should provide safe, good environment protection and good fuel economy. This means that there are three main objectives for engine control systems:

- Efficiency, which leads to lower fuel consumption
- Emissions should be lower to protect the environment
- Safety

As these demands, the role of testing, diagnosing engine for optimization parameters is very importance. But, if these devices are tested on the real vehicle will be expensive and consume much time. So, modeling the engine and subsystems based on mathematical model, and then connected with a Hardware-in-the-loop simulation is great solution for these problems.

With the aim above, in the thesis, engine model and some subsystems are created in Matlab/Simulink. These models are connected to HIL simulation equipment to control the engine. The results of simulation subsystems will be compared with standard data to diagnose some sensors, actuators, as well as engine ECU. I specially focus on the rotational signal from crankshaft sensor, which not only for defining the amount of fuel distributing for cylinders and to control advanced ignition angle, but this signal also used for evaluating angular velocity and angular acceleration – the very important factor to diagnose the health of the engine in the thesis. The engine model developed also could be useful for controller development for other modes of engine operation as well such as transient operation, steady state running, etc.

The thesis solved the problems:

- Describing generally equipments in the modern car and engine. The requirements with

the modern engine to reduce the fuel consumption and the emission of pollutant species, to increase safety, and also improving its reliability. It started the overview of automotive engine control with many sensors, actuators and electronic control unit (ECU) and the exchange signal between them. Moreover, many main control loops in spark ignition engines such as: air/fuel ratio control; ignition control; knock control and idle speed control are shown. Some methods of diagnostic automotive engine are presented as well.

- Extending the engine model of Weeks, R.W. & Moskwa, J.J. by modeling of the non-uniform driving torque in contrast to the original model assuming uniform driving torque. The thesis contains a description of the individual subsystems in the simulation program Matlab/Simulink from linear to none linear form. It begins with an overview of the engine and control system model briefly describing the various subsystems such as throttle body; intake manifold; torque generation; sensors and actuators. The equation for calculating the mass moment of inertia was found, and then written in Matlab program to show the response of the engine during the simulation process. The "brain" of the engine for controlling ECU was also modeled with many inputs from the sensors and many outputs to actuators. Angular variation equation of the engine was special attended, because the crankshaft acceleration which was evaluated from second derivative of angular variation is the main object to diagnose the engine. The simulations also are used to find out the spark advance to obtain the maximum brake torque (MBT).
- Introduction briefly the structure and functions of dSpace and Hardware-in-the-loop (HIL) simulation equipments, which was used to measure and evaluate the data for diagnostic engine. Signal flows in a real system for simulating the engine were presented also. Moreover, diagnostic - one important function of HIL was introduced quite clearly.
- Many results of the simulation engine and subsystems models were shown. These results display the relation between throttle angles and throttle flow with the throttle plate angle; manifold pressure and flow rate of air out of the manifold; mass flow rate in the cylinder for combustion. Torque of engine at some values of spark advance was simulated to compare and found out the best angle to obtain the maximum brake torque (BMT). Engine speed (include idle and load mode) and moment of inertia which describing the relationship between angular momentum and angular velocity, torque and angular acceleration were presented, as well. Crankshaft angular variation,

velocity and acceleration are one of the most important simulation results. It is used as the reference standard form to compare and diagnose the IC engine. By observing and analyzing these signals allow us to diagnose the engine such as evaluate the static and dynamic compression for each cylinder; identify faults in the ignition system; evaluate the condition of the injectors; obtain information about the ignition timing; identify the rotational characteristics of the flywheel; identify missing and bent teeth of the flywheel.

- Diagnostic internal combustion engine. This is the main work of the thesis. By approving the reason why the instantaneous angular acceleration of crankshaft is used for diagnostic engine, the relation between volume and pressure in the cylinder was presented. Phase demodulation using Hilbert transform was used as the method to evaluate the crankshaft angular acceleration. Non-uniform of angular acceleration at many spark advances was evaluated to diagnose the engine.

7. REFERENCES

[1] STOTSKY, A.A. 2009. *Automotive engine - Control, Estimation, Statistical Detection.* Spring. ISBN 978-3-642-00163-5, e-ISBN 978-3-642-00164.

[2] BONNICK, A.W.M. 2001. *Automotive Computer Controlled Systems: diagnostic tools and techniques*. Great Britain. ISBN: 0-7506-5089-3.

[3] BONNICK, A.W.M. 2008. *Automotive Science and Mathematics*. Elsevier Ltd. ISBN: 978-0-7506-8522-1

[4] NASSRHARAND, A.; SZE HONG THE. 2010. *Application of Describing Function Technique to Idle Speed Control.* American Control Conference. Pp 5351-5355.

[5] FIJALKOWSKI, B.T. *Automotive Mechatronics: Operational and Practical Issues (Volume 1, 2).* Springer. e-ISBN 978-94-007-0409-1.

[6] FRITZSCHES, C. & DUNOW, H.P. *Advanced Torque Control. New Approaches in Automation and Robotics.* ISBN 978-3-902613-26-4, pp. 392, May 2008, I-Tech Education and Publishing, Vienna, Austria.

[7] BAUMGARTEN, C. 2006. *Mixture Formation in Internal Combustion Engines.* Springer. ISBN-13 978-3-540-30835-5.

[8] CLOSE, C.M.; FREDERCK, D. H. & NEWELL, J. C. 2001. *Modeling and Analysis of Dynamic Systems*. United States of America. ISBN 0-471-39442-4

[9] RAKOPOLOS, C.D. & GIAKOUMIS, E. G. 2009. *Diesel Engine Transient Operation. Principles of Operation and Simulation Analysis.* Springer. e-ISBN 978-1-84882-375-4.

[10] SILVERLIND, D. 2001. *Mean Value Engine Modeling with Modelica*. Master thesis.

[11] PROKHOROV, D. 2008. *Computational Intelligence in Automotive Applications.* Springer-Verlag Berlin Heidelberg. e-ISBN 978-3-540-79257-4.

[12] SCHWARZMANN, D. 2007. *Nonlinear Internal Model Control with Automotive Applications.* PhD Thesis.

[13] EI EI MOE, ZAW MIN AUNG & KYAWT KHIN. 2010. *Design and Simulation of Air-Fuel Ratio Control System for Distributorless CNG Engine*. pp776-779.

[14] SHER, E. 1998. *Handbook of Air Pollution from Internal Combustion Engines Pollutant Formation and Control*. United States of America. ISBN: 0-12-639855-0.

[15] F. ZHAO; M.-C. LAI; D.L. HARRINGTON. 1999. *Automotive spark-ignited direct-injection gasoline engines*. Great Britain. ISBN: 0-08 043676-5.

[16] CONNOLLY, F. T. & YAGLE, A. E. 1994. *Modeling and Identification of the Combustion Pressure Process in Internal Combustion Engines*. Mechanical Systems and Signal Processing. P. 01-19.

[17] JONES, F. & JEZEK, C. 2008. *Diesel Combustion Modeling and Simulation for Torque Estimation and Parameter Optimization*. Master's thesis.

[18] BENGTSSON, F. 2006. *Estimation of Indicated - and Load - Torque from Engine Speed Variations*. Master Thesis.

[19] VACHTSEVANOS, G.; LEWIS, F.; ROEMER, M.; HESS A. & BIQING WU. 2006. *Intelligent fault diagnosis and prognosis for engineering systems*. USA. ISBN - 13: 978-0-0471-72999-0.

[20] GERARD, C. & MEIJER, M 2008. *Smart Sensor Systems*. Great Britain. ISBN: 9780470866917.

[21] GUNTER, P.M; SCHWARZ, C. & TEICHMANN, R. 2009. *Combustion Engines Development: Mixture Formation, Combustion, Emissions and Simulation*. Springer. e-ISBN 978-3-642-14094-5.

[22] KRISP, H.; LAMBERG, K. & LEINFELLNER, R. 2007. *Automated Real-Time Testing of Electronic Control Units*. USA. ISSN 0148-7191.

[23] MAREK, J. H.; MAREK, P. T.; SUZUKI, Y. & YOKOMORI, I. 2003. *Sensors for Automotive Applications.* (Sensors Applications Volume 4). ISBN: 3-527-29553-4.

[24] GRIZZLE. J. W.; BUCKLAND, J. and JING SUN. *Idle Speed Control of a Direct Injection Spark Ignition Stratified Charge Engine*. Invited paper for Int. J. Rob & Non-Lin Control, John Wiley.

[25] GRIZZLE, J.W.; COOKTAND, J.A. & MILAMI, W.P. 1994. *Improved Cylinder Air Charge Estimation for Transient Air Fuel Ratio Control*. Proceeding of the American Control Conference. Baltimore, Maryland. Pp1568-1573.

[26] HALDERMAN, J. D. *Automotive fuel and emissions control systems*. Prentice Hall ISBN 13: 978-0-13-254292-0.

[27] BALL, J. K. & BOWE, M. J. *Torque Estimation and Misfire Detection using Block Angular Acceleration.* SAE 2000 World Congress Detroit, Michigan. March 6-9, 2000. ISSN 0148-7191.

[28] HALDERMAN, J. 2012. *Automotive Technology: Principles, Diagnosis, and Service* (Fourth edition). Prentice Hall. ISBN-13: 978-0-13-254261-6.

[29] WEBSTER, J. G. (Editor-in-Chief). 1999. *Measurement, Instrumentation, and Sensors Handbook.*

[30] MOSKVA, J. J.; HEDRICK, J. K. *Automotive engine modeling for real time control application.*

[31] JAMES, J. V.; LAKE, W.; DOSDALL, J.M.; ILE, G.; MARKO, K. A. & ARBOR, A. 1992. *Determining Crankshaft Acceleration in an Internal Combustion Engine.* United States Patent.

[32] VALLDORF, J & GESSNER, W. 2007. *Advanced Microsystems for Automotive Applications.* Springer Berlin Heidelberg New York. ISBN-13 978-3-540-71324-1.

[33] KIHONG SHIN & HAMMOND, J. K. 2008. *Fundamentals of Signal Processing for Sound and Vibration Engineers.* John Wiley & Sons Ltd. ISBN-13 978-0470-51188-6.

[34] LAMBERG, K.; FLEISCHER, D. *One-Stop Solutions - ECU Test and Diagnostics Converging.* dSPACE GmbH.

[35] ERICKSSON, L. 1999. *Spark Advance Modeling and Control.* Sweden. ISBN 91-7219-479-0.

[36] GUZZELLA, L.; ONDER, C. H. 2010. *Introduction to Modeling and Control of Internal Combustion Engine Systems*. ISBN 978-3-642-10774-0.

[37] SMUTNY, L.; TUMA, J. & FARANA, R. *Calibration of Sensors for Angular Vibration Measurements.* XVIII Imeko World Congress Metrology for a Sustainable Development. September, 17 - 22, 2006, Rio de Janeiro, Brazil.

[38] DEL RE, L.; ALLGOWER, F.; GLIELME, L.; GUARDIOLA, C. & KOLMANOVSKY, L. 2010. *Automotive Model Predictive Control: Models, Methods and Applications*. Springer. e-ISBN 978-1-84996-071-7.

[39] FARFAN-RAMOS, L. 2011. *Real-time Fault Diagnosis of Automotive Electrical Power Generation and Storage System*. Master Thesis.

[40] HELLSTROM, M. 2005. *Engine Speed Based Estimation of the Indicated Engine Torque.* Master Thesis.

[41] CONCEPCION, M. 2011. *Diagnostics Strategies of Modern Automotive Systems.*USA.

[42] SCHMIDT M.; KIMMICH, F.; STRAKY, H. & ISERMANN, R. *Combustion Supervision by Evaluating the Crankshaft Speed and Acceleration.* Electronic Engine Controls 2000. ISSN 0148-7191.

[43] GEVECI, M.; OSBURN, A. W. & FRANCHEK, M. A. 2005. *An investigation of crankshaft oscillations for cylinder health diagnostics.* Mechanical Systems and Signal Processing 19. pp1107-1134.

[44] FELDMAN, M. 2011. *Hilbert Transform Applications in Mechanical Vibration*. Wiley. E-PDF ISBN 9781119991649.

[45] MINGHUI KAO & MOSKWA, J.J. 1994. *Model-Based Engine Fault Detection Using Cylinder Pressure Estimates from Nonlinear Observers*. Proceedings of the 33rd Conference on Decision and Control Lake Buena Vista. pp2742-2747.

[46] DINLER, N. & YUCEL, N. 2010. *Combustion simulation spark ignition engine cylinder: Effects of air-fuel ratio on the combustion duration*. Thermal science. pp. 1001-1012.

[47] LARSES, O. 2003. *Modern Automotive Electronics from an OEM perspective*. Stockholm.

[48] WALTERMANN, P. 2009 Hardware-in-the-Loop: *The Technology for Testing Electronic Controls in Automotive Engineering*. dSPACE GmbH.

[49] REN YUNPENG, HU TIANYOU, YANG PING & LIU XIN. *Approach to Diesel Engine Fault Diagnosis Based on Crankshaft Angular Acceleration Measurement and its Realization*. Proceedings of the IEEE International Conference on Mechatronics & Automation Niagara Falls, Canada. July 2005. pp 1451 - 1454.

[50] ATKINS, R. D. 2009. *An Introduction to Engine Testing and Development.* United States of America. ISBN 978-0-7680-2099-1

[51] ZURAWSKI, R. 2009. *Automotive Embedded Systems Handbook*. United States of America. ISBN-13: 978-0-8493-8026-6.

[52] LONGXIN ZHEN; ZIJUN AN & QIANG LI. *Calculate Engine Crankshaft Angular Acceleration Based on Original Flywheel Data*. ISBN: 978-1-4244-7739-5.

[53] BOND, R. R. 2011. *Vibration-based condition monitoring: industrial, aerospace and automotive applications*. John Wiley & Sons Ltd. ePDF ISBN: 978-0-470-97765-1.

[54] WEEKS, R. W. & MOSKWA J. J. *Automotive Engine Modeling for Real-Time Control Using Matlab/Simulink*. SAE 950417.

[55] CRISTI, R. *Modern Digital Signal Processing*. USA.

[56] STUDENER, S. *Combustion Engine Air Intake Theoretical Modeling, Model-Verification & Application to Optimal Valve Actuation*. ITK Engineering AG, Lochhamer Straße 15 D-82152 Martinsried, Germany.

[57] BEEBY, S.; ENSELL, G.; KRAFT, M. & WHITE, N. 2001. *MEMS Mechanical Sensors*. Boston-London. ISBN: 1-58053-536-4.

[58] KOHL, S. & JEGMINAT, D. 2005. *How to Do Hardware-in-the-Loop Simulation Right*. SAE World Congress. ISSN 0148-7191

[59] TAKAFUMI NAGANO, TAKASHI IWAMOTO & TOMOKO TANABE. 2009. *Angular Velocity/ Angular Acceleration Calculator, Torque Estimator, and Combustion State Estimator*. United States Patent.

[60] SEKOZAWA, T. *Model-based Control and Learning Control Method for Automobile Idle Speed Control using Electric Throttle*. WSEAS TRANSACTIONS on SYSTEMS and CONTROL. ISSN: 1991-8763. Pp.125-136.

[61] GILLES, T.2011. *Automotive Engines: Diagnosis, Repair and Rebuilding* (6th Edition). United States of America. ISBN-13: 978-1-4354-8641-6.

[62] DENTON, T. 2004. *Automobile Electrical and Electronic Systems* (Third edition). Great Britain. ISBN 0 7506 62190.

[63] DENTON, T. 2006. *Advanced Automotive Fault Diagnosis*. United Kingdom. ISBN - 13: 978-0-75-066991-7.

[64] TUMA, J. 2004. *Angular Vibration Measurements of the Power Driwing Systems*. Acta Metallurgica Slovaca. pp245 - 252.

[65] TUMA, J. 2003. *Signal Phase demodulation of impulse signals in machine shift angular vibration measurements*. In Proceedings of Tenth international congress on sound and vibration. Stockholm.

[66] TUMA, J. 2008. *Laser Doppler vibrometer and impulse signal phase demodulation in rotation uniformity measurements*. In Proceedings of 15th International Congress on Sound and Vibration. Daejeon, Korea.

[67] TUMA, J.; KOCI, P.; SKUTA, J. & JURAK, M. 2002. *Analysis of a car burst shaking while the car engine is running at idle.* In proceeding of 3rd International Carpathian Control Conference. Ostrava: VŠB-TU Ostrava. pp105-110. ISBN 80-248-0089-6.

[68] TUMA, J. *Lecture on Angular Vibration Measurements Based on Phase Demodulation.* VSB Technical University of Ostrava. Czech Republic.

[69] TUMA, J. 2009. *Signal processing*. VSB Technical University of Ostrava. Czech Republic.

[70] KIENCKE, U. & NIELSEN, L. 2005. *Automotive Control Systems: For Engine, Driveline, and Vehicle* (Second edition). Germany. ISBN 3-540-23139-0.

[71] WEBSTER, J. G. 1999. *The measurement, instrumentation, and sensors handbook*. CRC Press LLC, Boca Taton, Florida.

[72] PULKRABEK, W. W. *Engineering Fundamentals of the Internal Combustion Engine.* Prentice Hall.

[73] RIBBENS, W. B. 1998. *Understanding Automotive Etrectronics*. USA. ISBN 0-7506-7008-8

[74] YAOJUNG SHIAO & MOSKWA, J. J. 1995. *Cylinder Pressure and Combustion Heat Release Estimation for SI Engine Diagnostics Using Nonlinear Sliding Observers*. IEEE Transactions on Control Systems Technology. Vol 3, no.I. pp70-78.

[75] YILDIZ, Y.; ANNASWAMYA, A. M.; YANAKIEVB, D. & KOLMANOVSKY, I. 2009. *Spark Ignition Engine Fuel-to-Air Ratio Control: An Adaptive Control Approach.*

[76] NILSSON, Y. 2007. *Modeling for Fuel Optimal Control of a Variable Compression Engine.* Sweden. ISBN 978-91-85831-36-4.

[77] YU SHI, HAI WEN GE and REITZ, R. D. 2010. *Computational Optimization of Internal Combustion Engines.* Springer. e-ISBN 978-0-85729-619-1.

[78] YUE-YUN WANG, IBRAHIM HASKARA, CHOL-BUM M KWEON, FREDERIC ANTON MATEKUNAS & PAUL ANTHONY BATTISTON. 2010. *Fuel System Diagnostics by Analyzing Engine Cylinder pressure Signal and Crankshaft Speed Signal.* United States Patent.

[79] KIERNICKI, Z. 2005. *Some output parameters of indirect injection diesels running on rape biofuel under transient conditions*. TEKA Kom. Mot. Energ. Roln. pp87-95.

[80] http://forums.pelicanparts.com/porsche-911-technical-forum/279322-megasquirt-setup-930-dual-plug-edis-3.html.

[81] http://en.wikipedia.org/wiki/Fuel_injection

[82] http://www.hitachi-c-m.com/global/products/excavator/wheel/zx170w-3/feature_1.html

[83] http://kids.britannica.com/comptons/art-89315/An-internal-combustion-engine-goes-through-four-strokes-intake-compression

[84] http://universityoftoyota.com/

[85] Using Simulink and Stateflow in Automotive Application. www.mathworks.com.

[86] HEDRICK, C. D. 1989. *Automotive Powertrain Modeling for Control.* ASME Journal of Dynamic Systems Measurement and Control, vol. 111, December, pp.568-576.

8. LIST OF MY PAPERS

[1] LE KHAC BINH, PETR KOCI. *The Effect of Air Gap, Wheel Speed and Drive Angle on the Anti-Lock Braking System Efficiency*. 2011. The 12th International Carpathian Control Conference (ICCC). 25 – 28 May 2011. Velké Karlovice, Czech Republic. pp247-252. ISBN 978-1-61284-361-2.

[2] LE KHAC BINH, JIRI TUMA. *Diagnostics Internal Combustion Engine Based on Crankshaft Angular Acceleration.* 2011. In Proceedings of Technical computing Prague 2011, 1st. ed. Prague, November 8, 2011. ISBN 978-80-7080-794-1.

[3] LE KHAC BINH, JIRI TUMA. *Diagnostics Gasoline Engine by Phase Demodulation Method.* Transaction of the VSB – Technical University of Ostrava, Mechanical Series. No.2, vol. LVII, article No. 1865. Pp1-6. ISBN 1804 – 0993.

[4] LE KHAC BINH, JIRI TUMA. *Approach to Gasoline Engine Faults Diagnosis Based on Crankshaft Instantaneous Angular Acceleration*. 2012. The 13th International Carpathian Control Conference (ICCC). 25 – 28 May 2012. High Tatras, Podbanské, Grand hotel Permon, Slovak Republic. pp35-39. ISBN: 978-1-4577-1866-3